DEUTERIUM NMR STUDIES OF MODEL MEMBRANES CONTAINING 1-ALKANOL ANESTHETICS OR ALPHA-TOCOPHEROL

by

Jenifer L. Thewalt

B.Sc. (Hons.), Simon Fraser University, 1979

A THESIS SUBMITTED IN PARTIAL FULFILLMENT OF THE REQUIREMENTS FOR THE DEGREE OF DOCTOR OF PHILOSOPHY

in the Department

of

Chemistry

Simon Fraser University

February 1986

APPROVAL

Name: Jenifer L. Thewalt

Degree: Doctor of Philosophy

Title of Thesis: Deuterium NMR Studies of Model Membranes Containing 1-Alkanol Anesthetics or Alpha-tocopherol

Examining Committee: Chairman: Dr. F.W.B. Einstein

Dr. R.J. Cushley
Senior Supervisor

Dr. I.D. Gay

Dr. E.J. Wells

Dr. A.C. Oehlschlager

Dr. Eric Oldfield
External Examiner
School of Chemical Science
University of Illinois
Urbana, Illinois

Date Approved: April 8, 1986

PARTIAL COPYRIGHT LICENSE

I hereby grant to Simon Fraser University the right to lend my thesis, project or extended essay (the title of which is shown below) to users of the Simon Fraser University Library, and to make partial or single copies only for such users or in response to a request from the library of any other university, or other educational institution, on its own behalf or for one of its users. I further agree that permission for multiple copying of this work for scholarly purposes may be granted by me or the Dean of Graduate Studies. It is understood that copying or publication of this work for financial gain shall not be allowed without my written permission.

Title of Thesis/Project/Extended Essay

"Deuterium NMR Studies of Model Membranes Containing 1-Alkanol Anesthetics or α-Tocopherol"

Author: _____
(signature)

Jenifer L. Thewalt
(name)

April 7, 1986
(date)

ABSTRACT

The phase behaviour of model membranes containing 1-alkanol anesthetics has been studied using deuterium nuclear magnetic resonance spectroscopy (^{2}H NMR). The model membrane systems were aqueous multilamellar dispersions composed of either a saturated phosphatidylcholine perdeuterated on the *sn*-2 chain containing 1-octanol or 1-decanol or 1,2-dipalmitoyl-*sn*-glycero-3-phosphorylcholine (DPPC) containing [$^2H_{17}$]1-octanol or selectively deuterated 1-decanol. The phase changes monitored by ^{2}H NMR are corroborated using differential scanning calorimetry (DSC).

Incorporated 1-octanol or 1-decanol causes the lipid's gel to liquid crystalline phase transition to broaden and its onset temperature (T_m) to decrease. Octanol has more effect than decanol, indicating that it disrupts the gel phase packing of the phospholipid to a greater extent. The phase transition can also be observed in changes in the labelled 1-alkanols' ^{2}H NMR spectra with temperature. Using specifically deuterated decanols it is found that the phase change is sensed at different temperatures depending on the position of the ^{2}H label.

For liquid crystalline systems plots of C-^{2}H bond order parameter S_{CD} vs. position of deuteration have been constructed. At 50°C there is no significant change in the phospholipid S_{CD} due to 25 mol % incorporation of either 1-octanol or 1-decanol. This implies that the liquid crystalline phase can accommodate a

large number of linear anesthetic molecules without changing the orientational order in the acyl chain region of the lipid bilayer. The order parameter profile of 1-decanol in DPPC shows that 1-decanol aligns approximately parallel to the C-3 to C-13 segment of the lipid's *sn*-2 chain. The deuterium relaxation time characterized by the time constant T_{2e} lengthens dramatically in the presence of 1-alkanol. This is taken to mean that the slow motions thought to be responsible for this relaxation occur at a faster rate when 1-alkanol is dissolved in the lipid. These results are discussed in terms of the currently proposed theories of anesthesia where findings using model membrane systems are applicable.

The second area of study concerns the effect of α-tocopherol on aqueous dispersions of saturated, acyl chain perdeuterated phosphatidylcholine. ^2H NMR and DSC show that α-tocopherol broadens and reduces T_m of the phospholipid gel to liquid crystalline phase transition, and that the gel phase lipid is disrupted by the presence of α-tocopherol. Above the phase transition α-tocopherol increases the phospholipid S_{CD}. These results imply that the structural effects of α-tocopherol on lipid bilayers are similar to those of cholesterol.

ACKNOWLEDGEMENTS

I am grateful to my supervisor, Professor R. J. Cushley, for his expert guidance and for his support during the course of this study. The syntheses of selectively deuterated compounds was performed by Dr. A. P. Tulloch (National Research Council, Saskatchewan) to whom I am indebted.

I also thank the members of my supervisory committee, Professors I.D. Gay and E.J. Wells for their advice, especially Dr. I.D. Gay whose generosity in providing various computer programs was much appreciated. As well, the members of Professor M. Bloom's research group (Physics Department, University of British Columbia) were very helpful, particularly Mr. E. Sternin who donated his depaking program. Thanks go to Dr. C. Irwin and Mr. G. Jackle (Physics Department, S.F.U.) for the use of their DSC facility.

The companionship of the present and past members of Dr. Cushley's group has been rewarding. In particular Drs. H. Gorrissen, Y. Parmar, W.D. Treleaven and S.R. Wassall provided assistance with many aspects of this work. I also acknowledge Mr. R. Chana's help with syntheses.

Finally, my family deserves special thanks. My parents Mr. and Mrs. E. Tribe were supportive throughout my education, and my sister Dr. A. McMillan was a source of inspiration. The encouragement of my husband Dr. M.L.W. Thewalt has been immeasurably valuable.

TABLE OF CONTENTS

TABLE OF CONTENTS (Cont.)

TABLE OF CONTENTS (Cont.)

LIST OF TABLES

LIST OF FIGURES

LIST OF PLATES

INTRODUCTION

I. Anesthesia

One may define anesthesia as being the temporary loss of sensation. 'Loss of sensation' is difficult to monitor scientifically, and more practical definitions of anesthesia are linked to readily observed effects such as the absence of muscle movement upon surgical incision. The mechanism by which anesthesia occurs is not well understood and is being researched extensively. Two recent reviews of this research are Dluzewski et al. (1983) and Janoff and Miller (1982).

Anesthetics generally act on the nerve and interfere with either the nerve impulses which transmit stimuli or with communication from one nerve to another across the synapses. The former can affect just one part of the body as in local anesthesia while the latter is thought to result in general anesthesia. Hypothetical anesthesia mechanisms usually attribute anesthetic activity to either direct interactions between protein and anesthetic, or to indirect, lipid-mediated effects of the anesthetic on protein. It is the second class of hypotheses which is relevant to the work in this thesis. Early evidence in favour of an indirect mode of anesthetic action came from the observation that a wide variety of chemicals have anesthetic properties. These range from inert gases (eg. Xe) through the clinically used inhalation anesthetics (eg. halothane, $CF_3CHClBr$), to aliphatic alcohols, alkanes and

steroids. There is a correlation between the potency of these anesthetics and their solubility in lipid, but no other obvious correlations with chemical properties. Specific 'lipid' hypotheses of anesthesia are introduced in section II of this chapter.

The 1-alkanol or long chain alcohol family of anesthetics has been the subject of numerous investigations into the molecular mechanisms of anesthesia. Alcohols block both conduction along nerves, as measured for the squid giant axon (Armstrong and Binstock, 1964) and synaptic transmission, reflected in loss of consciousness as determined in tadpoles (Pringle et al., 1981). Ascending the homologous series of 1-alkanols it is found that the concentration of alcohol in the aqueous medium needed to produce anesthesia is progressively reduced. At a certain chain length (approximately 13-14 carbons) the alcohols' anesthetic capacity is lost. These observations can be explained in terms of the 1-alkanols' lipid:water partition coefficients, which increase with increasing chain length and then suddenly drop off at a length of thirteen or fourteen carbons. Taking into account the relative anesthetic concentrations in the aqueous medium and in the membrane, it has been shown that the anesthetic concentration in the membrane is similar for 1-alkanols from ethanol to dodecanol, varying between 0.01 and 0.04 moles per litre (Pringle et al., 1981).

A. Model membrane studies

Diacyl phosphatidylcholines spontaneously form bilayer structures upon hydration. Gentle mixing of the lipid and water yields multi-bilayered, irregular shapes with diameters on the order of several thousand angstroms. These mixtures will in general be referred to as 'multilamellar dispersions' (Plate I) in this thesis. Another common name for them is 'liposomes', but this term is sometimes used to mean unilamellar spherical lipid particles. The formation of bimolecular leaflets of phospholipid is a result of the lipid's chemical structure, as it possesses a polar (hydrophilic) headgroup and non-polar (hydrophobic) fatty acyl chains. The hydrophobic chains point toward each other to form the core of the bilayer while the headgroup region interacts with water, forming the lipid/water interface. In a multilamellar dispersion, many concentric bilayers, separated by water, make up each large, closed, onion-like structure. The structures tumble slowly, on the order of one second. Within each bilayer, lipid molecules undergo fast lateral diffusion ($\approx 10^{-8}$ cm^2 s^{-1}).

Plate I: Multilamellar Dispersion

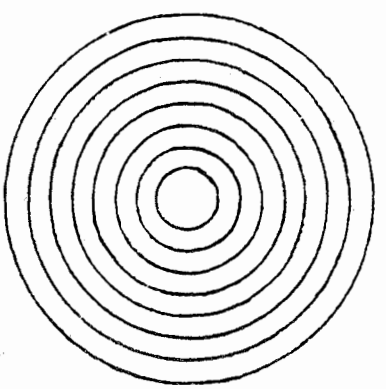

The bilayer structure is common in natural membranes, which in addition to various types of lipid, contain proteins and other fat-soluble molecules such as cholesterol. Model membrane systems, whose compositions are accurately known, and whose properties are intrinsically simpler, are the logical starting point for investigations into many subjects of biological relevance. The question of anesthesia mechanism is particularly suited to this type of study, since many hypotheses have identified the lipid constituent of membranes as the primary site of anesthetic/membrane interactions. It is interesting that biophysical measurements on natural membranes often give results similar to those obtained in the absence of protein. Recently Curatolo et al. (1985) reported a ^{2}H NMR spectroscopic study of mammalian neural tissue whose choline headgroups were biosynthetically deuterated. Their results led them to conclude that there were no strong interactions between neural proteins and choline-containing lipids in intact nerve membranes. Another recent study (Smith and Butler, 1985) presented evidence from ^{2}H NMR that the local anesthetic tetracaine (which had been deuterated) behaved similarly in model membranes, intact bovine spinal cord or the lipid extracts of bovine spinal cord.

B. Phosphatidylcholine phase transitions: effect of 1-alkanols

Multilamellar dispersions of fully hydrated 1,2-dipalmitoyl-*sn*-glycero-3-phosphorylcholine (DPPC) display a number of phase changes as they are heated (Tardieu et al.,

1973; Ruocco and Shipley, 1982a). The two which will be focussed on are the pretransition, at ≈35°C and the main gel to liquid crystalline transition, at 42°C. At temperatures below the pretransition (and above ≈15°C) the lipid is in the gel phase ($L_{\beta'}$) which is characterized by extended acyl chains which are tilted with respect to the bilayer normal, and by lipid packing which is approximately orthorhombic. In this phase the acyl chains are in close contact with each other, and motion in one chain occurs in tandem with neighbouring chain motion.

At the pretransition the lipid assumes hexagonal packing and a rippled surface develops ($P_{\beta'}$ phase), with a period of about two hundred angstroms. The motion of the acyl chains is less restricted than in the $L_{\beta'}$ phase, and rotation of the chains about their long axes occurs at an increased rate (Meier et al., 1983). The details of this rippled gel phase structure are still controversial (see, for instance, Marder et al., 1984).

At the main transition the bilayer becomes liquid crystalline (L_{α} phase) and trans-gauche isomerisations of the acyl chains lead to an elimination of the tilt and to a decrease in thickness of the hydrocarbon core by about twenty per cent. The orientational freedom of the acyl chains is constant from about C-2 to C-9 and then increases towards the middle of the bilayer as shown by ^{2}H NMR (for a review see Seelig, 1977).

Numerous studies using model membranes have reported changes in the phospholipid phase transition behaviour upon 1-alkanol incorporation. A brief summary of the results is

presented here. Hill (1974) found, using light scattering, that 1-alkanols with from three to nine carbons lowered the main phase transition temperature of DPPC. Jain and Wu (1977) and Jain et al. (1975), using differential scanning calorimetry (DSC), reported that the alcohols 1-pentanol to 1-octanol lower T_m and broaden the transition of DPPC. Also using DSC on DPPC Eliasz et al. (1976) studied the C-8 to C-18 (even chain) 1-alkanols and observed that those with fewer than twelve carbons lowered T_m while the rest raised T_m. (For 1-dodecanol an increased T_m was seen only at concentrations greater than 20 mol %.) Lee (1976a) used chlorophyll a as a fluorescent probe in DPPC, DMPC and 1,2-dipalmitoyl-*sn*-glycero-3-phosphoryl-ethanolamine (DMPE) containing 1-butanol to 1-dodecanol. Those 1-alkanols with fewer than ten carbons lowered T_m for all three lipids, while 1-decanol raised T_m for DMPC and 1-dodecanol raised T_m for DMPC and DPPC. By measuring the volume expansion that accompanies the main transition MacDonald (1978) found that 1-propanol to 1-pentanol decreased T_m without broadening the transition while 1-hexanol decreased T_m and increased the transition width. Using an ESR spin labelling technique Richards et al. (1980) reported the effects of 1-alkanols from six to fourteen carbons long on DMPC. 1-Hexanol to 1-nonanol reduced T_m while 1-decanol to 1-tetradecanol raised it.

These results taken together imply that the phase transition effects of 1-alkanols on saturated phospholipid bilayer systems depend on the chain lengths of both the alkanol and lipid acyl moieties. The phosphatidylcholine/alcohol

mixtures with a difference in chain length of four or fewer carbons display increased T_m's compared with the pure lipid while a greater chain length disparity results in lower T_m's.

It has been proposed that the lowering of the phospholipid main phase transition temperature could be linked to the mechanism by which 1-alkanols induce anesthesia. Early speculations (Lee, 1976b; Trudell, 1977) were that phase separations normally present in nerves were disrupted by anesthetics. These ideas relied on regions of lipid which were near their gel to liquid crystalline transition temperatures and in close proximity to excitable proteins. In support of the phase separation idea bacterial membranes have phase transitions near the temperatures at which the bacteria were grown. Recently these ideas have been criticised (Janoff and Miller, 1982) in that mammalian nerve membranes contain cholesterol and unsaturated lipid acyl chains. The former has the effect of broadening the transition while the latter lowers the transition temperature so that transitions at physiological temperatures are not expected to occur. As well, no convincing evidence for long-lived lipid-protein complexes in nerves has been presented.

The 'phase separation' anesthesia mechanisms are viewed with considerable doubt. Nevertheless it is important to know what changes an anesthetic causes in the phase behaviour of the membrane system under study in order to interpret anesthetic-induced changes in lipid acyl chain order or 'fluidity'. Such changes are discussed in section IIB of this chapter. For example, a recent publication (Fesik and Makriyannis, 1985)

reports differences in the ^2H NMR spectra of DMPC containing two closely related steroids, one of which is anesthetic and the other inactive. The anesthetic steroid was found to reduce the deuterated phospholipid's quadrupolar splittings (which are proportional to the C-^2H order parameters) while the inactive steroid did not, at a given temperature. However it was also noted that the anesthetic steroid reduced T_m of DPPC much more than the nonanesthetic steroid, so that the differences in quadrupolar splitting observed are not surprising. Many studies have reported a decline in phospholipid ^2H NMR order parameters with increasing temperature above the phase transition (eg. Davis, 1979).

C. Lipid disordering/'fluidizing' effect of 1-alkanols

Another area where model membrane studies have been utilized extensively is in the determination of changes in membrane order and/or 'fluidity' due to 1-alkanol incorporation. The term 'order' defines the degree of orientational freedom of the lipid acyl chains while 'fluidity' is related to the rates of motion that lipid components experience. The two terms should not be used interchangeably, although reduced order is often accompanied by increased fluidity. Two techniques have provided most of the results: ESR of spin-labelled lipid systems and fluorescence measurements using some form of fluorescent probe in the lipid bilayer system. These techniques have a common drawback in that they rely on indirect and

possibly probe-modulated information about the bilayer core, due to steric effects on the neighbouring phospholipids.

ESR studies have consistently reported a negative change in ESR order parameter upon addition of anesthetic alcohols. The first such study (Paterson et al., 1972) determined the effects of 1-propanol to 1-octanol on oriented multibilayers of human erythrocyte or beef brain lipids as monitored by a steroid spin label. It was found that all the alcohols disordered the ESR spectrum of the spin label in both types of membrane, the longer homologues exerting their effect at lower aqueous concentrations. Subsequently, a 21 mol % lipid concentration of 1-octanol was found to disorder a spin-labelled DPPC derivative in egg lecithin/cholesterol liposomes (mol ratio 1.0:0.9) (Lawrence and Gill, 1975). The order parameter of the label, which was attached to C-8 of the lipid *sn*-2 chain, was reduced by 0.09. Lyon et al. (1981) determined that the alkanols from ethanol to 1-octanol reduced the order of a C-5 spin-labelled stearic acid probe in mouse synaptosomal plasma membrane preparations. The magnitude of the reduction was linear with alcohol concentration, and the disordering capabilities of the alcohols were consistent with their membrane/buffer partition coefficients. Pringle et al. (1981) measured the disordering effect of a 25 mol % concentration of 1-alkanols having lengths of between ten and twenty carbons on the order parameter of C-5 labelled palmitic acid in egg lecithin/cholesterol (2:1) liposomes. They found that the change in order parameter was reduced as the 1-alkanol chain length was increased, so that 1-eicosanol had no

effect, while 1-decanol reduced the order parameter by about four per cent. More recently Boigegrain et al. (1984) studied the effects of methanol to 1-octanol on C-5 labelled stearic acid incorporated into rat intestinal membrane preparations. They reported that these alcohols reduce the probe order in a manner that correlated with their partition coefficients. Specifically, a five per cent reduction in order was found for all the alkanols when they were present in the membrane at concentrations between 0.15 and 0.30 mol/kg.

Fluorescence measurements on labelled model membrane systems containing alcohols yield values which can be related to the microviscosity of the bilayer near the fluorescent probe. Analysis of these experiments is complicated by variables such as the choice of probe (and hence its preferred location in the bilayer), and also by the fact that anisotropic reorientation of the probe can lead to errors in the determination of microviscosity (Heyn, 1979; Jahnig, 1979). Zavoico and Kutchai (1980) determined that the alkanols 1-butanol to 1-octanol reduced a microviscosity-related parameter of the probe diphenylhexatriene (DPH) in microsomal membranes isolated from chick hearts. When the alkanols were compared at equivalent membrane concentrations their effects were similar and increased linearly with concentration. In another study employing DPH, (Ingram et al., 1982) the results were interpreted to mean that ethanol increased the fluidity of neural membranes isolated from fish. A very recent report by Zavoico et al. (1985) compares the information obtained from five different fluorescent probes

which, due to their structure and polarity, are located in different regions of the bilayer. Two of the probes were DPH analogues while the other three were fluorescent stearic acid derivatives whose fluorescent moieties were attached to C-2, C-7, or C-12 of the acid. The lipids used were egg yolk lecithin (egg PC) or DPPC with incorporated 1-pentanol, 1-decanol or 1-tetradecanol. In the liquid crystalline phases studied 1-pentanol decreased probe order and increased its rate of rotation, independent of the particular probe employed. The results concerning 1-decanol or 1-tetradecanol were more complicated. For instance, 1-decanol decreased the order of the fatty acid probes but had no effect, or increased order, when the DPH probes were used. Decanol slightly increased the rotation rate for all probes. The 1-decanol:phospholipid molar ratios used were approximately 1:2. These results point out that the properties of the particular fluorescent probe must be known before fluorescence measurements can be interpreted accurately, since the information inferred about lipid order and dynamics is markedly probe-dependent.

A popularly held mechanism of anesthesia is that anesthetics dissolve into phospholipid membranes and disrupt their structure in a way which critically alters the function of proteins suspended in the bilayer. This is attractive in that it removes the need to explain the potency of molecules whose structures and chemical properties are similar only in that they are lipid-soluble. Changes detected in ESR order parameters due to 1-alkanol incorporation are quite small when clinical

concentrations of alcohols are used. For this reason the theory has been criticised in that temperature increases which cause the same change in order parameter do not cause anesthesia. Another characteristic of experiments which support the disordered or fluidised lipid hypothesis is that the model membranes employed generally contain large concentrations of cholesterol. It has been shown that the observed perturbations are amplified in the presence of cholesterol, although the reason for this is not clear (Miller and Pang, 1976).

D. Outline of research

Few reports using NMR have been published concerning the properties of phospholipid bilayers containing long chain alcohols. An early paper (Colley and Metcalfe, 1972) used proton NMR to study DPPC and egg PC vesicles containing phenyl alcohols or aliphatic alcohols. The latter were found to have no effect on the chemical shift of the lipids' choline headgroups.

Deuterium NMR has two major advantages over other techniques. It is possible to interpret the experimental results in a straightforward manner since, unlike proton NMR, ^{2}H's natural abundance is low, and any spectrum observed is directly attributable to the known deuterated compounds in the system. In addition deuterium introduces the least amount of perturbation possible into the experiment unlike ESR and fluorescence whose probes, being structurally dissimilar to the neighbouring

phospholipids, likely induce changes in their local environments so that the lipids in these environments are no longer in their natural state.

Very few ^2H NMR studies investigating phospholipid/1-alcohol interactions have been published. In 1979, looking at a closely related topic, Turner and Oldfield reported that the effect of high concentrations of the local anesthetic benzyl alcohol on DMPCs selectively deuterated on the *sn*-2 chain was a decrease in the lipids' quadrupolar splittings at 38°C. More recently Pope et al. (1984) studied aqueous dispersions of DMPC/[$^2H_{17}$]1-octanol and found that the alcohol was ordered in a manner similar to phospholipid acyl chains and was anchored at the lipid/water interface.

The goal of the work presented in this thesis is to determine the effects of anesthetic 1-alkanols on aqueous dispersions of saturated phosphatidylcholine. ^2H NMR is used to study both the phase behaviour of lipid/alcohol systems and the orientational order in the acyl chain regions of these systems when in the liquid crystalline phase. In this way any changes in order may be related to changes in phase transition temperature upon addition of 1-alkanols to the phospholipid. The phase behaviour as described by ^2H NMR is compared with that found using DSC which monitors the bulk phase behaviour of the dispersions. The phospholipids employed are DPPC and 1-palmitoyl(stearoyl)-2-[$^2H_{31}$]palmitoyl-*sn*-glycero-3-phosphorylcholine (PC-d_{31}). The latter is illustrated below.

PC-d_{31}: 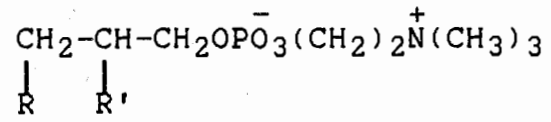

where R= palmitoyl ($CH_3(CH_2)_{14}COO-$) or

stearoyl ($CH_3(CH_2)_{16}COO-$)

R'= [$^2H_{31}$]palmitoyl

Two members of the alcohol anesthetic family are studied: 1-octanol and 1-decanol. These alkanols were chosen for a number of reasons. First, they are among the most potent of the alcohol anesthetics when potency is defined in terms of the aqueous concentration of anesthetic needed to produce anesthesia. Also their lipid:water partition coefficients are high, so that the ^2H NMR spectra are not complicated by the presence of a significant concentration of alkanol in the aqueous phase. Lastly, deuterium-labelled long chain alcohols are not generally commercially available, with the exception of [$^2H_{17}$]1-octanol. Selectively deuterated 1-decanols were available through collaboration with Dr. A. P. Tulloch (N.R.C., Saskatoon).

The results from experiments using the systems of deuterated phosphatidylcholine/1-alkanol and phosphatidylcholine/deuterated 1-alkanol dispersions are complementary. Taken together they enable a more complete understanding of the acyl chain region of the bilayers to be attained.

II. Alpha-tocopherol

"Vitamin E" consists of a variety of tocopherols, the most biologically active being α-tocopherol (Plate II). This compound was not discovered until the 1920's and much remains unknown about the details of its function. Most of the information about α-tocopherol deficiency comes from experiments with animals. Symptoms of severe deficiency vary from species to species and include reproductive failures, muscular degeneration, liver cell death, and brain malformation. In humans there is far less experimental knowledge of maladies caused by the lack of α-tocopherol. This is due to the lipid-soluble nature of the vitamin: it is stored in tissues for extended periods of time following dietary withdrawal and so controlled studies are difficult. Premature infants, though, are characteristically deficient in α-tocopherol and the condition of retrolental fibroplasia (blindness as a result of high oxygen concentrations in administered air) is thought to be ameliorated by doses of α-tocopherol. A summary of the current knowledge concerning α-tocopherol, including its chemistry, biochemistry and role as a nutrient is found in Machlin, 1980.

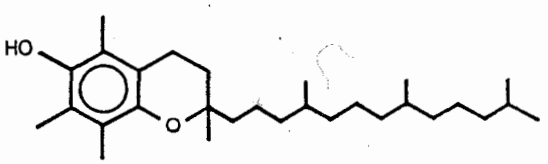

Plate II:

ALPHA - TOCOPHEROL

α-Tocopherol is primarily situated in subcellular organelle

membranes, particularly the inner mitochondrial and microsomal membranes. It is generally accepted that a major function of α-tocopherol is as an antioxidant, reacting with potentially damaging products of lipid breakdown. An interaction with selenium glutathione peroxidase, an integral protein whose function is to reduce peroxides, is also proposed. In addition it has been suggested that α-tocopherol fulfills the structural role of stabilizing membranes, particularly those containing polyunsaturated fatty acyl chains (Diplock and Lucy, 1973; Maggio et al., 1977). Perly et al. (1985) have estimated that the location of α-tocopherol in lipid bilayers is with its hydroxyl group near the lipid/water interface and its hydrocarbon phytyl chain extending into the bilayer core.

Investigations into the proposed structural function of α-tocopherol in lipid bilayers include measurements of phase transition effects, effects on phospholipid order and/or motion, permeability effects, and other effects such as antihemolysis. DSC (Cushley et al., 1979; Pohlmann and Kuiper, 1981; Massey et al., 1982; Lai et al., 1985), ESR (Srivastava et al., 1983) and fluorescence (Fukuzawa et al., 1980) have demonstrated that increasing concentrations of α-tocopherol progressively broaden the temperature range and reduce the enthalpy of the gel to liquid crystalline transition in DMPC and DPPC bilayers.

Considerable disagreement exists as to α-tocopherol's effect(s) on membrane order and motion. Negligible effect on membrane order by α-tocopherol was detected using ESR of 5-doxyl spin labelled palmitic acid intercalated in oriented egg

phosphatidylcholine multilayers (Cushley et al., 1979). On the basis of increased ^{13}C NMR spin lattice relaxation times measured for egg phosphatidylcholine vesicles containing 25 mol % α-tocopherol at 11°C Cushley and Forrest (1977) concluded that motion is increased within the bilayer. Srivastava et al. (1983) were unable to measure ^{13}C NMR spin lattice relaxation times for DPPC vesicles containing 50 mol % α-tocopherol at 50°C due to spectral broadening but, estimating spin-spin relaxation times from linewidths, they concluded that there is a loss in lipid mobility. Fluorescence measurements on the probe DPH in liquid crystalline DPPC or egg PC liposomes show that α-tocopherol increases polarization (Fukuzawa et al., 1980). Similarly DPH in DMPC dispersions exhibits increased polarization values at 37°C as the α-tocopherol concentration is raised (Massey et al., 1982).

Permeability studies also show that α-tocopherol modifies phospholipid model membranes, and again the situation is somewhat confused. Using a ^{31}P NMR-lanthanide induced shift method, Cushley and coworkers (Cushley and Forrest, 1977; Cushley et al., 1979) saw that incorporation of α-tocopherol into egg PC vesicles substantially increases Pr^{3+} permeability at 33°C. Increased DPPC vesicle permeability to sodium ascorbate at 45°C as detected by ESR was reported by Srivastava et al. (1983) upon addition of α-tocopherol. In contrast, Diplock et al. (1977) observed that α-tocopherol decreases the permeability of egg PC/phosphatidic acid liposomes to D-glucose and chromate at 30°C. The effect was greater for egg PC samples

which contained higher proportions of arachidonic acid residues. Reduced permeability to urea was observed in egg PC liposomes at 25°C by Stillwell and Bryant (1983) upon addition of α-tocopherol. These permeability effects are dependent on the phospholipid phase, and thus show complex temperature variability. Pohlmann and Kuiper (1981) found that α-tocopherol enhances osmotic water transport in DPPC liposomes below the gel to liquid crystalline transition temperature but has little effect above. Experiments by Fukuzawa et al. (1979) on DPPC and DMPC liposomes containing dicetyl phosphate indicated that the rate of glucose permeation is decreased by α-tocopherol in the liquid crystalline state but increased below the phase transition temperature. For DPPC liposomes at 37°C a biphasic variation was exhibited where D-glucose permeability increased at α-tocopherol levels of less than 5 mol % but decreased at levels greater than 5 mol %.

Heightened membrane stability due to the presence of α-tocopherol is also implied by studies of red blood cell hemolysis. Lucy and Dingle (1964) found that α-tocopherol inhibited retinol-induced hemolysis, while Brown (1983) reported that α-tocopherol protected against radiation-induced hemolysis.

^{2}H NMR of aqueous phospholipid dispersions produces results which are comparatively straightforward regarding the determination of acyl chain order in bilayers but until now (Wassall et al., 1986) has not been used to investigate phosphatidylcholine/α-tocopherol interactions. The final section of the Results and Discussion describes the study of PC-

d_{31} containing various concentrations of α-tocopherol. Both the phase behaviour (confirmed by DSC) and the acyl chain order parameters of these dispersions are documented.

THEORY

I. Introduction

This chapter outlines the theory behind the measurements and calculations found in this thesis. In each section reference is made to texts and/or review articles containing comprehensive explanations. An introduction to the nature of the NMR spectra expected from deuterons in liquid crystalline unoriented samples is given first, together with the definition of the carbon-deuterium bond order parameter. The background to the techniques of spectral depaking and of the quadrupolar echo pulse sequence is then presented in some detail. Following this are brief explanations of the measurements used in studying the temperature-induced changes in model membrane systems. These measurements are: (i) calculation of spectral moments; (ii) calculation of the echo height decay time; (iii) differential scanning calorimetry.

II. Deuterium NMR

The ^{2}H NMR technique measures transitions between nuclear energy levels in an external magnetic field. These levels are the sum of magnetic (Zeeman) and quadrupolar energies. A good introduction to the nature of quadrupolar interactions may be found in the first three sections of Cohen and Reif (1957), while Slichter (1978) and Harris (1983) are good general NMR

texts. ^2H NMR applied to lipid membranes is discussed in excellent reviews by Seelig (1977) and Davis (1983).

The Zeeman Hamiltonian is the scalar product of the nuclear magnetic moment μ and the magnetic field B_o, with associated energy levels $E_m = -\gamma h B_o m/2\pi$. B_o defines the z direction, and m = +1, 0, or -1 for deuterium, whose nuclear spin I=1. The gyromagnetic ratio γ equals 4.1×10^7 T^{-1} s^{-1} for ^2H.

The quadrupolar Hamiltonian describes the interaction between a non-spherically symmetric nuclear charge distribution and an external charge distribution that gives rise to non-zero electric field gradients at the nucleus. The quadrupolar interaction depends on the orientation of the nucleus with respect to the magnetic field, so that ^2H NMR can be used to gain information about the positions of deuterons in the sample. The electric field gradient at the ^2H nucleus may be expressed in terms of a diagonal, traceless tensor with elements $V_{zz} \geq V_{xx} \geq V_{yy}$ where the x and y components are related by defining an 'asymmetry parameter' $\eta = (V_{xx} - V_{yy})/V_{zz}$.

At the fields of several tesla commonly employed in NMR, the quadrupolar Hamiltonian results in only a small shift of the Zeeman energy levels. The energy levels for ^2H in a magnetic field parallel to the z component V_{zz} of the electric field gradient tensor are:

$$E_m = -\gamma h B_o m/2\pi + e^2 qQ(3m^2-2)/4 \qquad (1)$$

where: e is the nuclear charge, eq equals V_{zz}, and Q is the

nuclear electric quadrupole moment (2.875×10^{-27} cm^2 for ^{2}H). The frequencies of the allowed transitions are thus displaced from the Larmor precession frequency $\nu_o = \gamma B_o/2\pi$ by $\pm 3e^2qQ/4h$, resulting in a doublet of separation $\Delta\nu = 3e^2qQ/2h$. This is the maximum obtainable splitting, since B_o was defined as being parallel to V_{zz}.

For a powder sample, consisting of a random distribution of V_{zz}'s, the NMR spectrum is made up of contributions from all orientations of the molecule-fixed V_{zz} with respect to the external B_o. For a given orientation the splitting is given by:

$$\Delta\nu = 3/2\ (e^2qQ/h)\ \left|(3\cos^2\theta - 1)/2 + \eta\sin^2\theta\cos 2\phi/2\right| \qquad (2)$$

where ϕ and θ are the azimuthal and polar angles, respectively, between the two sets of axes, as shown in Fig. 1. The quantity e^2qQ/h is termed the 'static quadrupolar coupling constant', which varies according to the chemical environment and equals $\approx$168 kHz for C-D bonds in an alkane (Burnett and Müller, 1971). Also pertaining to C-D bonds V_{zz} is essentially parallel to the bond direction and η, the asymmetry parameter, is very close to zero so that the second term in Eq. (2) may be ignored. Thus the orientation dependence of the splitting $\Delta\nu$ is given by the factor $(3\cos^2\theta - 1)/2$. The probability of finding a given angle θ between V_{zz} and B_o varies as $\sin\theta$, so that the most probable relative orientation is $\theta = 90°$, yielding $(3\cos^2\theta - 1)/2 = -1/2$. Correspondingly the frequency separation $\Delta\nu_Q$, called the quadrupolar splitting, of the most intense absorptions in the

Figure 1: The relationship between the laboratory coordinate system (x,y,z; B_o parallel to z) and the principal component V_{zz} (parallel to the C-D bond) of the molecule-fixed electric field gradient coordinate system. The angles θ and ϕ define the relative orientation of the axes.

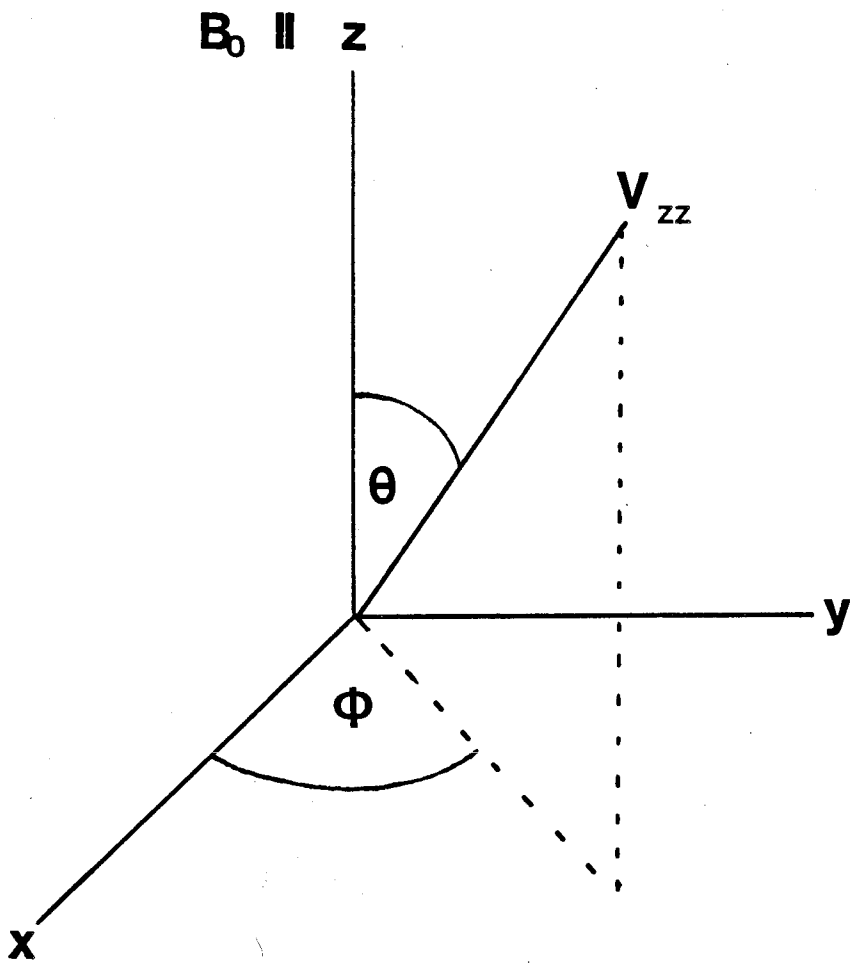
B0 ∥ z
Vzz
θ
y
Φ
x

powder lineshape is:

$$\Delta\nu_Q = 3/4\ (e^2qQ/h) \tag{3}$$

Fig. 2 illustrates a typical ^2H NMR powder spectrum and $\Delta\nu_Q$. In liquid crystalline samples, such as membrane systems of biochemical interest, motion occurs which narrows the splitting from that observed in powders. This motion is generally a rotation about the long axis (termed the 'director') of the liquid crystalline constituent molecule so that only the average orientation is detected by the NMR technique. For an oriented liquid crystal with its director parallel to B_o the observed splitting is:

$$\begin{aligned}\Delta\nu_Q &= 3/2\ (e^2qQ/h)\ |\langle 3\cos^2\Phi - 1\rangle/2| \\ &= 3/2\ (e^2qQ/h)\ |S_{CD}|\end{aligned} \tag{4}$$

where the angular brackets indicate the time average, Φ is the instantaneous angle between V_{zz} and the director axis, and S_{CD} is the order parameter of the C-D bond. For a liquid crystalline sample of random director axes such as occurs in multilamellar dispersions of phosphatidylcholine in water, the most probable angle between a given director axis and B_o is 90°, by analogy with powders. This gives rise to a measured splitting:

$$\Delta\nu_Q = 3/4\ (e^2qQ/h)\ |S_{CD}| \tag{5}$$

Figure 2: A ^2H NMR powder pattern. The spectrum is of [7,7-$^2H_2$]1-decanol in DPPC at 50°C.

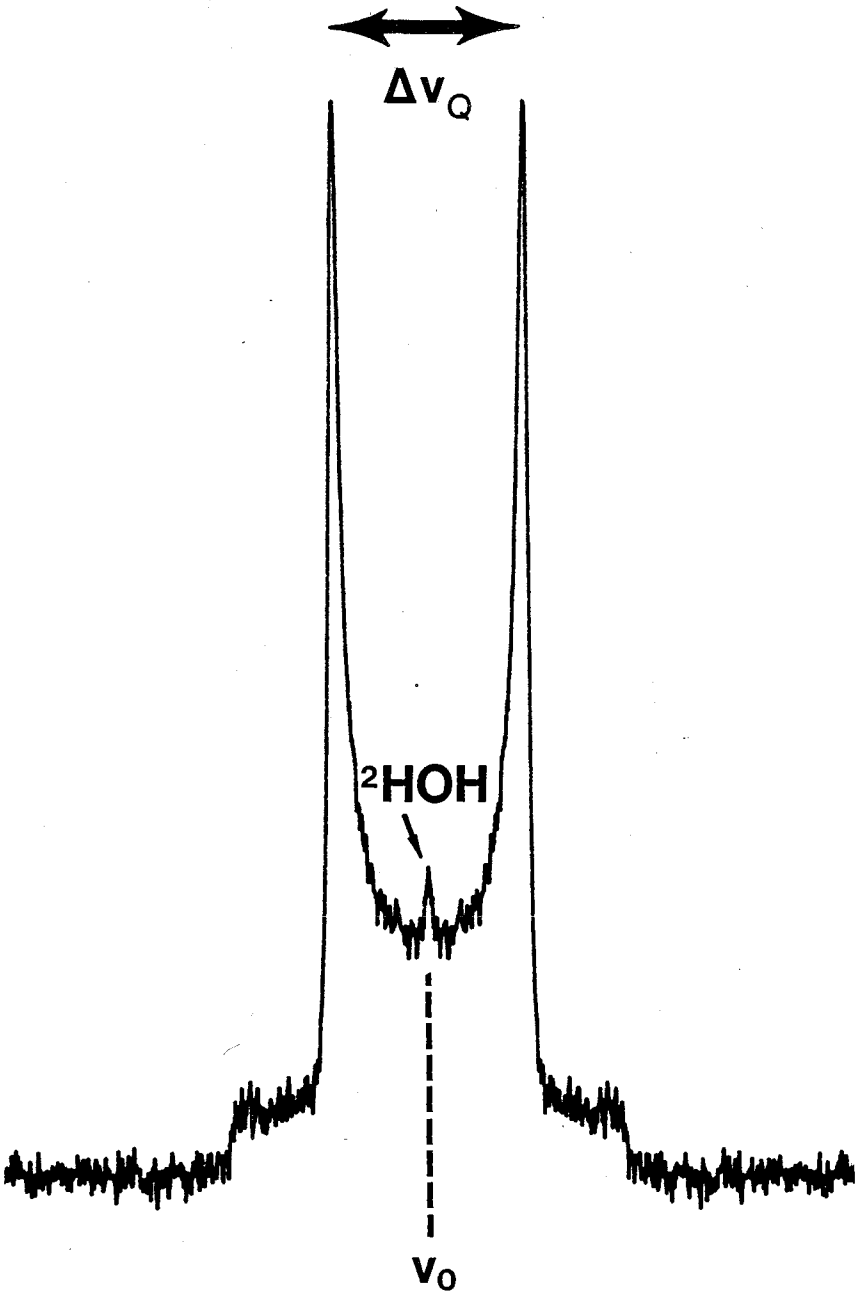
$\Delta\nu_Q$
^{2}HOH
ν_0

Thus the powder lineshape, Eq. (3), is reduced by the anisotropic motions by a factor = $|S_{CD}|$. The sign of S_{CD} must be determined independently if $|S_{CD}| \leq 0.5$.

The functional form of the portion of the axially symmetric ^2H NMR powder pattern which results from the m=0 to m=-1 absorption (i.e. one-half of the quadrupolar doublet) is given by:

$$\text{Powder}(\omega) = \int_0^{\pi/2} \text{Orient}_\theta(\omega) \sin\theta \, d\theta \qquad (6)$$

where $\text{Orient}_\theta(\omega)$, the oriented spectral shape, has not been specified. This can be expressed in terms of frequency using the relationship between ω and θ:

$$\omega(\theta) = x \, (3\cos^2\theta - 1)/2 \qquad (7)$$

where x is the maximum value of ω, found when $\theta = 0$, while the minimum ω equals $-x/2$. In frequency terms Eq. (6) is, then:

$$\text{Powder}(\omega) = \int_{-x/2}^{x} \text{Orient}_\theta(\omega) \, [3x(2\omega + x)]^{-1/2} \, d\omega \qquad (8)$$

where $\text{Orient}_\theta(\omega)$ is usually assumed to be Gaussian or Lorentzian.

The symmetrical powder pattern illustrated in Fig. (2)

results from the sum of Eq. (8) and its mirror image (reflected through the $\omega = 0$ axis), which stems from the low-frequency (m=1 to m=0) absorption and whose limits of integration would be $-x$ and $x/2$. Neglecting the broadening caused by the oriented lines' finite widths (i.e. omitting the convolution with $Orient_\theta(\omega)$ shown in Eq. (8)) the powder pattern has the behaviour: $[-2\omega + x]^{-1/2}$ for $-x \leq \omega < -x/2$; $\{[-2\omega + x]^{-1/2} + [2\omega + x]^{-1/2}\}$ for $-x/2 < \omega < x/2$; and $[2\omega + x]^{-1/2}$ for $x/2 < \omega \leq x$.

A. Depaking

Depaking has been recently developed to calculate 'aligned' NMR spectra from powder patterns (Bloom et al., 1981; Sternin, 1982; Sternin et al., 1983). The technique yields the spectrum that would result from an oriented liquid crystal having its director axis parallel to B_o. For ^2H powder patterns, then, the splitting measured from the depaked spectrum is twice that measured from the powder pattern. Depaking is used to enhance the resolution of spectra consisting of superimposed powder patterns with differing $\Delta\nu_Q$'s. Assignment of the various resonances from perdeuterated molecules is facilitated since the integrated intensities of the peaks in the depaked spectrum are those that would be measured from an oriented spectrum, so that the proportion of the sample's deuterons contributing to a given peak may be determined. Powder spectra must have high signal-to-noise ratios to be suitable for depaking, since the enhanced resolution is accompanied by a concomitant increase in noise.

An outline of the depaking procedure follows. For simplicity it is best to consider only half of the ^2H powder pattern. Fig. (3) shows how the powder and oriented ($\theta = 0°$) spectra are related. The experimentally-determined powder pattern is a superposition of oriented spectra having a sin θ distribution of angles θ between their molecular symmetry axes and B_o, as has been previously discussed. The depaking routine deconvolutes this powder pattern and converts it to the spectrum which would arise from a homogeneously oriented sample with $\theta = 0°$. Axial symmetry is assumed, so that given a certain lineshape $Orient_{\theta=0°}(x)$, the oriented spectra at angles $\theta \neq 0°$ are related to $Orient_{\theta=0°}(x)$ by the factor $(3\cos^2\theta - 1)/2$ according to (Sternin, 1982):

$$Orient_{\theta}(\omega) = Orient_{0°}(x) \; / \; |(3\cos^2\theta - 1)/2| \qquad (9)$$

This relationship implies that the maximum height of $Orient_{0°}(x)$ is smaller than for any other orientation, and that, correspondingly, $Orient_{0°}(x)$ has a larger width than the oriented spectrum at any other angle, since the integrated intensity of the oriented spectrum is not θ-dependent.

Now it is possible to define $Powder(\omega)$ in terms of $Orient_{0°}(x)$, integrating over x:

$$Powder(\omega) = \int_0^1 Orient_{0°}(x) \; [3x(2\omega + x)]^{-1/2} \; dx \qquad (10)$$

Figure 3: One-half of a (simulated) ^2H NMR powder pattern and the associated "oriented" spectrum which would result from a crystal with V_{zz} parallel to B_o. Adapted from Fig. 2 of Sternin (1982), with permission.

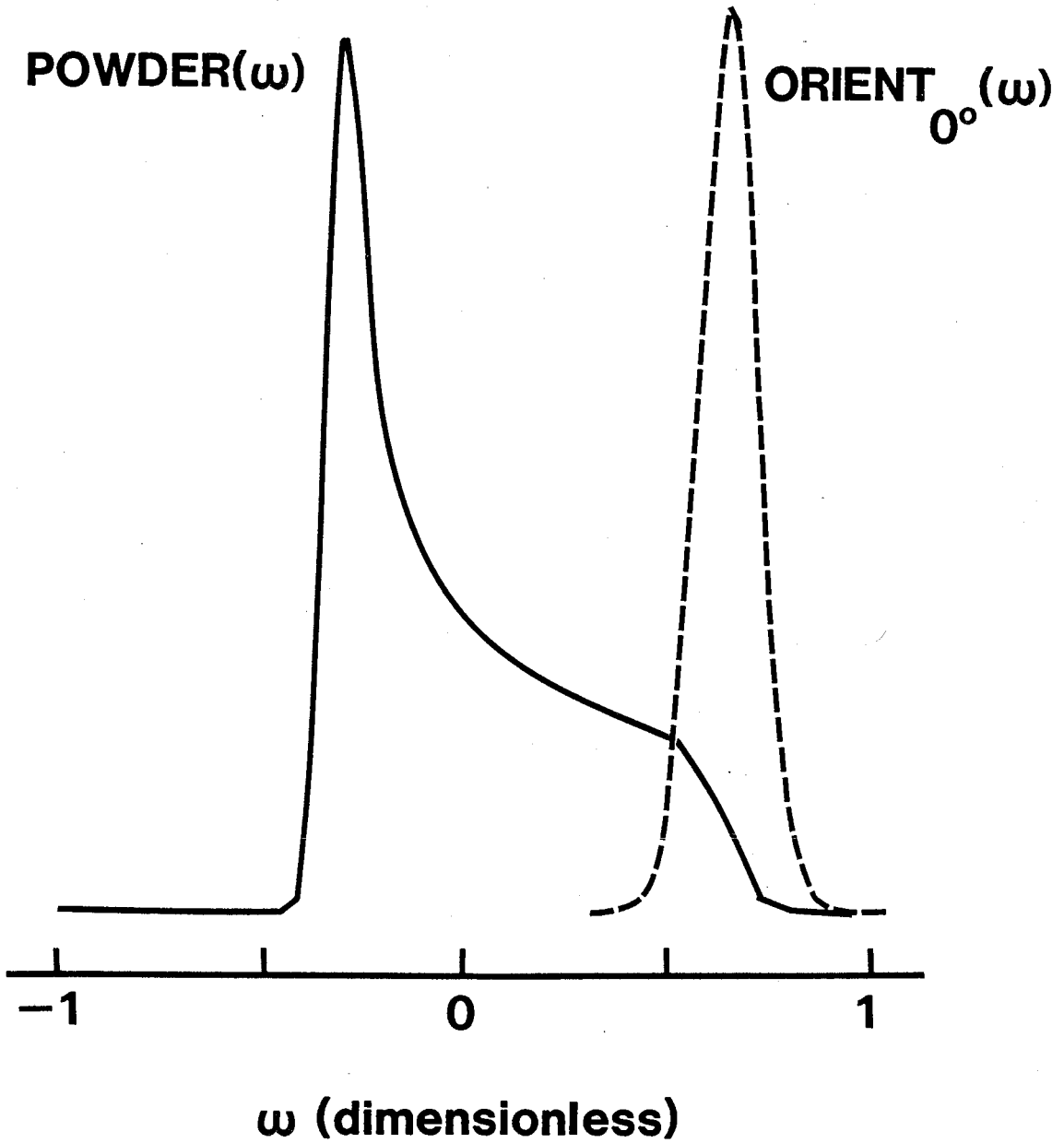
POWDER(ω)
ORIENT 0° (ω)
−1
0
1
ω (dimensionless)

The limits of integration indicate that $Orient_{0o}(x)$ has been scaled so that it lies within the frequency range $0 < \omega < 1$. In addition, since $\omega = x\,(3\cos^2\theta - 1)/2$, $-x/2 \leq \omega \leq x$ are the only possible values of ω, and the integrand is set equal to zero for values outside this range.

Eq. (10) forms the basis for the depaking program. When dealing with experimental data, however, $Powder(\omega)$ is only known at N discrete frequencies ω_i. In order to compute $Orient_{0o}(x)$, Eq. (10) must be converted into a form containing histograms instead of the continuous functions $Powder(\omega)$ and $Orient_{0o}(x)$. The integral in Eq. (10) may then be solved, since $Orient_{0o}(x)$ is constant over a given histogram interval and thus may be taken outside the integral. The resulting formula, outlined in Eq. (11), may then be used to systematically calculate the oriented spectrum from the known powder pattern. The functions

$$Powder(-\omega_n) = \sum_{i>n}^{N/2} Orient_{0o}(2\omega_i)\; A(\omega_i,\omega_n) + Orient_{0o}(2\omega_n)\; B(\omega_n) \qquad (11)$$

A and B result from the integration, and their precise forms are not necessary for this discussion.

Starting from the $-\omega$ side of the spectrum, a point is chosen well beyond the edge of the powder pattern, where it has disappeared into the baseline noise. Thus, $Powder(-\omega_n) = 0$. It is then assumed that $Orient_{0o}(2\omega_n)$ will also be indistinguishable from noise, so that $Orient_{0o}(2\omega_i) = 0$ for all $i > n$.

$Orient_{00}(2\omega_n)$ may then be uniquely determined from Eq. (11). $Powder(-\omega_{n-1})$ is then sufficient to calculate $Orient_{00}(2\omega_{n-1})$, and this process may be continued until $Orient_{00}(\omega_i)$ is known for all ω_i.

The actual depaking process is somewhat more complex, for two reasons. One is that the ^2H NMR spectra are symmetric, so that each side of the powder pattern contains contributions from both edge and shoulder intensity. Also, random noise tends to obscure the point where the spectrum disappears into noise. This second problem is especially serious when taking the first systematic intensity found in the powder spectrum as 'shoulder' intensity, since the shoulders are intrinsically more susceptible to being obscured by noise than are the edges. The program overcomes these difficulties by taking an iterative approach. The first iteration treats all intensity in half the powder spectrum as 'edge' intensity. This is a purposeful overestimation which is countered in the second iteration by subtracting from the other half of the powder pattern a contribution from the first half's 'shoulder' intensity which, since it was calculated in the first iteration, is of greater magnitude than the true shoulder intensity. After only a few iterations ($\approx$ 4) the two sides of the calculated oriented spectrum converge to the same intensity. An example of a simple ^2H NMR powder pattern and its associated depaked spectrum is given in Fig. (4).

The assumption central to successful depaking is that the interaction giving rise to the powder pattern is axially

Figure 4: A ^2H NMR powder pattern with its associated depaked spectrum. The powder pattern is from [7,7-$^2H_2$]1-decanol in a phospholipid bilayer system. Seven iterations were performed on the data to yield the lower spectrum.

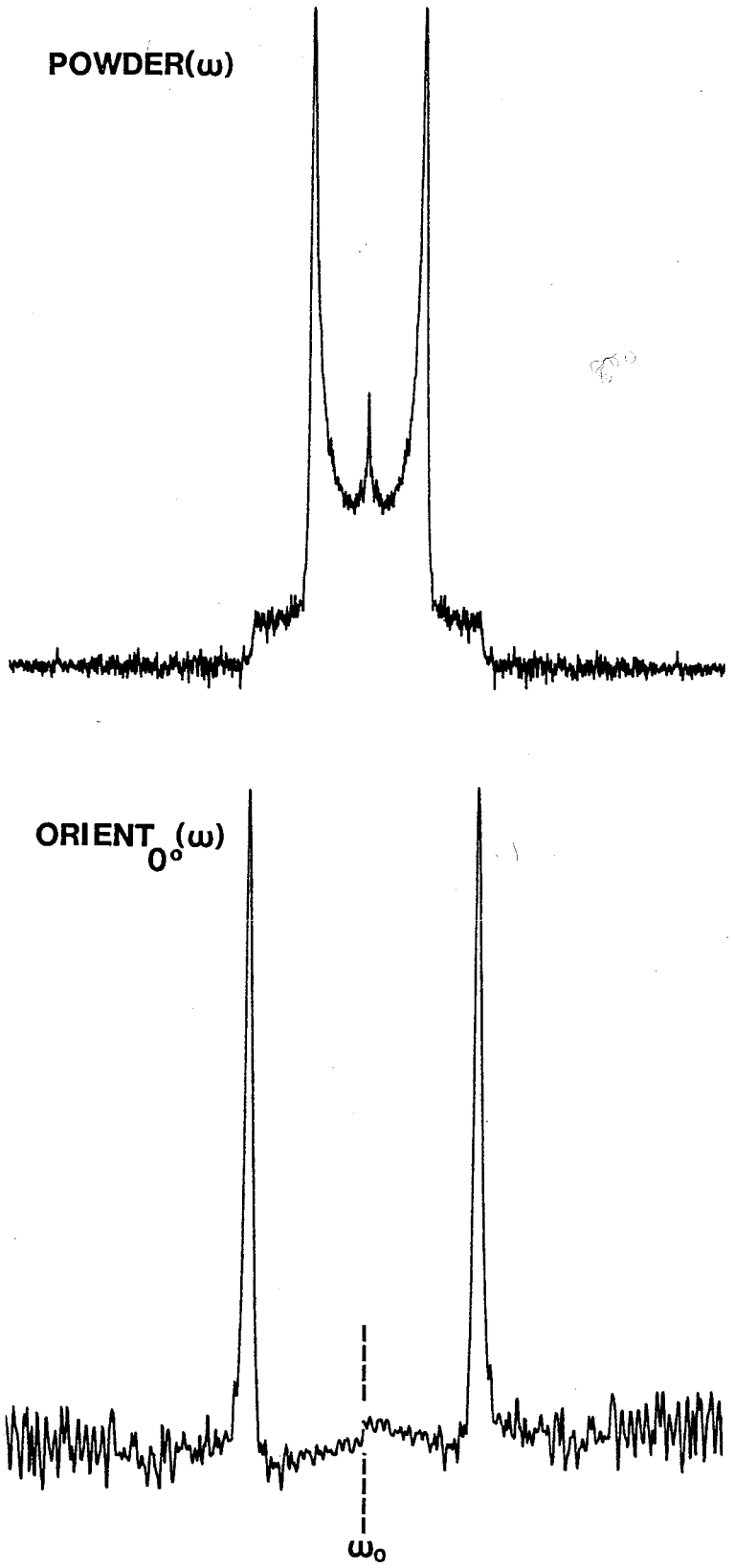
POWDER(ω)
ORIENT 0°(ω)
ω₀

symmetric, so that the oriented spectrum is scaled according to $(3\cos^2\theta - 1)/2$. Caution must be exercised if the powder spectrum arises from a non-zero asymmetry parameter, but useful information may still be obtained (Sternin et al., 1983). A second potential difficulty occurs when orientation-independent line broadening is present. This is encountered, for example, when the time-domain spectrum is filtered using exponential multiplication and gives rise to artifacts in the depaked spectrum at twice the frequency displacement (from ω_o) of the oriented spectral resonances. Fortunately these problems do not interfere with splitting measurements.

B. The quadrupolar echo technique

The first ^2H NMR studies on lipid/water systems (Oldfield et al., 1971) did not employ the pulsed Fourier transform technique and suffered from the lack of sensitivity associated with the older continuous wave method. Early Fourier transform NMR studies (e.g. Seelig and Seelig, 1974) also produced distorted spectra. The free induction decay (FID) from a 90° pulse, which is the usual method of acquiring data in systems with narrow resonances, is not adequate to give fidelity to the ^2H NMR powder lineshape. Because of the large frequencies (up to 250 kHz) encountered in ^2H powder spectra, time domain information diminishes extremely rapidly. The finite 'dead-time' of the receiver following the RF pulse causes the initial data points of the FID to be lost, and the Fourier-transformed

spectrum is thus inaccurate.

To overcome this problem the quadrupolar echo pulse sequence was applied to lipids by Davis et al. (1976). Neglecting relaxation and losses due to magnetic field inhomogeneities, the signal from the static quadrupolar interactions is completely refocussed by the two-pulse sequence $90°_y - \tau - 90°_x - \tau$ - echo, illustrated in Fig. (5). The powder pattern is then obtained by Fourier transformation of the last half of the echo.

It is very difficult to give a classical view of the quadrupolar echo pulse sequence. Two useful references on solid echoes are Solomon (1958) and Mansfield (1965). Solomon (1958) examined the echoes obtained by sequential pulses about the y axis for a nucleus with I=5/2, and his treatment may be readily adapted for two pulses 90° out of phase and for ^2H, with I=1. Following Solomon (1958), we show that the signal amplitude of the echo at $t=2\tau$ following the quadrupolar echo pulse sequence is equal to the signal amplitude which would be measured by an ideal (zero dead-time) receiver coil immediately after the first 90° pulse.

In thermal equilibrium the spin density matrix behaves like I_z. The first 90° pulse is equivalent to a rotation about the y axis and immediately after this pulse (t=0) $\rho(0)$ is proportional to I_x. The density matrix evolves in time according to the quadrupolar interaction which is proportional to I_z^2:

$$\rho(t) = \exp(-iaI_z^2t)\ \rho(0)\ \exp(iaI_z^2t) \qquad (12)$$

Figure 5: The quadrupolar echo pulse sequence. Fourier transformation begins at the top of the echo. Pulses are assumed to be infinitely short for purposes of illustration. The digitization rate is 5 μs and τ is 125 μs.

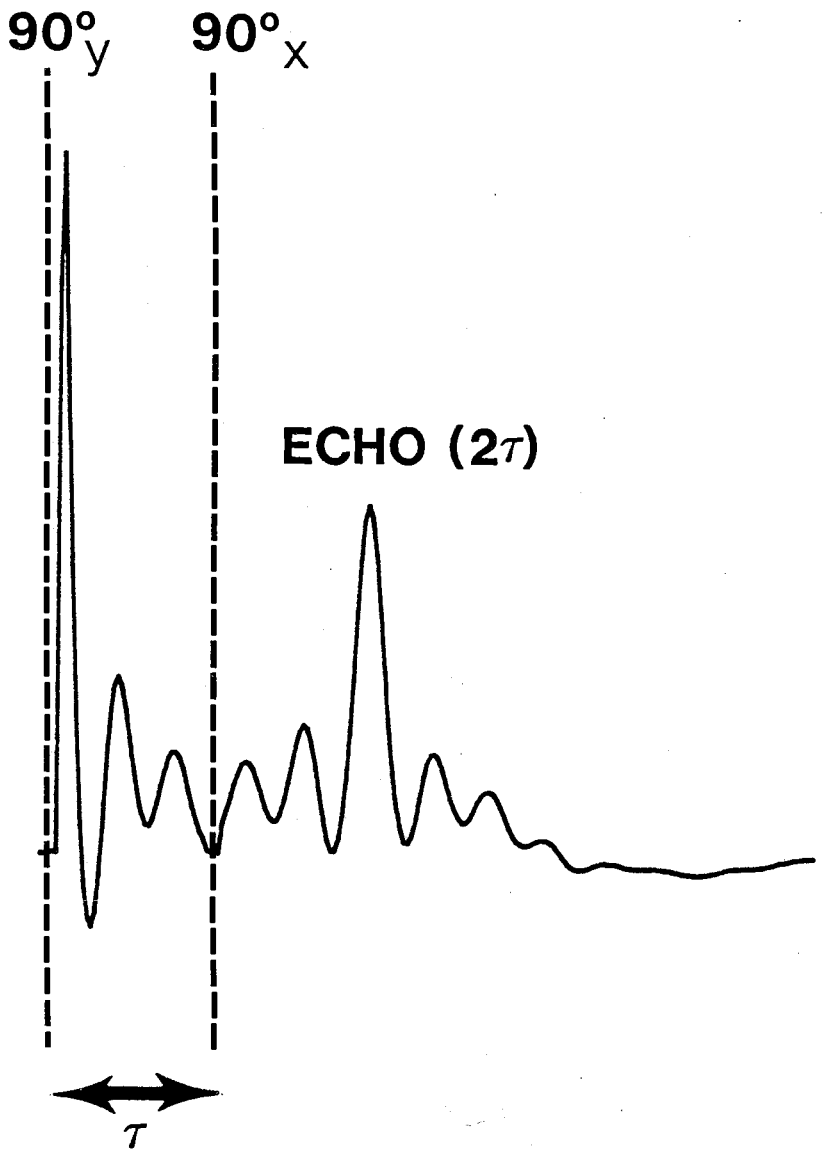
90°y
90°x
ECHO (2τ)
τ

The constant 'a' is related to the strength of the quadrupolar interaction for a given nucleus. The signal amplitude in the coil, S(t), is proportional to:

$$S(t) = Tr[\rho(t) I_+] \tag{13}$$

where $I_+ = I_x + iI_y$. Substituting Eq. (12) into Eq. (13), expanding the exponentials with Taylor series and taking the sum of the diagonal matrix elements gives:

$$S(t) = \sum_m \langle m|\rho(0)|m+1\rangle \; [I(I+1)-m(m+1)]^{1/2} \times \exp(ia(2m+1)t) \tag{14}$$

At $t = \tau$ the second pulse is applied, which performs a rotation R about the x axis. Immediately after this pulse we have:

$$\rho'(\tau) = R \; \rho(\tau) \; R^{-1} \tag{15}$$

where R^{-1} is the inverse matrix of R, with a signal established in the coil at times $t > \tau$ of:

$$S(t) = Tr\{\exp[-iaI_z^2(t-\tau)] \; R \; \exp[-iaI_z^2\tau] \; \rho(0) \times \exp[iaI_z^2\tau] \; R^{-1} \; \exp[iaI_z^2(t-\tau)] \; I_+\} \tag{16}$$

Eq. (16) can be expanded in a similar manner to Eq. (13),

yielding:

$$S(t) = \sum_{m,m',m''} \langle m|R|m''\rangle \langle m''|\rho(0)|m'\rangle \langle m'|R^{-1}|m+1\rangle \times [I(I+1)-m(m+1)]^{1/2} \times \exp\{ia[(2m+1)(t-\tau) - (m''^2-m'^2)\tau]\} \quad (17)$$

An echo occurs when S(t) is independent of 'a', meaning that all nuclei are 'in phase'. The time at which this refocussing happens is given by:

$$(t-\tau)/\tau = (m''^2 - m'^2)/(2m + 1) > 0 \quad (18)$$

Since $\rho(0) = I_x$, the only non-zero matrix elements occur for $(m'' - m') = \pm 1$. Also, when $m = I = 1$, $[I(I+1)-m(m+1)]^{1/2} = 0$ in Eq. (17). The only values m, m' and m'' which are allowed, then, are: $m = 0$, $m' = 0$, $m'' = \pm 1$; $m = -1$, $m' = \pm 1$, $m'' = 0$. Thus the ratio in Eq. (18) equals one, so that the echo occurs at $t = 2\tau$.

In the quadrupolar echo pulse sequence the second pulse is a rotation R about the x axis. This rotation is accomplished by means of the Euler angles $(\alpha,\beta,\gamma) = (-\pi/2, \pi/2, \pi/2)$ as illustrated in Fig. (6). The matrix elements $\langle m|R|m''\rangle$ are found using the Wigner rotation matrix $D^1(-\pi/2, \pi/2, \pi/2)$ which is shown in Table I. The matrix elements $\langle m'|R^{-1}|m+1\rangle$ are found using the adjoint of $D^1(-\pi/2, \pi/2, \pi/2)$. The non-zero matrix elements $\langle m''|\rho(0)|m'\rangle$ are all equal to $1/\sqrt{2}$ (Planck's constant having been set equal to one by convention).

Figure 6: The Euler angles (α,β,γ) needed for a 90° clockwise rotation about the x axis. The 90° rotation about the x axis is illustrated on the left, showing its equivalence to the sequence of rotations: $-\pi/2$ about the z axis, $\pi/2$ about the new y axis, and $\pi/2$ about the new z axis.

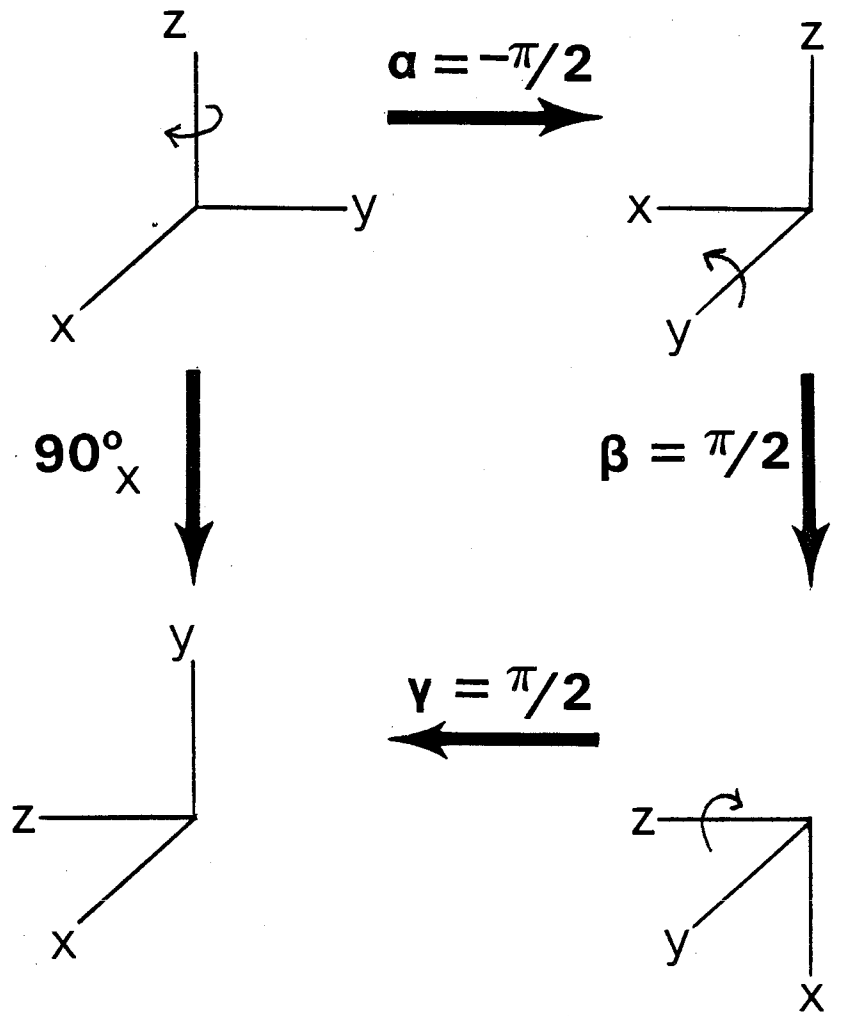
z
y
x
α = −π/2
z
x
y
90°x
β = π/2
y
z
x
γ = π/2
z
y
x

TABLE I: The matrix elements of $D^1(-\pi/2,\pi/2,\pi/2)$.

$$D^1(-\pi/2,\pi/2,\pi/2) = \begin{bmatrix} 1/2 & -i/\sqrt{2} & -1/2 \\ -i/\sqrt{2} & 0 & -i/\sqrt{2} \\ -1/2 & -i/\sqrt{2} & 1/2 \end{bmatrix}$$

$S(t=2\tau)$ may now be evaluated from Eq. (17) and is found to equal one. Similarly, the signal immediately after the first pulse (assuming zero dead-time) may be calculated from Eq. (14) with t=0, and is found to equal one. This proves that the quadrupolar echo completely refocusses the quadrupolar interactions, neglecting the effects of relaxation, etc., as mentioned previously.

C. Method of moments

The NMR spectral moments M_n can be defined by:

$$M_n = \int_0^\infty \omega^n \, f(\omega) \, d\omega \; / \; \int_0^\infty f(\omega) \, d\omega \qquad (19)$$

where $f(\omega)$ is the intensity of the frequency-domain spectrum as a function of the frequency displacement ω from the central (Larmor) frequency. The denominator of Eq. (19), then, is just the spectral area. Note that integration commences at the center of the symmetrical spectrum and is carried out over only half of it. This allows useful values to be measured for the odd moments, which are zero when the limits of integration are the more usual $\pm \infty$.

Qualitatively, the n^{th} spectral moment is a measure of the frequency range over which the ^2H NMR spectrum extends. The higher moments give increasing weight to the low-intensity

shoulders of the spectrum, and thus are more susceptible to errors stemming from low signal-to-noise ratios or from instrumental factors which cause frequency-dependent distortion (see the Experimental Methods). M_1 is least prone to these errors, and the reduction in M_1 as the model membrane is heated through its gel to liquid crystalline transition provides a quantitative measurement of the ^2H NMR spectral narrowing which is qualitatively obvious (Davis, 1979).

In the liquid crystalline lipid phase the first moment may be related to the mean quadrupolar splitting of a perdeuterated sample (Davis, 1979, 1983). For axially-symmetric systems $M_n = c_n \langle(\Delta\nu_Q)^n\rangle$, where c_n is constant for a given integer n. Thus $M_1 = 4\pi/3\sqrt{3}\ \langle\Delta\nu_Q\rangle$, where $\langle\Delta\nu_Q\rangle$ is the mean quadrupolar splitting. Alternatively M_1 may be related to the mean order parameter of the system: $M_1 = \pi/\sqrt{3}\ (e^2qQ/h)\ \langle S_{CD}\rangle$. Similarly, $M_2 = 9\pi^2/20\ (e^2qQ/h)^2\ \langle S_{CD}^2\rangle$.

D. Relaxation: T_{2e}

When employing the quadrupolar echo technique the most accessible relaxation measurement is the measurement of the decay of the echo height $A(2\tau)$ as a function of the pulse spacing τ. This decay has a time constant of T_{2e}:

$$A(2\tau) = A(0)\exp(-2\tau/T_{2e}) \qquad (20)$$

where $A(0)$ is the initial intensity following the first 90°

pulse.

The interpretation of T_{2e} data is not straightforward, although it is generally accepted that time-dependent quadrupolar interactions are chiefly responsible for the loss of echo amplitude (Davis, 1979; Jeffrey, 1981). Dipolar interactions with nearby protons may also contribute, but are usually assumed negligible except for selectively deuterated systems (Pratum, T.K. and Klein, M.P., unpublished).

T_{2e} is orientation-dependent and thus when studying unoriented samples the decay should not be characterized by a single exponential (Pauls et al., 1985). In practise, however, the measured dependence of echo height on pulse spacing for lipid dispersions <u>is</u> exponential, at least for reasonably short pulse spacings ($\tau < \approx 150$ μs).

The examination of the behaviour of T_{2e} as a function of temperature allows correlations to be made with lipid phase changes. Pauls et al. (1984) have related T_{2e} to the rotational correlation time τ_c of a deuterated helical protein in a lipid bilayer through the gel to liquid crystalline phase transition. They find that T_{2e} is directly proportional to τ_c below the phase transition temperature (slow motion) and inversely proportional to τ_c above the transition (fast motion) (Eqs. (21) and (22), respectively). In the intermediate motional regime

$$T_{2e} = p\,\tau_c, \quad p = \text{constant} \tag{21}$$

$$T_{2e} = (\Delta M_2\,\tau_c)^{-1}, \tag{22}$$

ΔM_2 = measure of the extent of spectral narrowing

due to the motion

T_{2e} necessarily goes through a minimum. These changes will be more thoroughly discussed in the relevant sections of the Results and Discussion.

III. Differential Scanning Calorimetry (DSC)

DSC is a powerful thermodynamic tool for studying phase changes in lipid systems. McElhaney (1982) reviews some recent applications of DSC to membrane research. Although DSC may be used to quantitatively determine the change in enthalpy associated with a given phase transition the work in this thesis is chiefly concerned with the temperature of the transition, so that only qualitative results are shown.

DSC measures the difference in power required to keep a sample and reference cell at the same temperature. During a DSC scan the temperature is changed at a constant rate. If the sample goes through an endothermic phase change, more power must be supplied to it, causing a deflection on the recorder. After the phase transition, provided there has been no change in heat capacity, the recorder reattains its baseline level. All phase transitions examined in this thesis are first order, characterized by a discontinuity in the entropy vs. temperature curve (Stanley, 1971).

When comparing different lipid systems whose phase transition temperatures T_m are not equal it is useful to compare

them at a common reduced temperature (Seelig and Browning, 1978). The reduced temperature is defined as $\varepsilon = (T-T_m)/T_m$. This concept does not enable an exact correspondence to be drawn between any two systems at any temperatures, but has been fruitful when comparing model membranes near their respective gel to liquid crystalline transition temperatures.

EXPERIMENTAL METHODS

I. Materials

[$^2H_{31}$]Palmitic acid was a gift from W. Dale Treleaven. The synthesis was by way of hydrogen-deuterium exchange starting with palmitic acid and using palladium on activated charcoal as the catalyst (Hsiao et al., 1974). Egg yolk lysophosphatidylcholine, 1,2-dipalmitoyl-*sn*-glycero-3-phosphorylcholine (DPPC) (DL-α-; grade 1-S; crystalline, synthetic), α-tocopherol and deuterium depleted water were purchased from Sigma Chemical Co. (Sigma lysophosphatidylcholine contains 66-68% palmitic acid, 24-26% stearic acid, and 6-10% other saturated acids.) 1-Octanol was obtained from Matheson, Coleman and Bell and 1-decanol from Aldrich Chemical Co. [$^2H_{17}$]1-Octanol was purchased from MSD Isotopes. Selectively deuterated 1-decanols were synthesized by A. P. Tulloch (Plant Biotechnology Institute, N.R.C., Saskatoon) using recently published procedures (Tulloch, 1985a and 1985b).

II. Synthesis of Deuterated Phosphatidylcholine

1-palmitoyl(stearoyl)-2-[$^2H_{31}$]palmitoyl-*sn*-glycero-3-phosphorylcholine (PC-d_{31}) was synthesized according to published procedures (Grover and Cushley, 1979; Boss et al., 1975) with minor modifications. Briefly, [$^2H_{31}$]palmitic acid was dissolved in dry benzene, to which an equimolar quantity of

1,1'-carbonyldiimidazole is added. Formation of the activated palmitoylimidazole derivative is accompanied by CO_2 evolution. Lysolecithin was then added to the reaction vessel and the solvent evaporated. The dried reaction mixture was heated, during which imidazole crystals formed, indicating that the esterification of fatty acid to lysolecithin had taken place. The modifications to the published procedure were as follows: the reaction (using 3 g lysolecithin and 1.67 g [$^2H_{31}$]palmitic acid) was heated in an oil bath at 75-80°C for 2.5 hours; the crude product was dissolved in petroleum ether/ethanol (28 mL/4 mL) and precipitated by addition to cold acetone (100 mL); the precipitation step was repeated once; the product was purified on a 60 x 4 cm Baker Analyzed silica gel column, 60-200 mesh, and eluted with chloroform/methanol/water (70:26:4 v:v).

The mass spectrum of PC-d_{31} is characteristic of the proposed structure, with two sets of lines centred at m minus 183 (e.g. m minus $N(CH_3)_3(CH_2)_2OPO_3$: phosphorylcholine) = 580.1 and 608.1. The two sets were distributed as follows: m/e: 578 (4.5%), 579 (12.8%), 580 (14.7%), 581 (9.3%), 582 (4.0%) corresponding to phospholipid with a palmitoyl *sn*-1 chain and m/e: 606 (1.2%), 607 (2.9%), 608 (3.5%) 609 (2.9%), 610 (1.3%) corresponding to phospholipid with a stearoyl *sn*-1 chain.

III. Preparation of Multilamellar Dispersions

Fifty weight percent aqueous multilamellar dispersions of PC-d_{31} were prepared by adding ≈200 mg of PC-d_{31} to ≈0.20 mL of deuterium depleted water and thoroughly mixing using a spatula at ≈50°C. The PC-d_{31}/1-octanol and DPPC/[$^2H_{17}$]1-octanol samples were prepared by dissolving the phospholipid (≈200 mg or ≈300 mg, respectively) in chloroform, evaporating to near dryness with a stream of dry N_2, and further drying under high vacuum overnight. Deuterium depleted water (≈0.20 mL or ≈0.30 mL, respectively) and sufficient 1-octanol to bring the phospholipid/1-octanol mol ratio to the desired level were added. Vigorous mixing at ≈50°C using a spatula and a Vortex mixer produced a homogeneous sample. For the PC-d_{31}/1-decanol, DPPC/deuterated 1-decanol and PC-d_{31}/α-tocopherol samples, the alcohol or the tocopherol was codissolved with the lipid in $CHCl_3$ prior to vacuum pumping. Samples were stored at -18°C.

IV. NMR Spectroscopy

A. Instrumental

^2H NMR spectra were recorded at 38.8 MHz using a home-built spectrometer and a Nalorac 5.9 T superconducting magnet. Spectra were measured using the quadrupolar echo pulse sequence $90°|_x - \tau - 90°|_y - T$. Spectral parameters (see figure legends for others) were: data set size = 2K; delay time between

scans, T = 1.0 or 1.5 s. Sample temperature in the home-built probe was controlled to an accuracy of ±0.5°C, by means of a heated gas flow. Samples were allowed to equilibrate for a minimum of 20 min. at a given temperature. Data collection was accomplished with an Explorer III digital oscilloscope, while signal averaging, Fourier transformation and moment calculations were performed using a Nicolet BNC-12 computer. The spectra were symmetrized by zeroing the out-of-phase quadrature channel and reflecting the spectrum about the central (carrier) frequency, resulting in an increase in signal to noise ratio of $2^{1/2}$.

The low temperature spectra of multilamellar lipid dispersions are very broad (up to ±126 kHz), which leads to difficulty in irradiating the entire spectrum with available RF pulses. Our instrument had a 90° pulse of 6.5 or 8 μs in duration. This low value of ω_1 leads to a large reduction in intensity in the wings of the spectrum. The distortion $D(\omega)$ is given by $[\sin(\theta K)/K]^3$ (Bloom et al., 1980) where $K = (1 + \omega^2/4\omega_1^2)^{1/2}$ and where ω is the frequency separation from the Larmor frequency, ω_1 is the frequency of the pulse, and θ is the flip angle of the pulse (all 90° in this thesis). Even with the shorter pulse length of 6.5μs any intensity at ±126 kHz is severely attenuated. This problem is to some extent insoluble. The coil's response can be made more efficient (by increasing its "quality factor" Q) so that the pulse length is reduced, but Q, being inversely proportional to bandwidth, must be kept below about 100 in order that the radio-frequency irradiation is

homogeneous. Also, if Q is increased, the time constant governing the rate of decay of the pulse, which is proportional to Q, is lengthened. This leads to long "ringing" following the pulse which destroys the pulse shape, again resulting in spectral distortions (Rance, 1981). The measurements made and the conclusions reached in the Results and Discussion are not dependent on the exact spectral shape (with the exception of moment calculation, discussed below), especially of the broad, low temperature spectra. The liquid crystalline lipids' spectra should be virtually distortion-free.

B. Data analysis

Fourier transformation and calculation of spectral moments were performed on a Nicolet BNC-12 computer. Prior to transforming the time-domain data, the points were shifted a fraction of a dwell-time so that the initial point was at the top of the echo (Davis, 1983) using a program obtained from Dr. M. Bloom (Physics Dept., U.B.C.). The principle of the algorithm is that five data points are used to fit a fourth order polynomial which is evaluated at a specified shift from the central point. Moments were calculated on the Fourier-transformed data using a program written by Dr. J. Davis and obtained from M. Bloom. As noted above, broad spectra will be distorted, with their wings reduced in intensity. This will also reduce the value of the calculated moments, which are strongly dependent on contributions from the wings of the

spectra (see Theory chapter for the relevant equation). As a result we have measured only the first spectral moment, since this, while less sensitive to spectral narrowing, is much less affected by distortions due to the finite pulse length than the higher moments. The first moment vs. temperature plots presented in the Results and Discussion are not used to draw conclusions based on the absolute value of the moments at low temperatures.

Depaking was accomplished on an IBM 4341 computer using the program contained in Sternin (1982). Data was transferred between the Nicolet and the main-frame via an interface written by Dr. I. Gay (Chemistry, S.F.U.). In general six or seven iterations were performed on the data.

The decay rate of the quadrupolar echo height was measured by varying the time between pulses in the quadrupolar echo sequence. Echo heights were measured using the Nicolet "peak-pick" routine and normalized for the number of scans taken for a given delay time. Generally five times τ in the range 40μs to 150 μs were employed to determine the initial slope of the echo height vs. 2τ plot. The slope was calculated using the BMDP3R weighted nonlinear regression routine from the statistical package BMDP, on the IBM 4341.

V. Differential Scanning Calorimetry (DSC)

DSC traces were obtained using a DuPont Instruments Series 99 thermal analyzer fitted with a 910 DSC accessory, with ≈1-2 mg samples contained in sealed sample pans over the range -30°C to +70°C. The heating rate was 10°C per minute. This rate is too fast to accurately determine the width of very narrow endotherms but was used consistently throughout the thesis. The DSC results are intended to corroborate those obtained from NMR and thus are used in a qualitative way only. Numerous more comprehensive DSC studies have already been published (e.g. Eliasz et al., 1976). The instrument was calibrated using Ga, water and Hg.

The phase transition temperatures were determined as in Eliasz et al. (1976). T_m is measured as the temperature at which the tangent to the maximum slope of the endotherm (on the low-temperature side) intersects the baseline.

RESULTS AND DISCUSSION

The experimental results reported in this chapter have been organized into four broad sections. The first concerns the investigation of aqueous dispersions of a deuterated phosphatidylcholine using ^2H NMR and DSC. The second is a study of the effects that the alkanol anesthetics 1-octanol and 1-decanol produce on the NMR spectra and phase behaviour of these dispersions. The third section deals with the results obtained from a complementary study of aqueous dispersions of phosphatidylcholine with deuterated 1-octanol or 1-decanol added. These studies are summarized together to facilitate cross-comparison wherever possible. The final set of data is a departure from the anesthetic studies: the techniques of ^2H NMR and DSC are used to study aqueous dispersions of deuterated phosphatidylcholine and α-tocopherol. This data is discussed separately.

I. Deuterated Phosphatidylcholine

A. Differential Scanning Calorimetry (DSC)

A phospholipid, 1-palmitoyl(stearoyl)-2-[$^2H_{31}$]palmitoyl-*sn*-glycero-3-phosphorylcholine (PC-d_{31}), has been prepared from egg yolk lysophosphatidylcholine by attaching [$^2H_{31}$]palmitic acid as the *sn*-2 chain. PC-d_{31}, then, has the usual egg phosphatidylcholine distribution of acyl chains on the *sn*-1 position: 66-68% palmitoyl (16:0); 24-26% stearoyl (18:0); 6-10% others. PC-d_{31}, while retaining some of the heterogeneity typical of natural lipids, is expected to have thermotropic behaviour like 1,2-dipalmitoyl-*sn*-glycero-3-phosphorylcholine (DPPC) since both of its acyl chains are fully saturated.

The DSC profile of PC-d_{31} (Fig. 7) confirms this prediction. The DSC trace of a 50:50 wt:wt PC-d_{31}/water dispersion is given in Fig. 7a and shows a pretransition at 31°C and a main gel to liquid crystalline transition at 40°C (half-height width ≈2°C). Fig. 7b shows the DSC trace of a 50:50 wt:wt DPPC/water dispersion which exhibits a pretransition at 35°C and a main transition at 42°C (half-height width ≈2°C) in agreement with literature values (Eliasz et al., 1976; Boroske and Trahms, 1983). The fact that the DSC traces of both lipid dispersions display main transition peaks with half-height widths of 2°C indicates that the heterogeneity of the *sn*-1 chain of PC-d_{31} does not influence its gel to liquid crystalline transition to any appreciable extent.

Figure 7: DSC traces of 50 wt % aqueous dispersions of: (a) PC-d_{31}; (b) DPPC. The peak at 0°C is due to water. Scanning rate was 10°/min. over the range -30°C to +70°C.

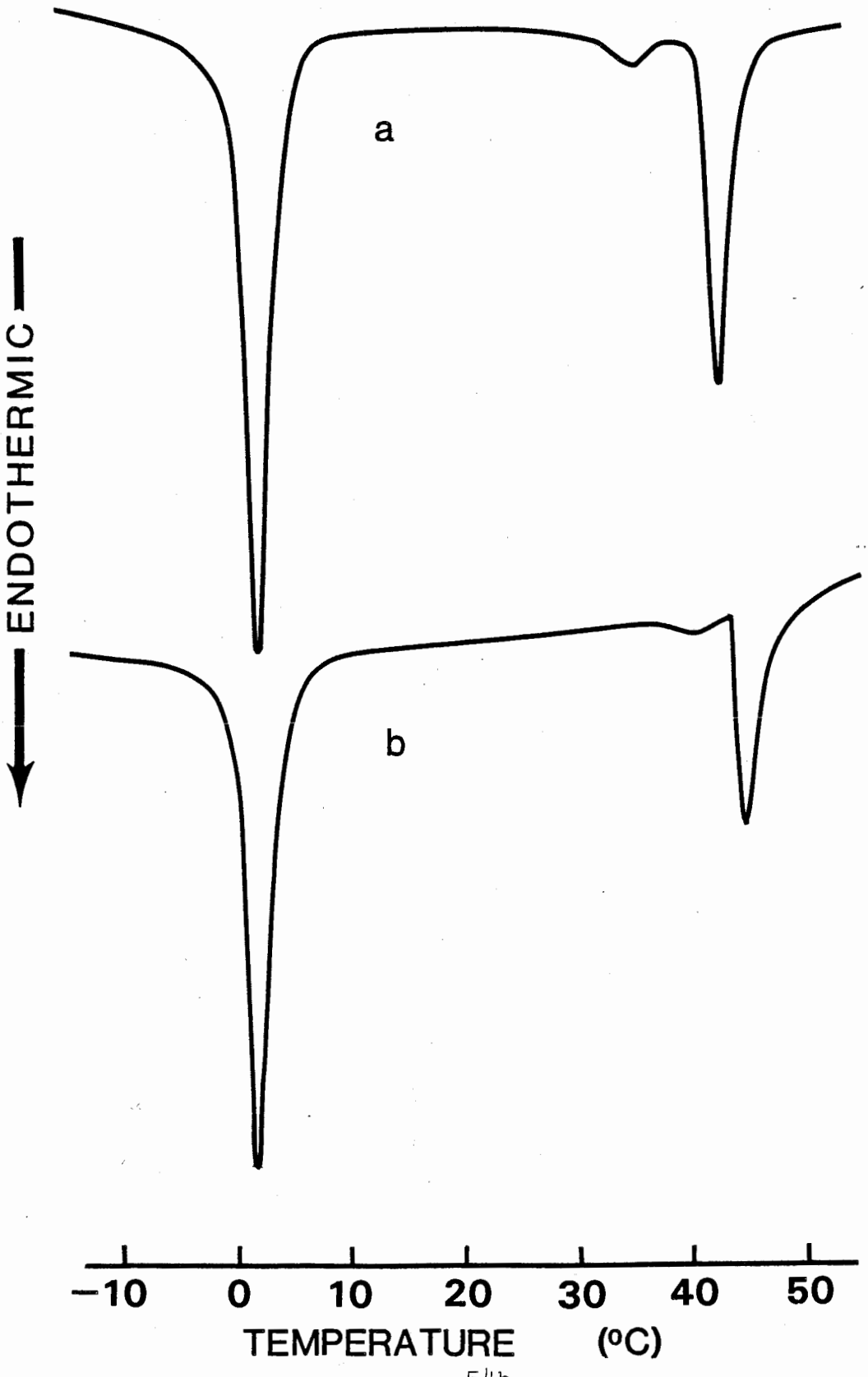
a
b
ENDOTHERMIC
−10
0
10
20
30
40
50
TEMPERATURE (°C)

The differences between Figs. 7a and 7b lie in the temperatures at which the pretransition and the main transition occur and the relative separation (in degrees) of the two endotherms, which defines the intermediate ($P_{\beta'}$) phase. The observed transition temperatures of 40°C and 31°C for PC-d_{31} are consistent with its degree of deuteration and with the presence of about 15% stearoyl chains. [$^2H_{62}$]DPPC has a main transition at 37°C and a pretransition at 30°C (Ruocco and Shipley, 1982b), due to isotope effects caused by the substitution of deuterium for hydrogen. The temperature range of the intermediate ($P_{\beta'}$) phase of PC-d_{31} is ≈9°, which is larger than the ≈7° range found for DPPC. This is consistent with the presence of *sn*-1 stearoyl chains since there is a 13°C difference between the pretransition and main transition for 1-stearoyl-2-palmitoyl-*sn*-glycero-3-phosphorylcholine (Chen and Sturtevant, 1981).

B. ^2H NMR

1. Spectral changes as a function of temperature.

The ^2H NMR spectra of PC-d_{31}/water dispersions have been measured for temperatures from -15°C to 60°C. Selected spectra are shown in Figs. 8-11. Low-temperature spectra are illustrated in Fig. 8. Referring to Fig. 8a it is apparent that there is a pair of 'edge' features at ±63 kHz, and another at ±9 kHz. The former pair corresponds to -C$^2H_2$- resonances from immobile *sn*-2 chains, since theoretically $\Delta\nu_Q(\max)$=126 kHz for

Figure 8: Low-temperature ^2H NMR spectra of a PC-d_{31}/water dispersion. Spectral parameters: pulse spacing = 75 µs; pulse length = 6.5 µs; line broadening = 50 Hz; sweep width = ±250 kHz, number of acquisitions = 1000.

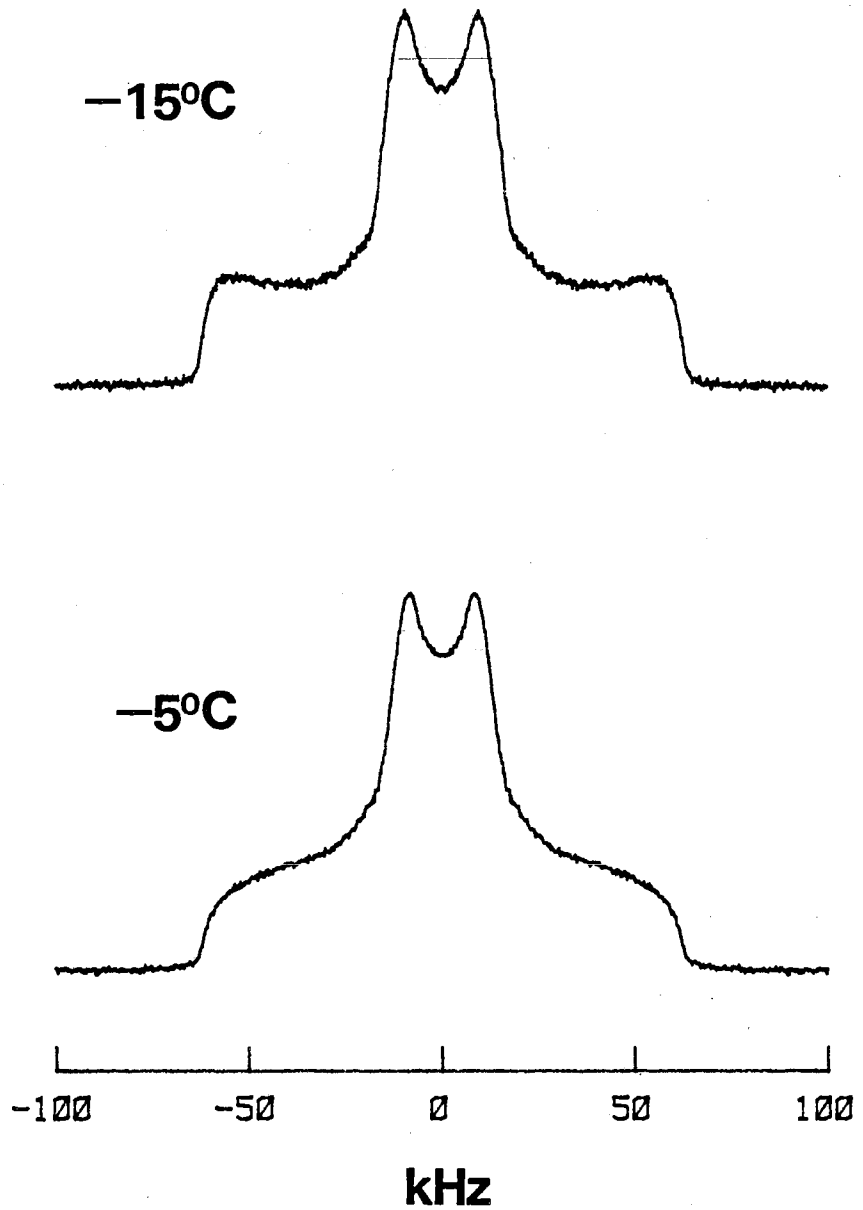
−15°C
−5°C
-100
-50
0
50
100
kHz

methylenes. Note that the shoulders at ±126 kHz are severely attenuated due to the finite pulse length. The latter pair of edges can be attributed to $-C^2H_3$ resonances. These spectra are likely those of lipid in a metastable state, however, since it has been found that an equilibration at low temperatures on the order of days was needed to convert DPPC liposomes into their low-temperature crystal phase (L_c) (Chen et al., 1980, Ruocco and Shipley, 1982a). This low temperature phase is not of primary relevance to the study of anesthetic-induced changes to the lipid bilayer and the main body of results concerns temperatures greater than 15°C. More discussion of low temperature ^2H NMR of DPPC dispersions may be found in Davis (1979).

Fig. 9 gives the temperature dependence of the ^2H NMR spectra of multilamellar dispersions of PC-d_{31} in the gel phase. Only small spectral changes are observed as the temperature is increased from 15°C to 28°C. All spectra are characterized by edges at ±63 kHz, rounded peaks at ±7 kHz and featureless sloping regions in between. These sloping regions gradually transform from nearly linear at 15°C to slightly rounded humps at 28°C. Such spectra are not simple powder patterns: they cannot be analyzed as such in terms of either zero or nonzero asymmetry parameter.

The ^2H NMR spectra of PC-d_{31} dispersions for temperatures from 30°C to 39°C are given in Fig. 10. This temperature range starts at the lipid's pretransition and goes to just below the main transition temperature, during which the lipid is in the

Figure 9: Gel phase ^2H NMR spectra of PC-d_{31}/water. Spectral parameters: pulse spacing = 75 µs; pulse length = 6.5 µs; line broadening = 50 Hz; sweep width = ±250 kHz; number of acquisitions = 1000.

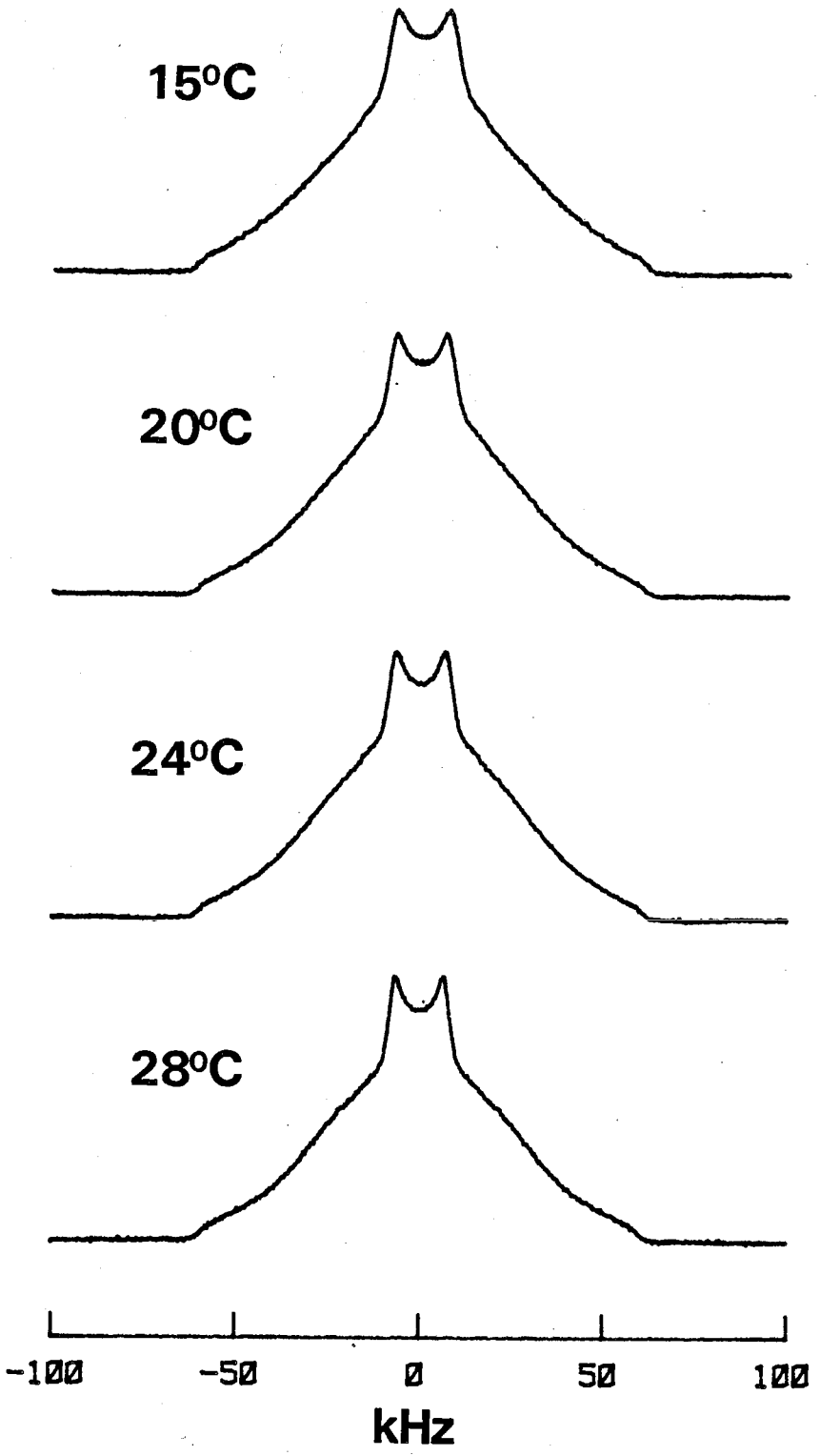
15°C
20°C
24°C
28°C
-100
-50
0
50
100
kHz

Figure 10: Intermediate phase ^2H NMR spectra of PC-d_{31}/water. Spectral parameters: pulse spacing = 75 µs; pulse length = 6.5 µs; line broadening = 50 Hz; sweep width = ±250 kHz, number of acquisitions = 1000.

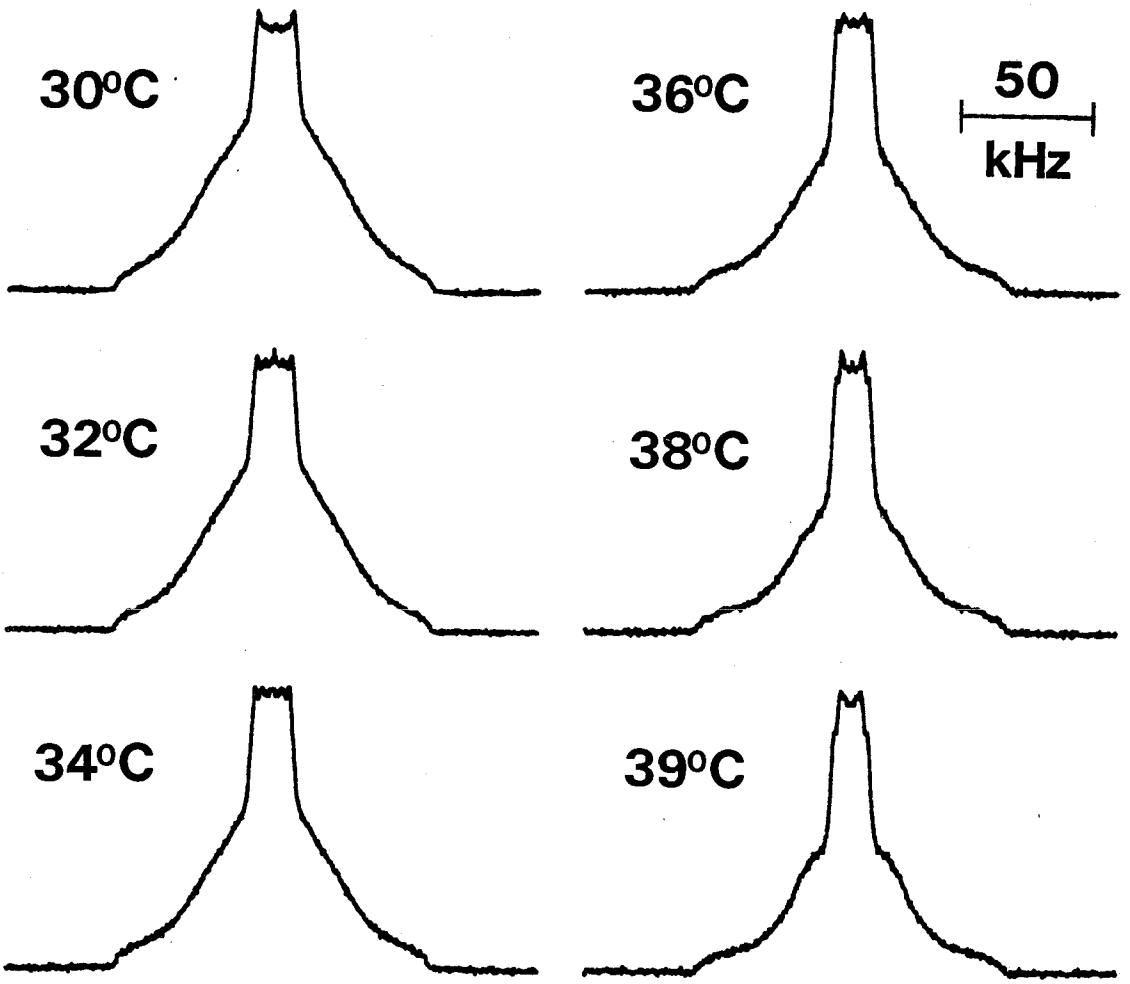
30°C
36°C
50
kHz
32°C
38°C
34°C
39°C

$P_{\beta'}$ phase. The spectra in Fig. 10 all have intensity at ±63 kHz as was seen in the gel phase as well as peaks at about ±7 kHz. The rounded humps seen at 28°C become slightly more curved as the sample is heated to 39°C. The most notable change is the growth of intensity in the central region of the spectrum. This manifests itself as first a 'filling in' of the dip between ±7 kHz, seen at 30°C (Fig. 10) compared with 28°C (Fig. 9). As the temperature is increased a second pair of peaks emerges at ±4 kHz, presumably due to the $-C^2H_3$ groups of a second population of lipid acyl chains. This second population might be small pools of lipid which are beginning to melt near their methyl groups, in the center of the bilayer. This gradual growth of a second spectral component as the temperature is increased between the pretransition and the main transition is also observed in multilamellar 1,2-dimyristoyl-*sn*-glycero-3-phosphorylcholine (DMPC) selectively deuterated at the methyl group of the *sn*-2 chain (see Fig. 6 of Meier et al., 1983). The ratio of the smaller splitting to the larger at a temperature of T_m minus 2°C is 0.64 ± 0.03 for PC-d_{31} (38°C) and 0.65 ± 0.03 for selectively deuterated DMPC (22°C). Meier et al. (1983) were able to simulate their intermediate phase spectra by introducing a second chain orientation parameter whose value was determined by extrapolation from the higher temperature liquid crystalline phase. This supports the idea of partially melted regions of phospholipid, but the authors kept speculation to a minimum and did not propose a detailed model.

Figure 11 illustrates the liquid crystalline lipid's ^2H NMR

Figure 11: Liquid crystalline phase ^2H NMR spectra of PC-d_{31}/water. Spectral parameters: pulse spacing = 75 µs; pulse length = 6.5 µs; line broadening = 50 Hz; sweep width = ±100 kHz, number of acquisitions = 1000 (41°C and 60°C), 2000 (50°C).

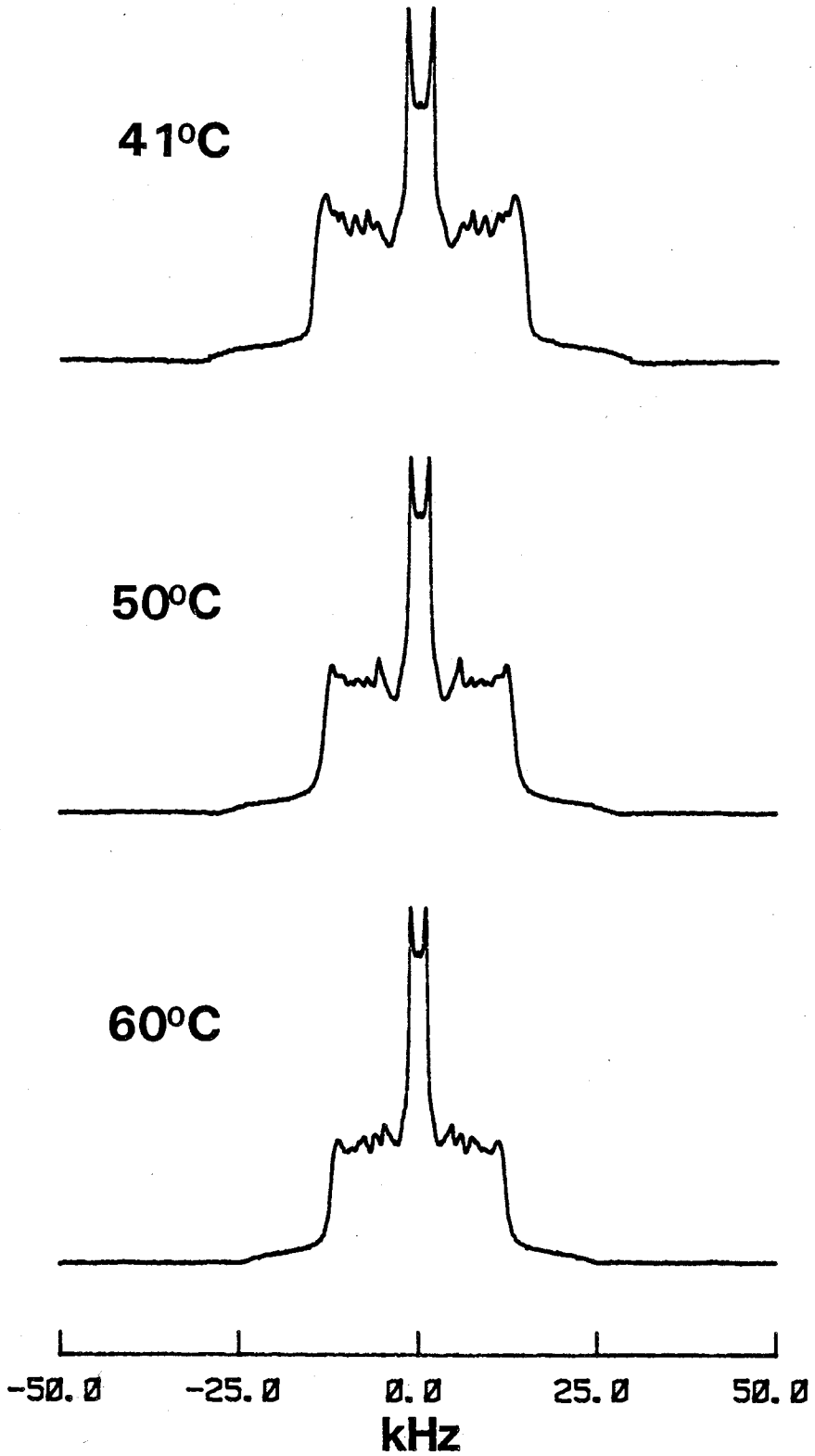
41°C
50°C
60°C
-50.0
-25.0
0.0
25.0
50.0
kHz

spectra. The main phase transition at 40°C is accompanied by a drastic narrowing and sharpening of the spectrum. There is no longer any intensity at ±63 kHz. At temperatures above 40°C only a gradual narrowing takes place. This narrowing reflects the decreasing order of the lipid acyl chains and indicates increasing thermal motion within the bilayer.

The preceding description of the changes observed in the ^2H NMR spectra of PC-d_{31} multilamellar dispersions with increasing temperature will be quantified via spectral moment and order parameter profile calculations in conjunction with the results from the PC-d_{31}/1-alkanol experiments detailed in Section II of this chapter.

2. T_{2e} as a function of temperature

The amplitude of the quadrupolar echo decays exponentially with increasing pulse spacing in the quadrupolar echo pulse sequence. The time constant of this decay, T_{2e}, is one of the most accessible relaxation times of deuterated multilamellar phospholipids.

The decay of the quadrupolar echo as a function of two times the pulse spacing is shown in Fig. 12 for PC-d_{31} at several temperatures. The first observation is that at all temperatures the semi-log plots are linear. The second observation is that, as the temperature is increased from 20°C to 37°C, just below the main phase transition, the slopes of the lines become progressively steeper. Above the phase transition the

Figure 12: Quadrupolar echo height vs. twice the pulse spacing for multilamellar dispersions of PC-d_{31} at several temperatures. (◆) 20°C; (■) 30°C; (●) 37°C; (△) 50°C.

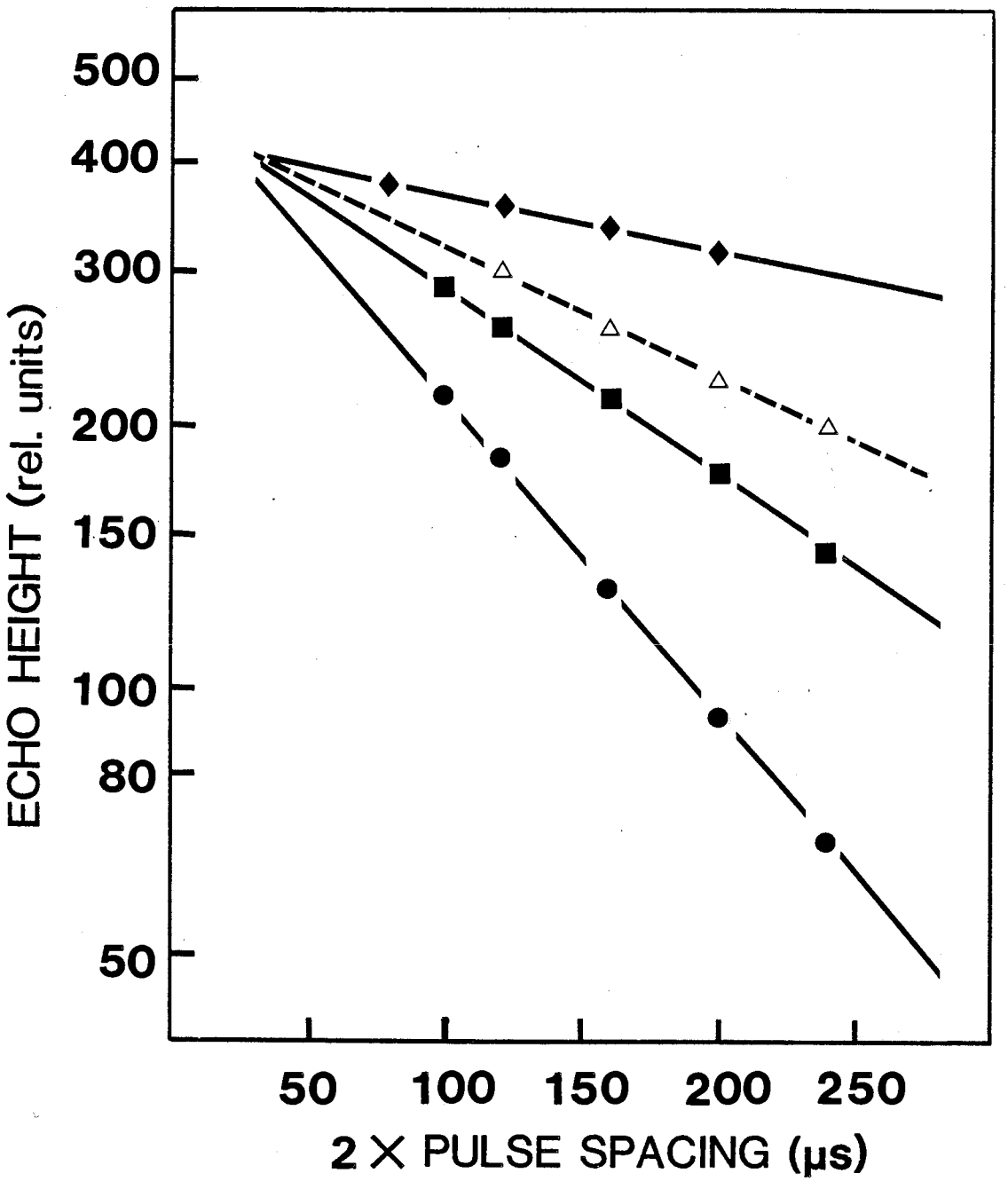
500
400
300
200
150
100
80
50
ECHO HEIGHT (rel. units)
50
100
150
200
250
2 X PULSE SPACING (μs)

slope returns to being more gradual.

The variation of T_{2e} with temperature for multilamellar dispersions of PC-d_{31} is shown in Fig. 13. The relaxation time correlates with the lipid phase as follows. In the gel phase T_{2e} decreases with increasing temperature. This decrease becomes more gradual at the pretransition temperature (31°C). In the intermediate phase T_{2e} changes only slightly, reaching a minimum of 120 μs at about 37°C. At the main phase transition T_{2e} lengthens considerably, reaching 290 ± 25 μs at 50°C.

Similar T_{2e} behaviour with increasing temperature has been observed for deuterons attached to the backbone of a synthetic protein in DPPC bilayers (Pauls et al., 1984). The T_{2e} minimum was explained as the result of the rotation of the helical protein about its long axis. The rotation was postulated to begin near the high-temperature gel phase boundary and increase in speed as the temperature was raised, reflecting the presence of more and more fluid phase lipid. At the T_{2e} minimum the rotation rate was correlated with the change in the average quadrupolar splitting due to the motion (Bloom and Smith, 1985). For temperatures above the lipid's main phase transition T_{2e} varies directly with the motional correlation time, so that faster rotation yields longer T_{2e} measurements.

It is probable that the T_{2e} minimum observed for PC-d_{31} bilayers reflects the increased rotational rate of the lipid acyl chains in the intermediate phase. Simulation of the ^2H NMR spectrum of methyl-deuterated DMPC at temperatures of 10°C (just below the pretransition) and 13°C (at the pretransition)

Figure 13: T_{2e} vs. temperature for a 50 wt % aqueous multilamellar dispersion of PC-d_{31}.

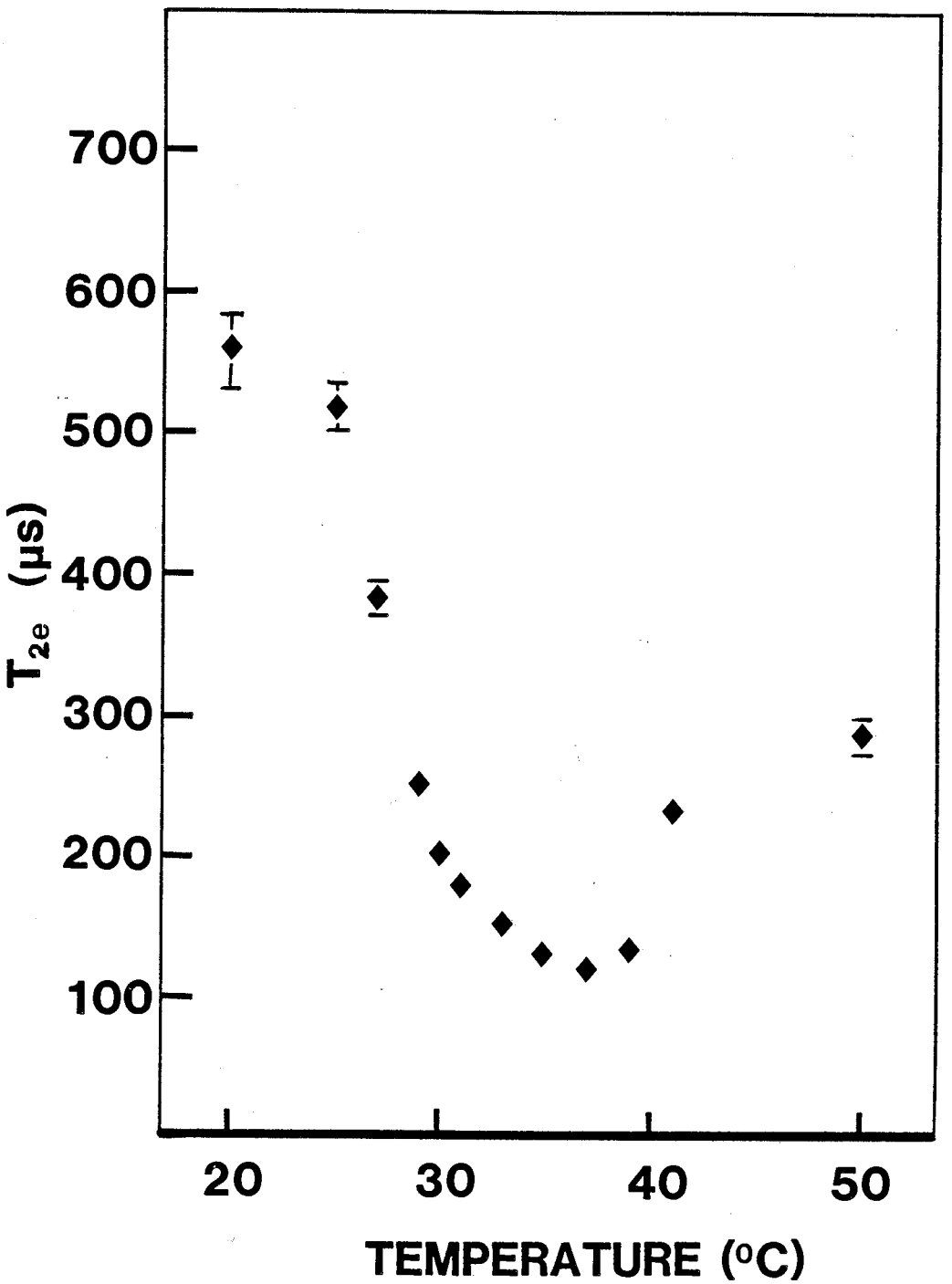
700
600
500
400
300
200
100
T_{2e} (μs)
20
30
40
50
TEMPERATURE (°C)

required an increase of nearly an order of magnitude in the rotation rate about the lipid long axis. In contrast the rate of motion perpendicular to the lipid long axis increases by only a factor of two over this temperature range and the rate of trans-gauche isomerization increases very little (Meier et al., 1983). The discussion concerning T_{2e} will be amplified in section II.B.4 of this chapter.

II. Deuterated Phosphatidylcholine + 1-Alkanol

Multilamellar dispersions (50 wt % deuterium depleted water) containing PC-d_{31} and 1-octanol or 1-decanol were prepared at 50°C. The molar ratio of phospholipid to 1-alkanol was 3:1 (eg. 25 mol % alcohol) in all cases except for the 5 mol % 1-octanol preparation discussed in Section IID. Both 1-octanol and 1-decanol have high lipid:water partition coefficients so that in a dispersion of equal weights of lipid and water the amount of alcohol in the aqueous phase is negligible (Jain et al., 1978).

A. DSC

Fig. 14 shows DSC traces for dispersions of PC-d_{31}/water, PC-d_{31}/1-decanol/water, and PC-d_{31}/1-octanol/water. Fig. 14a has already been discussed in Section I. Upon the addition of 1-decanol at a bilayer concentration of 25 mol % the DSC trace (Fig. 14b) shows that the PC-d_{31} pretransition has vanished and the main transition has been lowered (to 37°C) and broadened (half-height width ≈4°C). 1-Octanol has a greater effect than 1-decanol on the DSC profile of PC-d_{31} as Fig. 14c shows that the main transition occurs at 29°C with a half-height width of 7.5°C. The pretransition, as seen for the 1-decanol/PC-d_{31}/water system, has been eliminated.

It is interesting to compare the effects of 1-octanol and 1-decanol on the thermotropic behaviour of PC-d_{31} with the

Figure 14: Differential scanning calorimetry traces: 50 wt % aqueous multilamellar dispersions of: (a) PC-d_{31}; (b) PC-d_{31}/25 mol % 1-decanol; (c) PC-d_{31}/25 mol % 1-octanol. Scanning rate was 10°/min. over the range -30°C to +70°C.

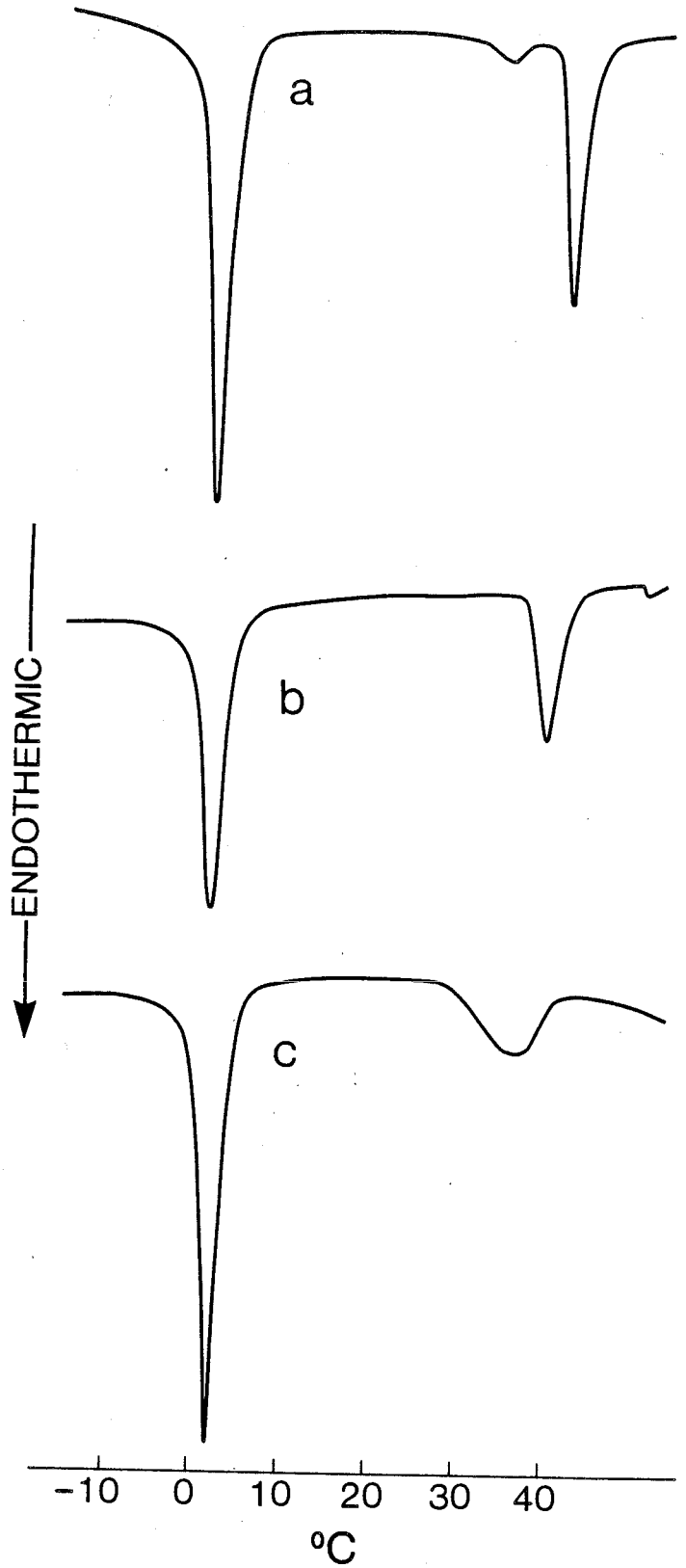
a
b
c
ENDOTHERMIC
-10
0
10
20
30
40
°C

results of Lee (1976) and Eliasz et al. (1976). Lee examined the change in chlorophyll fluorescence intensity in DPPC liposomes as a function of temperature and alcohol concentration. At a 1-octanol concentration of 25 mol % (2.3 mM) Lee observed a phase transition temperature of 31°C compared with 41°C for DPPC with no added 1-octanol. This compares well with our results of T_m = 29°C (for 25 % 1-octanol) and 40°C (for 0 % 1-octanol). For 22 mol % 1-decanol (0.13 mM) Lee observes a 3° reduction in T_m. We similarly see a reduction in T_m of 3° upon incorporation of 25 mol % 1-decanol. Eliasz et al. used DSC to determine the change in T_m of DPPC dispersions in the presence of 1-octanol and 1-decanol. A 25 mol % 1-decanol concentration caused a 4° drop in T_m, while 25 mol % 1-octanol produced a 15° drop in T_m. These are slightly larger T_m depressions than we observed.

B. ^2H NMR

1. Temperature dependence

^2H NMR spectra were measured for temperatures from -15°C to 50°C for 50 wt % aqueous multilamellar dispersions of PC-d_{31}/1-octanol, molar ratio 3:1. Fig. 15 shows representative spectra for dispersions of PC-d_{31} with and without incorporated 1-octanol. At -15°C (Figs. 15a and 15e) both samples display essentially the same spectral shape, discussed in Section IB. At 15°C (Figs. 15b and 15f) both samples produce a typical gel

Figure 15: Temperature dependence of the ^2H NMR spectra of multilamellar dispersions of: (a-d) PC-d_{31} with 25 mol % 1-octanol incorporated; (e-h) PC-d_{31} alone. Spectral parameters: pulse spacing = 75 µs; pulse length = 6.5 µs; line broadening = 50 Hz; sweep width = ±250 kHz except (d) and (h), ±100 kHz; number of acquisitions = 1000 except (d) and (h), 2000.

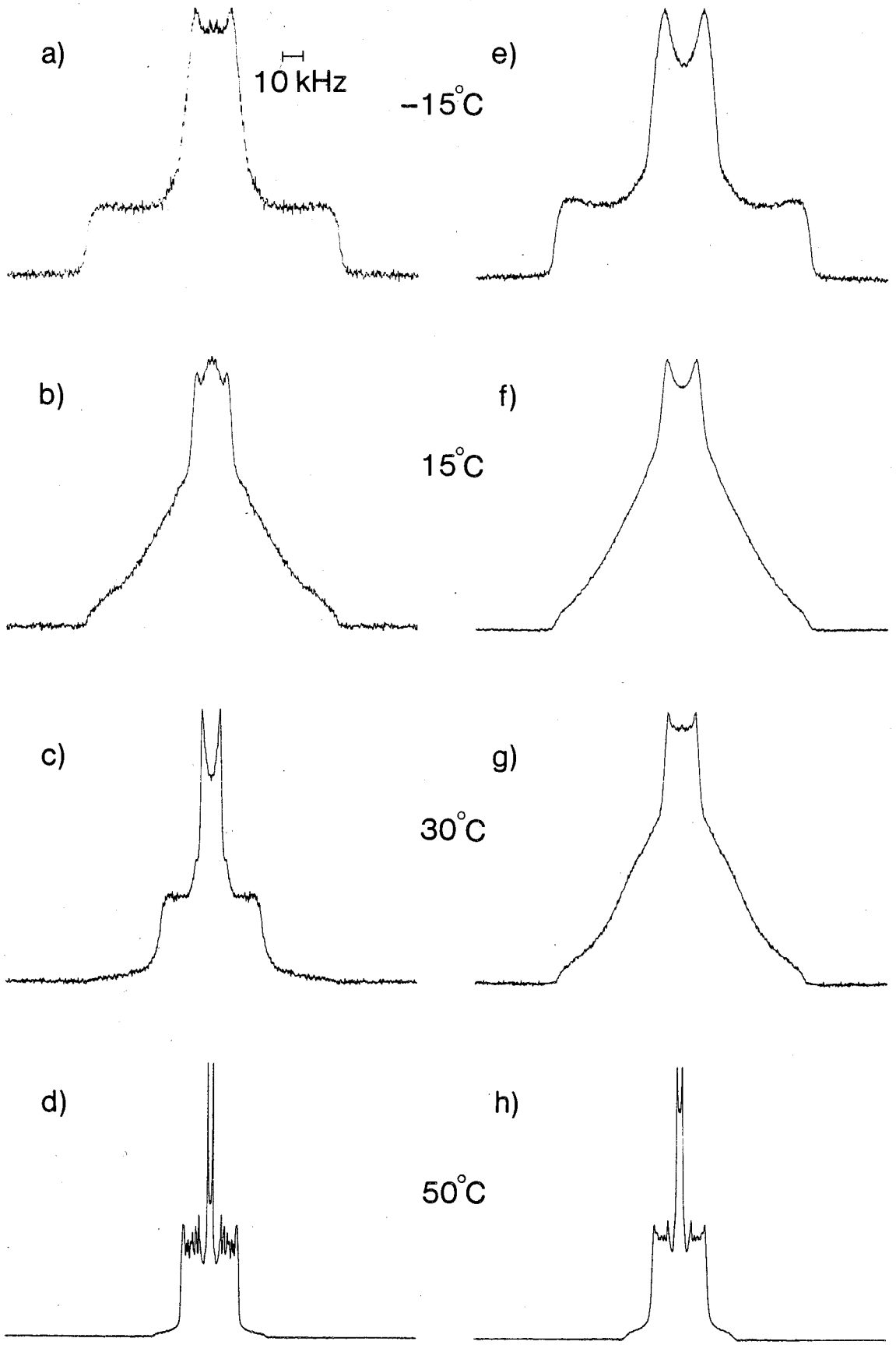
a)
10 kHz
−15°C
e)
b)
15°C
f)
c)
30°C
g)
d)
50°C
h)

phase spectrum with an absence of distinct shoulders and a broad, featureless central region. At 30°C the PC-d_{31} sample (Fig. 15g) is still in the gel phase but the 1-octanol-containing sample (Fig. 15c) is in an intermediate phase between gel and liquid crystal: the broad gel phase component has almost disappeared and sharp edges are beginning to form at ±24 kHz. When the temperature is raised to 50°C (Figs. 15d and 15h), both samples are in the liquid-crystalline phase. This phase is characterized by an axially symmetric powder pattern ^2H NMR spectrum possessing well-defined, sharp edges (at ±13-14 kHz) associated with a plateau in the variation of the C-^2H bond order parameter S_{CD} with position along the phospholipid acyl chain. The 1-octanol/PC-d_{31} sample, Fig. 15d, appears to have sharper and more numerous component peaks than Fig. 15h - a feature that is discussed in Section IIC.

The temperature variation of ^2H NMR spectra for the PC-d_{31} sample containing 25 mol % 1-decanol is qualitatively the same as the one containing 25 mol % 1-octanol except that the temperature of the gel to liquid crystalline transition occurs at a higher temperature with 1-decanol. Thus, 1-decanol/PC-d_{31}/water dispersions gave a 50°C spectrum virtually identical to Fig. 15d, and a 15°C gel phase spectrum very similar to Fig. 15b. Differences in the ^2H NMR spectra of lipid plus 1-octanol and lipid plus 1-decanol occurred only at temperatures near their respective gel to liquid crystalline phase transitions.

The behaviour of 1-octanol/PC-d_{31}/water and PC-d_{31}/water dispersions throughout the gel to liquid crystalline phase

Figure 16: Changes in ^2H NMR spectra at the main gel to liquid crystalline phase transition: (a-d) PC-d_{31}/25 mol % 1-octanol; (e-f) PC-d_{31} alone. Spectral parameters: pulse spacing = 75 µs; pulse length = 6.5 µs; line broadening = 50 Hz; sweep width = ±250 kHz, number of acquisitions = 1000.

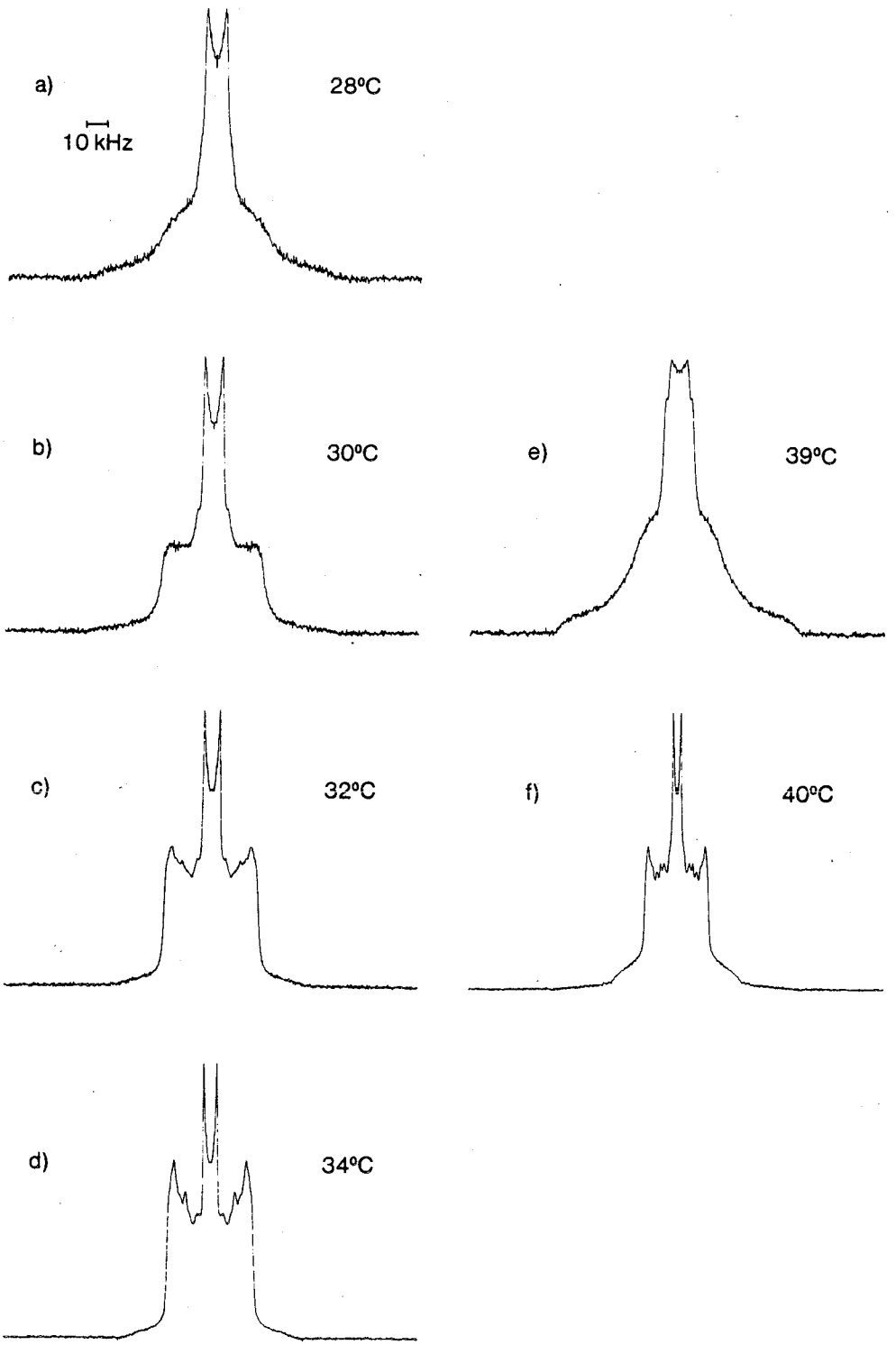
a)
28°C
10 kHz
b)
30°C
c)
32°C
d)
34°C
e)
39°C
f)
40°C

transition region, as shown by ^2H NMR, is depicted in Fig. 16. Figs. 16a to 16d show the spectra at 2-degree intervals through the main transition of the 1-octanol/PC-d_{31}/water dispersion. The spectral changes are much more gradual than those shown in Figs. 16e and 16f, which occur in the absence of 1-octanol. The phase transition region of a multilamellar dispersion of 1-decanol/PC-d_{31}/water is illustrated in Fig. 17. ^2H NMR spectra at 35°, 36° and 37°C indicate that the gel to liquid crystalline transition occurs over a narrower temperature range than in the 1-octanol/PC-d_{31}/water dispersion (Fig. 16).

The transition behaviour of the ^2H NMR spectra in the vicinity of the gel to liquid crystalline phase change can be examined more clearly using spectral moments, which quantify the spectral narrowing that occurs as the temperature is raised. Fig. 18 shows the variation of the first moment M_1 with temperature for PC-d_{31}/water, 25 mol % 1-octanol/PC-d_{31}/water and 25 mol % 1-decanol/PC-d_{31}/water. The uncertainty in the M_1 measurements is small except at the phase transition. Here the first moment depends on the time τ between the two 90° pulses of the quadrupolar echo pulse sequence. This is discussed in Section IIE. The values plotted were obtained by visually extrapolating M_1 back to zero pulse spacing τ of M_1 recorded as a function of τ. Five τ values in the range 40-125 μs were generally employed and an uncertainty of not more than 5 % was introduced by this extrapolation.

From Fig. 18 it can be seen that the first moment decreases sharply as the temperature increases through the main gel to

Figure 17: Changes in ^2H NMR spectra at the main gel to liquid crystalline phase transition for PC-d_{31}/25 mol % 1-decanol. Spectral parameters: pulse spacing = 75 µs; pulse width = 6.5 µs; line broadening = 50 Hz; sweep width = ±250 kHz, number of acquisitions = 1000.

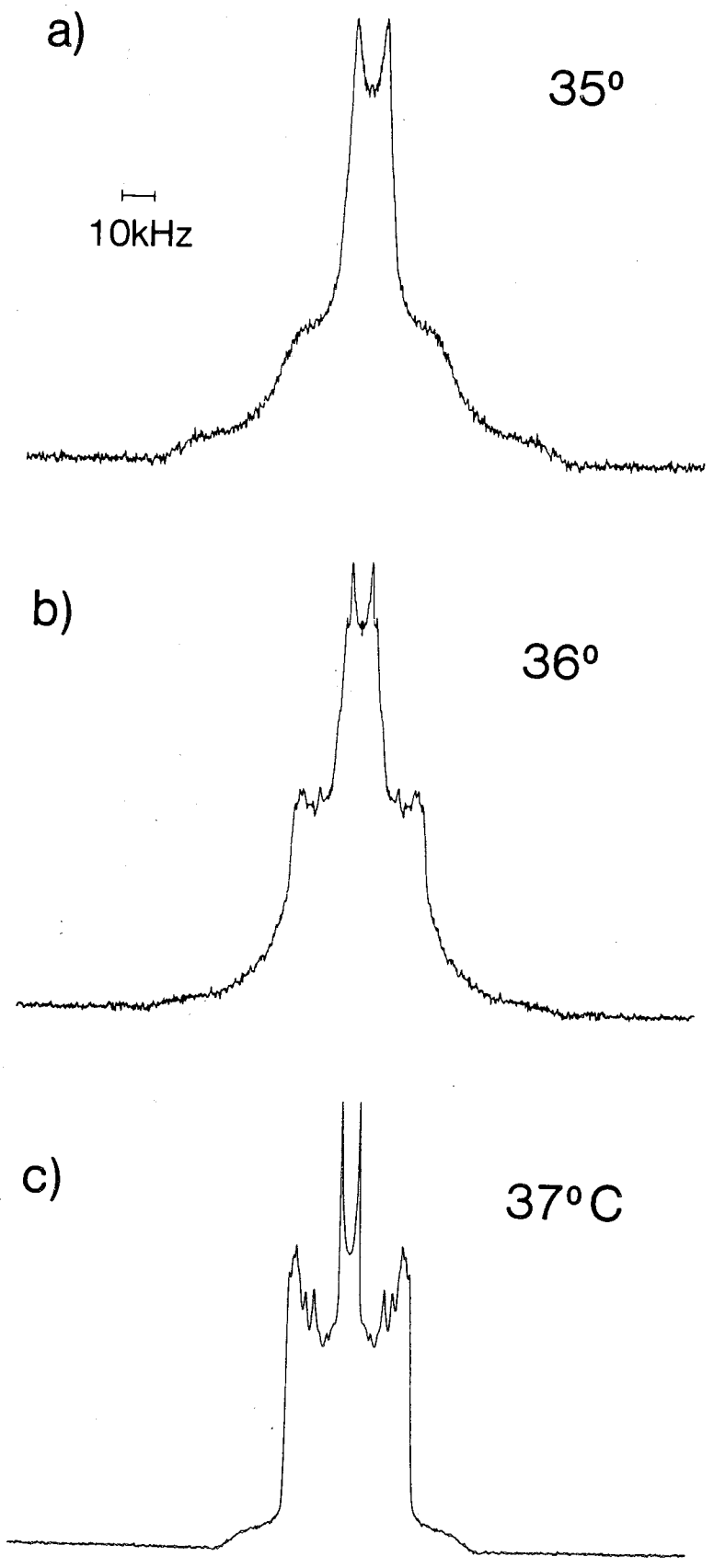
a)
35°
10kHz
b)
36°
c)
37°C

Figure 18: Variation of the first moment M_1 with temperature of 50 wt % aqueous multilamellar dispersions of: (●) PC-d_{31}; (○) PC-d_{31}/25 mol % 1-octanol; (△) PC-d_{31}/25 mol % 1-decanol. The uncertainty in temperature is estimated at ±0.5°C.

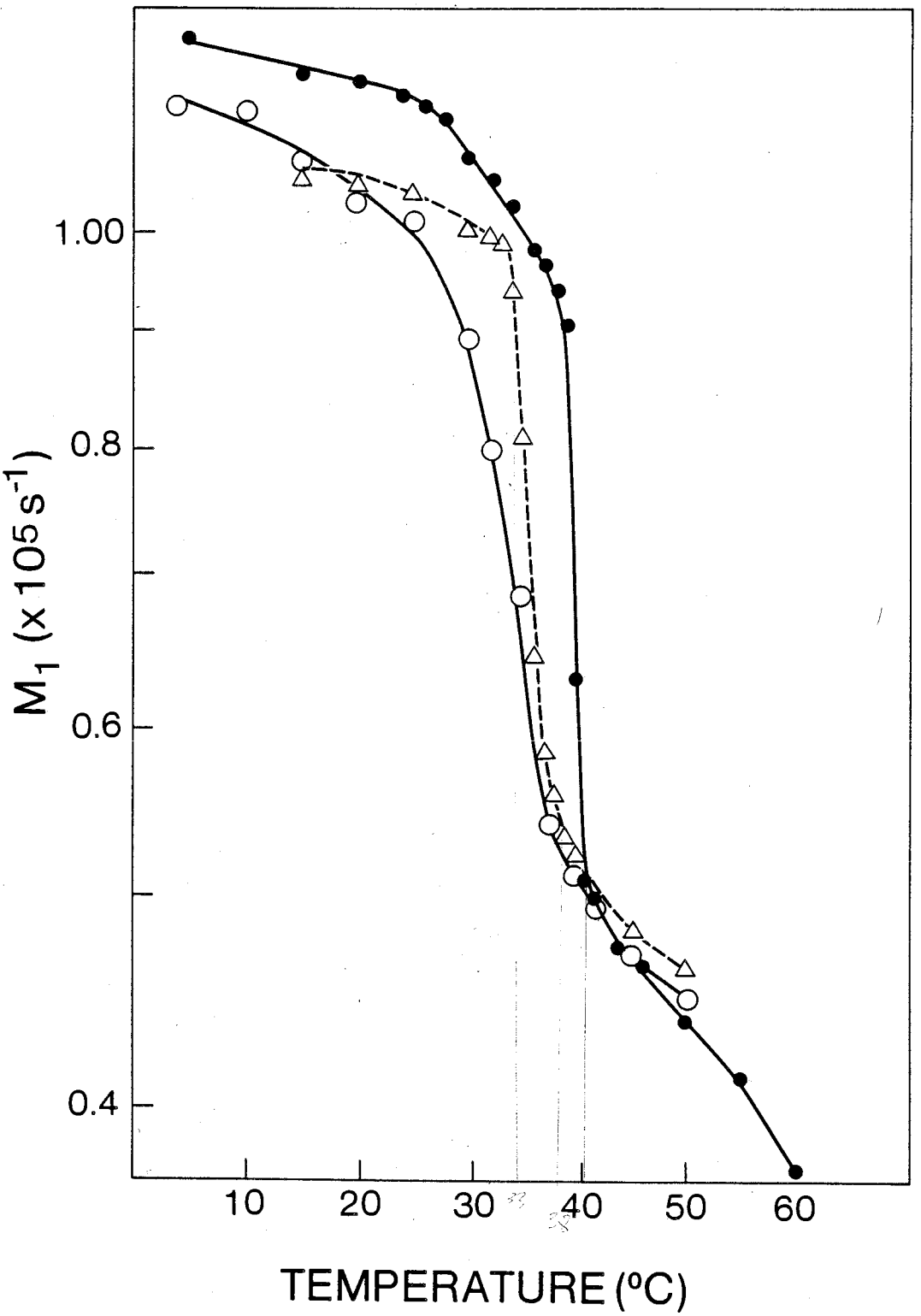
1.00
0.8
0.6
0.4
M_1 (x 105 s^{-1})
10
20
30
40
50
60
TEMPERATURE (°C)

liquid crystalline phase transition. For PC-d_{31}/water this melt occurs abruptly at 40°C, immediately preceded by a region, centered at 32°C, of more gradual decrease which we associate with the pretransition. For 1-octanol/PC-d_{31}/water a broad transition centered at 33°C on the M_1 vs. temperature plot is observed. The onset of the transition occurs at ≈28°C and it spans about 10°C. The 1-decanol-containing lipid dispersion has a narrower transition (Fig. 18) from ≈34°C to ≈39°C. The main phase transition onset temperatures determined by NMR are generally 1-3° lower than the melting points determined by DSC. The onset temperatures determined by NMR correspond more closely with the temperature at which the DSC signal first deviates from the baseline as the sample is heated through the endotherm.

The differential effects of 1-octanol and 1-decanol on the main phase transition temperature of PC-d_{31} are due to their respective chain lengths. 1-Octanol disrupts the gel-phase lipid's packing to a greater extent than 1-decanol due to the greater difference in acyl chain length between 1-octanol and PC-d_{31} (≈8 carbons) than between 1-decanol and PC-d_{31} (≈6 carbons). This has been discussed in the literature (Pringle et al., 1981). The abolition of the pretransition of PC-d_{31} by 1-octanol and 1-decanol is likely due to the changed gel phase packing of the lipid acyl chains in the presence of the alkanol. Tardieu et al. (1973) observed that the $L_{\beta'}$ and $P_{\beta'}$ phases of DMPC and DPPC could be transformed into an L_{β} phase by adding 7 % decane. The L_{β} phase, with no lipid acyl chain tilt, and hence a thicker hydrocarbon region than $L_{\beta'}$ or $P_{\beta'}$, is possibly

also induced by 1-alkanols.

2. Order parameters

The liquid crystalline ^2H NMR spectra observed for PC-d_{31} and PC-d_{31}/1-alkanol dispersions above the main transition temperature can be analyzed to give information about the molecular order along the entire lipid acyl chain. To compare the order parameters of the three systems PC-d_{31}, PC-d_{31}/1-octanol and PC-d_{31}/1-decanol a temperature of 50°C was chosen. This temperature is about ten degrees above the temperature at which the main phase transition is complete in all three cases as observed from the M_1 vs. temperature plot (Fig. 18). Using the depaking technique (Sternin et al., 1983), oriented spectra can be derived from the powder pattern spectra, enhancing the resolution of the quadrupolar splittings.

Fig. 19a and 19b contain the depaked spectra of 50 wt % aqueous multilamellar dispersions of PC-d_{31} and of 75 mol % PC-d_{31}/25 mol % 1-octanol, at 50°C. (The powder pattern spectra from which these depaked spectra were calculated are shown in Fig. 15d and 15h.)

Looking first at Fig. 19a, five well-defined quadrupole doublets, plus one pair of broad, composite outer peaks can be identified. Assignment of the various positions of the *sn*-2 [$^2H_{31}$]palmitoyl segments to the spectra in Fig. 19a is based on the work of Pauls et al. (1983) wherein it was assumed that, with the exception of the 2-position deuterons, the quadrupolar

Figure 19: The depaked ^{2}H NMR spectra at 50°C of 50 wt % aqueous multilamellar dispersions of: (a) PC-d_{31}; (b) PC-d_{31}/25 mol % 1-octanol. Digits on peaks indicate the number of deuterons assigned to each. Six iterations were performed on the powder pattern data for both (a) and (b).

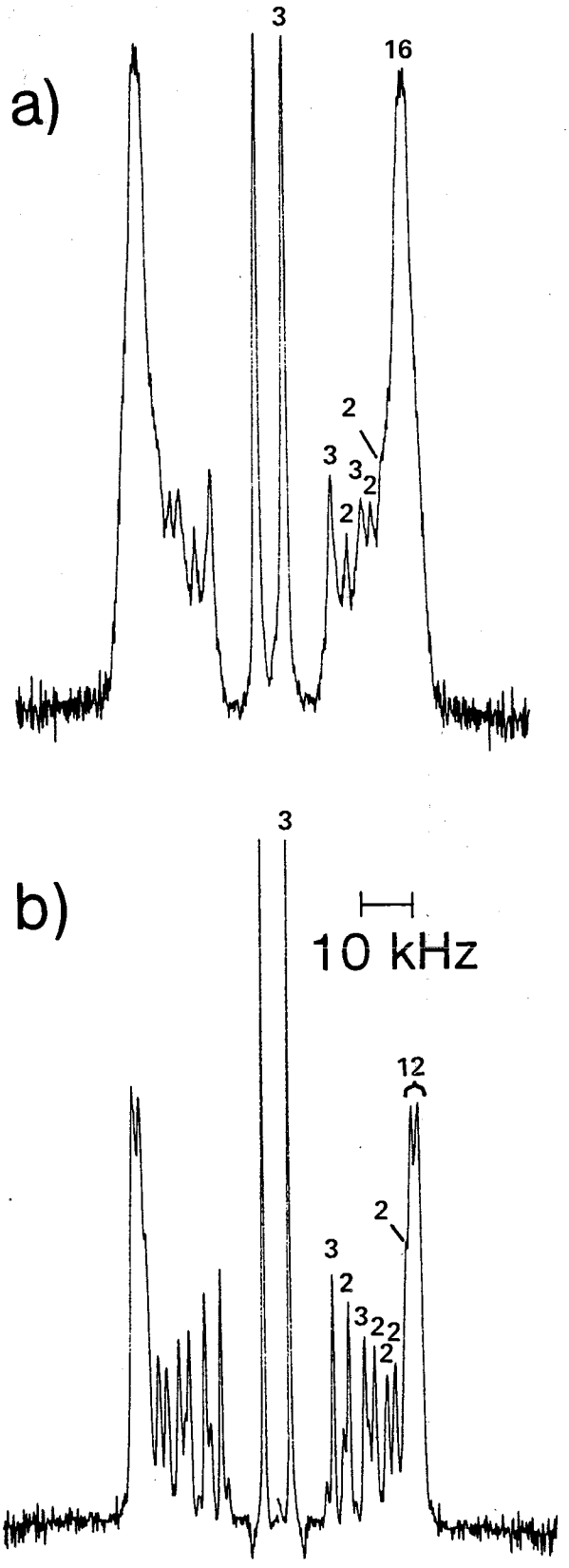
a)
3
16
2
3
3
2
2
b)
3
10 kHz
12
2
3
2
3
2
2
2

splittings decrease monotonically towards the C^2H_3 segment. Assignments of the resonances from the C-2 deuterons were based on results with ≈5 mol % 1-palmitoyl(stearoyl)-2-[2,2-$^2H_2$]palmitoyl-*sn*-glycero-3-phosphorylcholine (PC-d_2) in dispersions of either egg yolk phosphatidylcholine (egg PC) (25°C) (Parmar, 1985) or DPPC (48°C) (Y.I. Parmar, S.R. Wassall and R.J. Cushley, unpublished results). Table II lists the peak assignments and quadrupolar splittings ($\Delta\nu_Q$) associated with Fig. 19a, and also lists literature values for similar lipid systems for comparison purposes. Care must be exercised when comparing different lipid systems: the temperature of the gel to liquid crystalline phase transition must be taken into account. Therefore PC-d_{31} at 50°C would be expected to correspond closely with selectively deuterated DPPC at 52°C and with [$^2H_{62}$]DPPC at 47°C, all ten degrees above their respective T_m's. In Table II, then, the literature values listed for labelled DPPC should be slightly higher than those for PC-d_{31}. In general our data correspond to within 10% with published results. There is some discrepancy in the assignment of one of the C-2 deuteron resonances ($\Delta\nu_Q$=17.84 kHz), but those values still agree to within 20%.

Comparison of PC-d_{31} and PC-d_x (selectively deuterated at palmitoyl *sn*-2 chain position x) in egg PC is more difficult since egg PC has a rather broad phase transition at around -5°C. However, the splittings obtained for deuterons on C-4, C-7, C-11, C-12, and C-16 in both systems agree to within 10%.

Shifting attention to Fig. 19b, one observes seven pairs of

TABLE II: ^2H NMR quadrupolar splitting vs. acyl chain position for PC-d_{31} dispersions at 50°C. Literature values for comparable lipid systems are also shown.

Acyl Chain Position	$\Delta\nu_Q$ (kHz)				
	PC-d_{31} 50°C	DPPC[a] 50°C	[$^2H_{62}$]DPPC[b] 45°C	PC-d_x[c] in DPPC 48°C	PC-d_x[d] in EYL 25°C
C-2	11.75 17.84	12.0 19.2	11.7 21.8	12.2 16.9	11.6 17.9
C-3	26.03	23.2	25.2		
C-4	26.03	27.2	25.2		27.5
C-5	26.03	26.2	25.2		
C-6	26.03		25.2		
C-7	26.03		25.2	27.6	28.7
C-8	26.03		25.2		
C-9	26.03	24.2	24.3		
C-10	26.03	22.9	23.3		
C-11	22.03		22.1	22.9	22.7
C-12	19.59	18.3	20.2	21.2	20.3
C-13	17.84		18.3		
C-14	14.92	14.9	16.1		
C-15	11.75	11.1	12.6		
C-16	2.73		3.8	3.04	2.65

[a] Seelig and Seelig (1974). The DPPC was selectively deuterated in both chains. Values for the *sn*-2 chain are listed.

[b] Pauls et al. (1983, calculated from Fig. 10a).

[c] Parmar, Y.I., Wassall, S.R. and Cushley, R.J., unpublished results. PC-d_x is analogous to PC-d_{31} except that the *sn*-2 chain is selectively deuterated. x=2 except for the 11,12 position, where x=4, and the 16 position, where x=3.

[d] Parmar (1985).

TABLE III: Quadrupolar splittings ($\Delta\nu_Q$) for segments of aqueous dispersions of PC-d_{31} + 1-alkanol anesthetics (25 mol %) at 50°C.

Acyl Chain Position	$\Delta\nu_Q$ (kHz)[a]			
	PC-d_{31}	PC-d_{31}/1-octanol	PC-d_{31}/1-decanol Run I	PC-d_{31}/1-decanol Run II
C-2	11.75 17.84	10.95 17.21	11.11 17.43	11.62 18.20
C-3 to 8	26.03[b]	27.97[c] 26.63	26.83[c] 25.68	27.98[c] 26.73
C-9	26.03[b]	25.52	24.92	26.29
C-10	26.03[b]	23.25	22.94	24.05
C-11	22.03	21.59	21.59	22.49
C-12	19.59	19.24	19.43	20.28
C-13	17.84	17.21	17.43	18.20
C-14	14.92	14.13	14.30	15.03
C-15	11.75	10.95	11.11	11.62
C-16	2.73	2.54	2.54	2.77

[a] Quadrupole powder pattern splittings are reported (i.e. one-half of the depaked spectrum's splittings) to conform to common usage.

[b] These values are accurate to ±9%.

[c] These values are accurate to ±6%.

well resolved quadrupole peaks, plus one pair of composite peaks with two distinguishable splittings. Table III lists the peak assignments and quadrupolar splittings ($\Delta\nu_Q$) associated with Fig. 19. Included in Table III are the results of experiments run with two different PC-d_{31}/1-decanol/water samples. The differences in the $\Delta\nu_Q$ values for the two PC-d_{31}/1-decanol samples indicate the reproducibility of the technique. In all of the depaked spectra of alcohol-containing dispersions of PC-d_{31} the C-15 and C-14 doublets have shoulders of smaller splittings, $\Delta\nu_Q \approx 9.7 \pm 0.3$ and $\approx 12.7 \pm 0.15$ kHz, respectively (See Fig. 19b). These peaks result from a small amount of acyl chain migration during preparation of the PC-d_{31}. The splittings of the shoulders correspond very closely to values reported by Paddy et al. (1985) for deuterons at C-15 ($\Delta\nu_Q \approx 9.7$ kHz) and C-14 ($\Delta\nu_Q \approx 13.2$ kHz) of 1-[$^2H_{31}$]palmitoyl-2-palmitoyl-*sn*-glycero-3-phosphorylcholine.

The profiles of order parameter S_{CD} vs. acyl chain position for PC-d_{31}/water, PC-d_{31}/water/1-octanol (25 mol %) and PC-d_{31}/water/1-decanol (25 mol %) are shown in Fig. 20. The order parameter for C-10 of PC-d_{31}/water does not appear to fit the profile very well. From Fig. 19a one can see that, even in the depaked spectrum, the C-10 resonance is not resolved from the broad 'plateau' peak. The splittings in the plateau region do not necessarily correspond to the mean splitting (Table III) but lie within the error bar in Figure 20 which is determined by the width at half height of the composite peak in Figure 19a. Upon addition of 1-octanol or 1-decanol resolution is sufficiently

Figure 20: Order parameter profiles at 50°C: S_{CD} vs. position along the phospholipid *sn*-2 chain. (●) PC-d_{31}; (○) PC-d_{31}/25 mol % 1-octanol; (△) PC-d_{31}/25 mol % 1-decanol (average of two determinations). The order parameters for C-2 to C-9 of PC-d_{31} are indicated by an average value (bar).

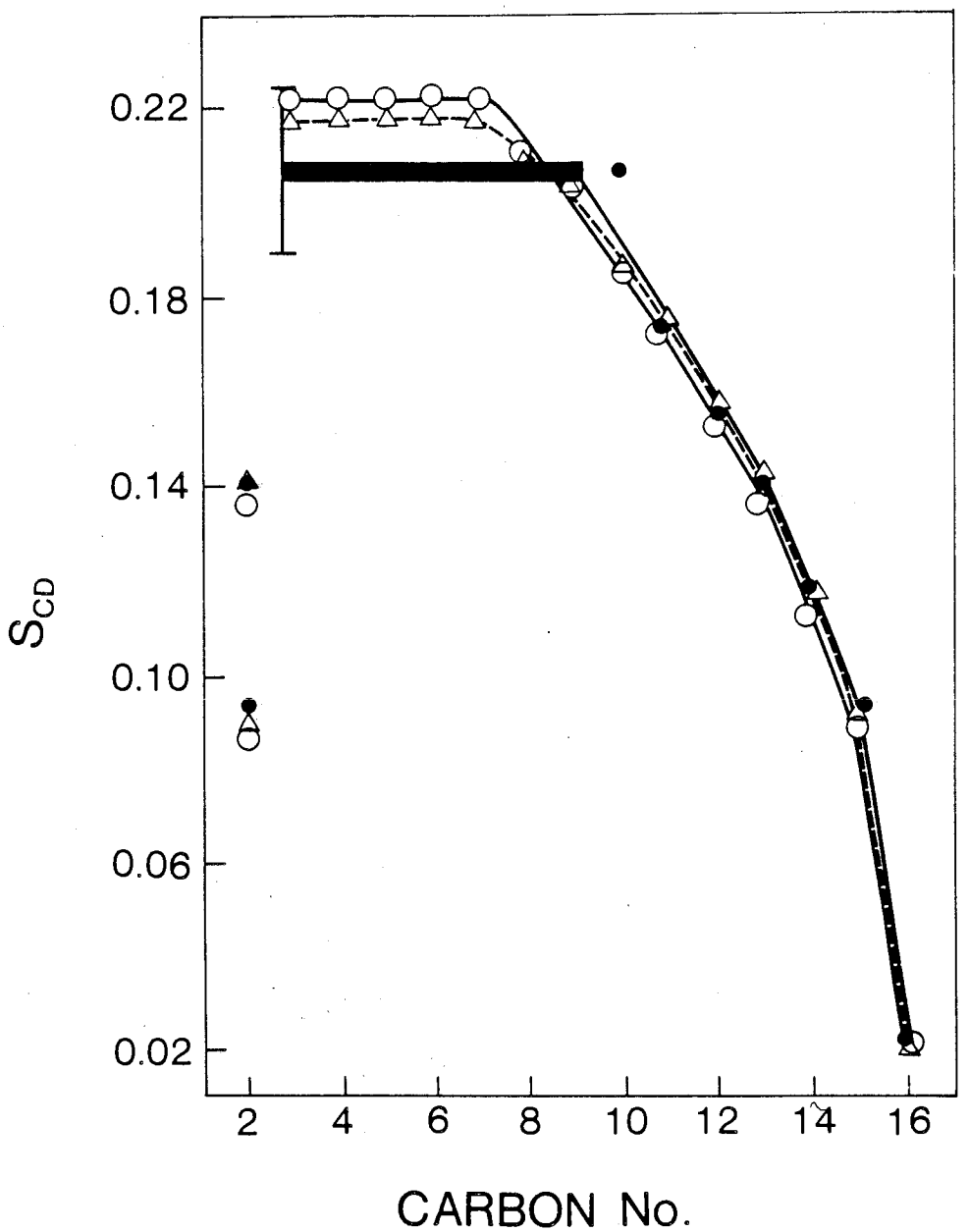
0.22
0.18
0.14
0.10
0.06
0.02
S_{CD}
2
4
6
8
10
12
14
16
CARBON No.

enhanced in the depaked ^2H NMR spectrum that the C-10 position becomes resolved and a slightly narrower splitting than the average 'plateau' value, leading to a smaller S_{CD} value for C-10, can be assigned. The enhanced resolution upon 1-alkanol addition is a result of the narrowing of the spectral lines. This is discussed in Section IIE.

The order parameter profile of PC-d_{31}/water is not significantly changed by the presence of 25 mol % 1-octanol or 1-decanol. The first moments (which are directly proportional to the average S_{CD} (Davis, 1983) for all three systems at 50°C are 0.455 x 10^5 s^{-1} ± 3% (see Fig. 18). Apparent differences in the plateau regions of the order parameter profiles (Fig. rd14) are the result of the enhanced resolution of peaks in the spectra of the alcohol-containing samples. This enhancement causes the length of the plateau to be reduced (due to the increased number of resolved peaks) and the order of the plateau region to increase (since splittings may be associated with previously unresolved outer peaks rather than with an average value). After this work was completed a paper appeared reporting preliminary results of 1-octanol incorporated into a related phospholipid, [$^2H_{54}$]DMPC (Pope et al., 1984). These workers also observed a small increase in order for the first few segments of the pohospholipid acyl chains when 1-octanol was present.

The lack of effect that 1-octanol and 1-decanol (25 mol %) have on the amplitude of lipid acyl chain motions as reflected in S_{CD} is in agreement with the results of a recent paper

(Jacobs and White, 1984) which concluded that hexane (26 mol %) dissolved in [$^2H_{54}$]DMPC did not change the lipid acyl chain order as determined by ^2H NMR.

Incorporation of 20 mol % palmitic acid into [$^2H_{62}$]DPPC bilayers has similarly been found to have only a small (≈10%) effect upon order within the membrane (Pauls et al., 1983) when the systems are compared at 51°C. It is probable that the ordering effect of palmitic acid on DPPC bilayers above the phase transition is related to palmitic acid's effect on the transition temperature. The pure DPPC bilayers are completely melted at a temperature ten degrees less than the DPPC/palmitic acid bilayers. When the order of the DPPC plateau region at 51°C (S_{CD} = 0.19) is compared with the order of the DPPC/palmitic acid plateau region at 61°C (S_{CD} = 0.20) the difference is only 5 %.

3. Concentration dependence

Aqueous multilamellar dispersions of PC-d_{31}/1-octanol at a molar ratio of 19:1 (e.g. 5 mol % 1-octanol) were studied to determine the effect of a lower concentration of anesthetic alcohol on the ^2H NMR spectrum of PC-d_{31}. The phase behaviour of DPPC/1-octanol dispersions has been studied for various 1-octanol concentrations (Eliasz et al., 1976), and the amount by which the phase transition temperature is lowered increases linearly with alcohol concentration to a mole ratio of 1-octanol:DPPC of 0.29, which corresponds to 22 mol % 1-octanol.

Figure 21: The temperature dependence of the ^2H NMR spectrum of PC-d_{31}/5 mol % 1-octanol aqueous multilamellar dispersions. Spectral parameters: pulse spacing = 75 µs; pulse length = 6.5 µs; line broadening = 50 Hz; sweep width = ±250 kHz (15°C to 35°C) or ±100 kHz (36°C to 50°C); number of aquisitions = 1000 except 4000 at 32°C and 8000 at 50°C.

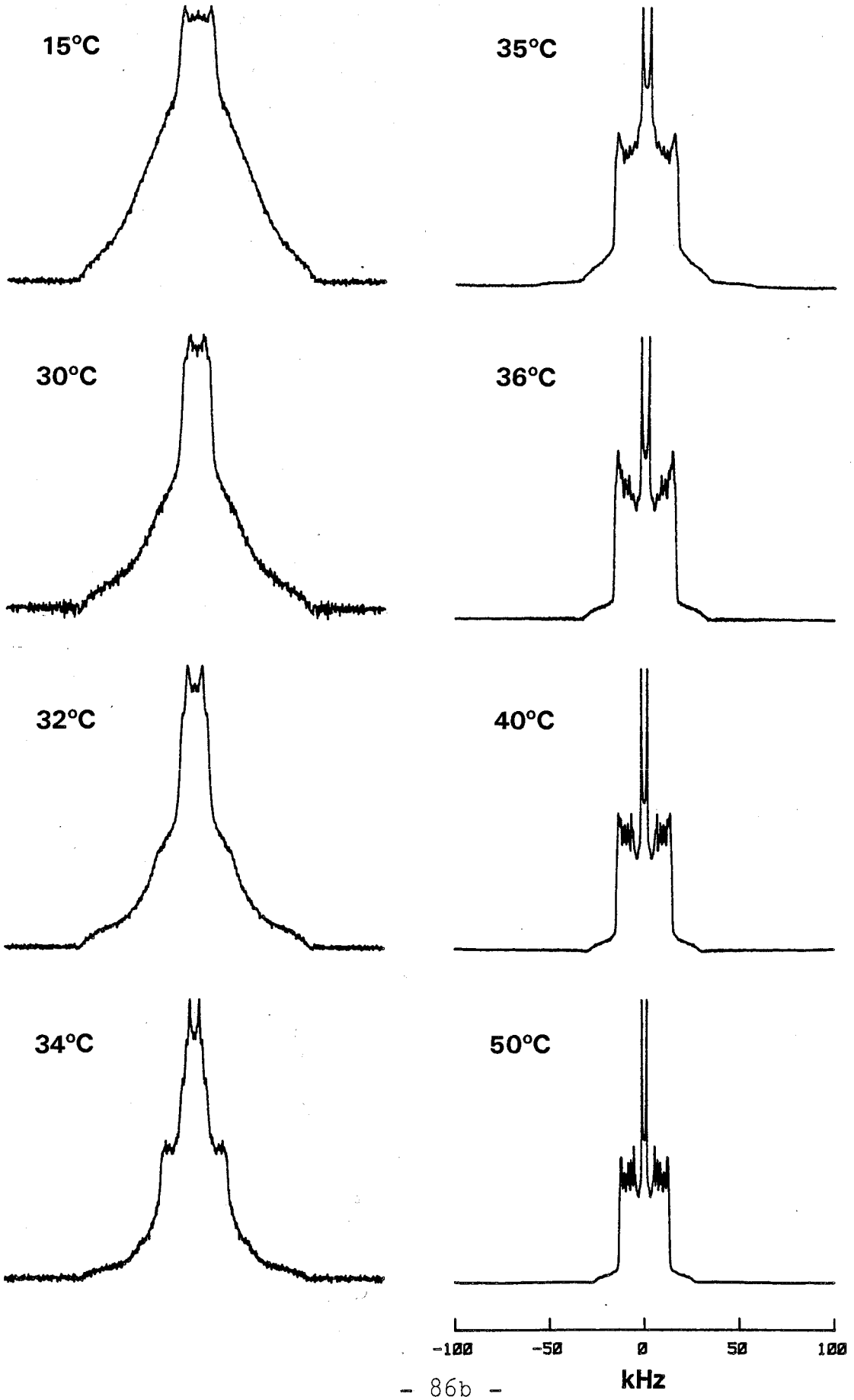
15°C
35°C
30°C
36°C
32°C
40°C
34°C
50°C
-100
-50
0
50
100
kHz

The temperature dependence of the ^2H NMR spectrum of PC-d_{31}/5 mol % 1-octanol is given in Fig. 21 for the range 15°C to 50°C. These spectra may be compared with those in Figs. 15 and 16 for PC-d_{31} multilayers containing 25 mol % 1-octanol. The 15°C (gel phase) spectrum in Fig. 21 corresponds well with Fig. 15 except that the hump spanning ≈ ±5 kHz around ν_o in Fig. 15b is more prominent. This feature appears to be related to the 1-octanol concentration as it is absent in pure PC-d_{31} dispersions. It is probably due to 1-octanol affecting neighbouring lipid acyl chains by lowering the microviscosity of their local environment. The 34°C spectrum in Fig. 21 corresponds roughly to the 30°C spectrum (Fig. 15c) at the higher alcohol concentration. The 50°C spectra in Figs. 21 and 15d are essentially the same. The spectra in the region of the phase transition (32°C - 36°C) of PC-d_{31}/5 mol % 1-octanol compare more closely with those in Fig. 17, for PC-d_{31}/25 mol % 1-decanol, than with those for PC-d_{31}/25 mol % 1-octanol. This is to be expected given the nature of the phase transition effect of the two 1-alkanols upon phospholipid bilayers.

4. Relaxation measurements

When the spectra for PC-d_{31}/1-alkanol aqueous multilamellar dispersions are recorded as a function of temperature with constant pulse spacing, the signal-to-noise ratio decreases markedly for temperatures just below and at the onset of the phase transition. See, for example, Fig. 16a-d, where the

signal-to-noise improves as the sample is heated through the phase transition. When the first moment is calculated for these spectra, an anomalous constant value of M_1 was found for T=31° to 34°C (midway through the phase transition) and a pulse spacing of 75 μs. This prompted a closer investigation of spectra in this region, and it was discovered that the spectral shape (and hence M_1) depended markedly on the pulse spacing for these temperatures. The variation of M_1 with pulse spacing is shown in Fig. 22 for PC-d_{31}/5 mol % 1-octanol, for those temperatures where this variation is significant. As stated in Section IIB, M_1 vs. temperature plots use the M_1 values determined from extrapolation to zero pulse spacing.

Fig. 23 illustrates the dependence of spectral shape on pulse spacing for PC-d_{31}/5 mol % 1-octanol at 32°C. The spectral region between about 10 and 50 kHz away from the Larmor frequency decays more rapidly than the other regions, causing M_1 to become smaller. There are several possible reasons for this. One is that the spectrum is composed of two superimposed spectra: one from PC-d_{31} in microdomains of melted lipid and one from PC-d_{31} still in the gel state, each with characteristic decay rates. A second reason is that since our phosphatidylcholine is perdeuterated, there may be a dependence of decay rate on acyl chain position, as seen with [$^2H_{62}$]DPPC in the liquid crystalline state (Pauls et al., 1983). The methyl decay rate is much slower than the methylene decay rate. A third reason is that there may be an orientation-dependence to the decay rate, so that microscopic crystallites whose director

Figure 22: Variation of M_1 with pulse spacing for those temperatures (indicated beside each curve in °C) where this variation is appreciable. Sample: PC-d_{31}/5 mol % 1-octanol.

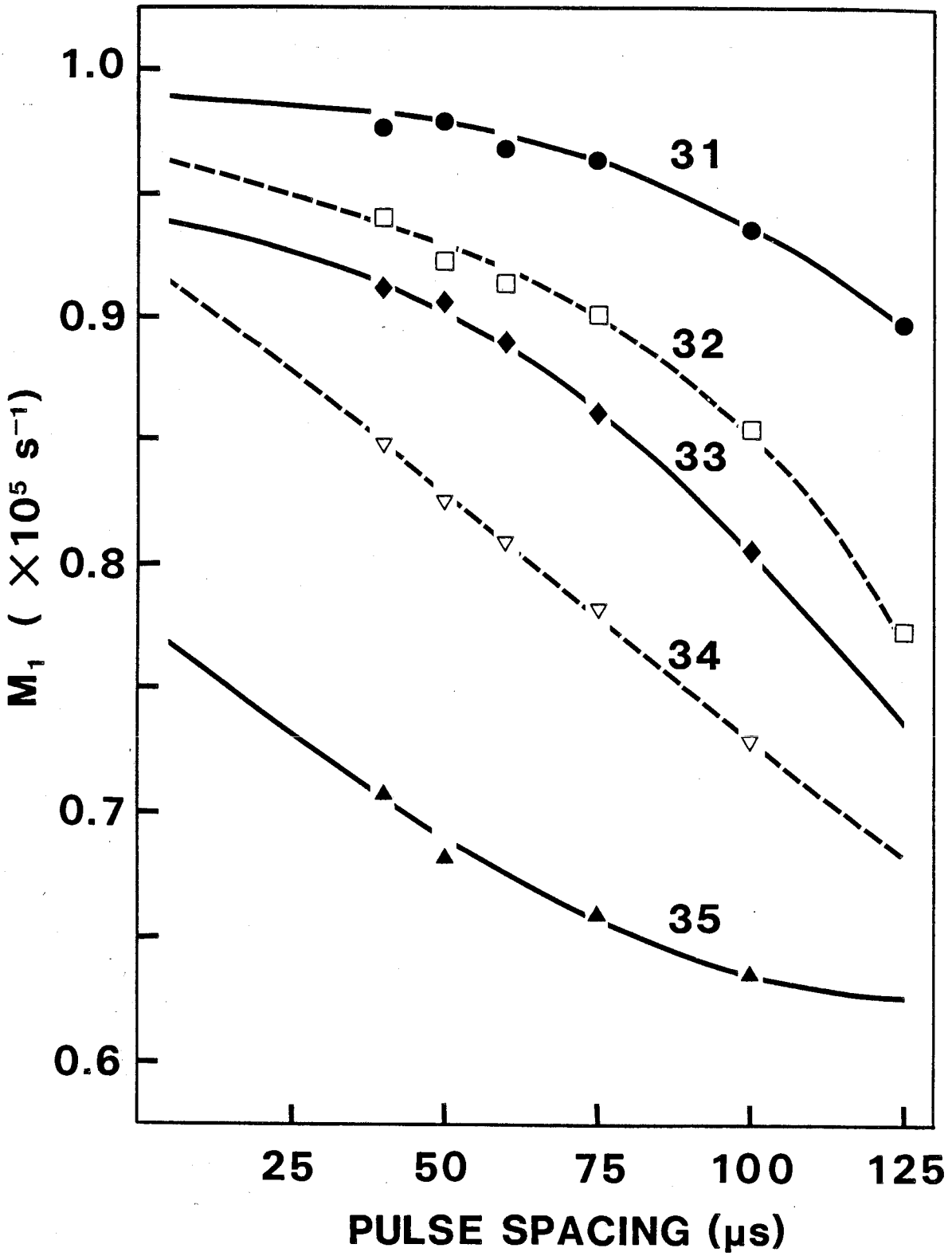
1.0
0.9
0.8
0.7
0.6
M_1 ($\times 10^5$ s^{-1})
31
32
33
34
35
25
50
75
100
125
PULSE SPACING (μs)

Figure 23: Variation of spectral shape with pulse spacing for PC-d_{31}/5 mol % 1-octanol at 32°C. Spectral parameters: pulse spacing: as indicated; pulse length = 6.5 µs; line broadening = 50 Hz; sweep width = ±250 kHz, number of acquisitions = 1000.

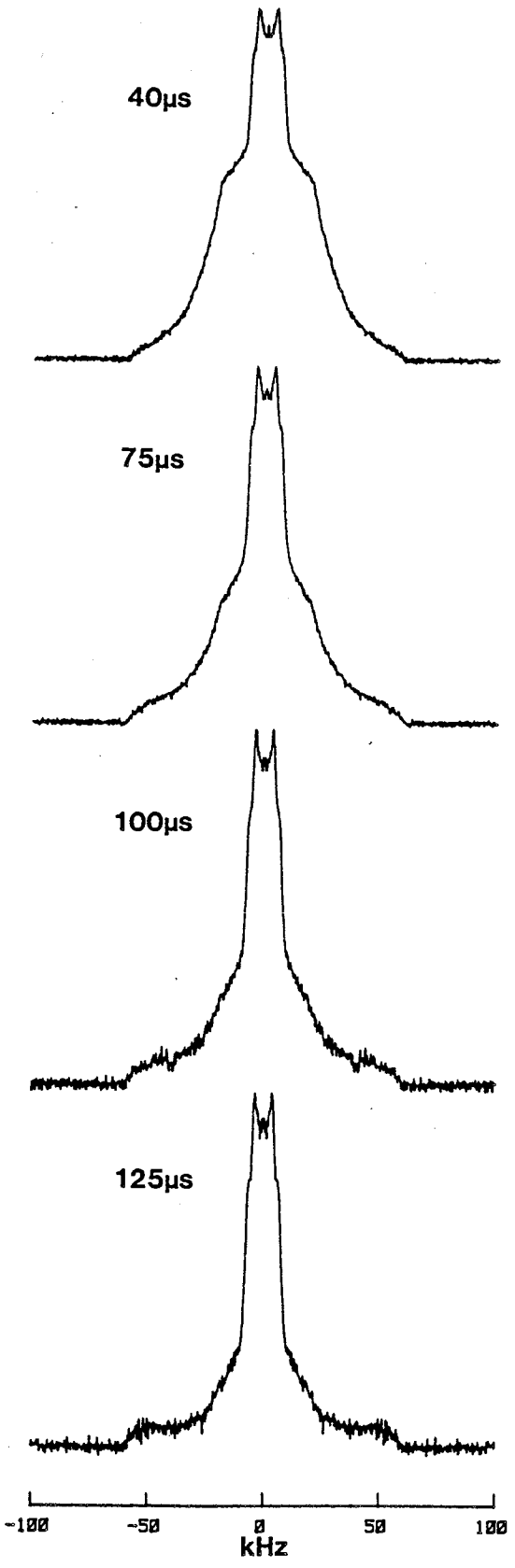
40μs
75μs
100μs
125μs
-100
-50
0
50
100
kHz

axes are parallel to B_o may behave differently from those whose axes are perpendicular to B_o. This has been observed with selectively deuterated phosphatidylcholines very recently (Perly et al., 1985). A final explanation is that the motion responsible for the decay has a characteristic time comparable to the pulse spacing for this temperature region, a condition which can lead to distortions in the NMR spectra obtained using the quadrupolar echo technique (Spiess and Sillescu, 1980). These distortions increase in severity with increasing pulse separation. Perly et al. (1985) have stated that lateral diffusion is possibly the motion responsible, although other motions such as chain rotation, director fluctuation or trans-gauche isomerization could be responsible in our case.

The M_1 dependence on pulse spacing is only seen (for short pulse spacings) at those temperatures where the $1/T_{2e}$ rate is a maximum. The temperature dependence of $1/T_{2e}$ is given in Fig. 24, for PC-d_{31}, PC-d_{31}/25 mol % 1-octanol and PC-d_{31}/25 mol % 1-decanol. For each of these three systems the $1/T_{2e}$ curve follows the same general shape. In the gel phase $1/T_{2e}$ increases as the sample is heated until a maximum is reached just before the onset of the gel to liquid crystalline phase transition. Through the transition $1/T_{2e}$ decreases, and when the transition is complete $1/T_{2e}$ appears to change only gradually with increasing temperature. Differences in the $1/T_{2e}$ behaviour for the three systems are also notable (Fig. 24). Firstly, the curves are displaced along the temperature axis in a way that correlates with the 1-alkanol's effect on the

Figure 24: The $1/T_{2e}$ relaxation rate vs. temperature for: (□) PC-d_{31}; (▽) PC-d_{31}/25 mol % 1-decanol; (◇) PC-d_{31}/25 mol % 1-octanol.

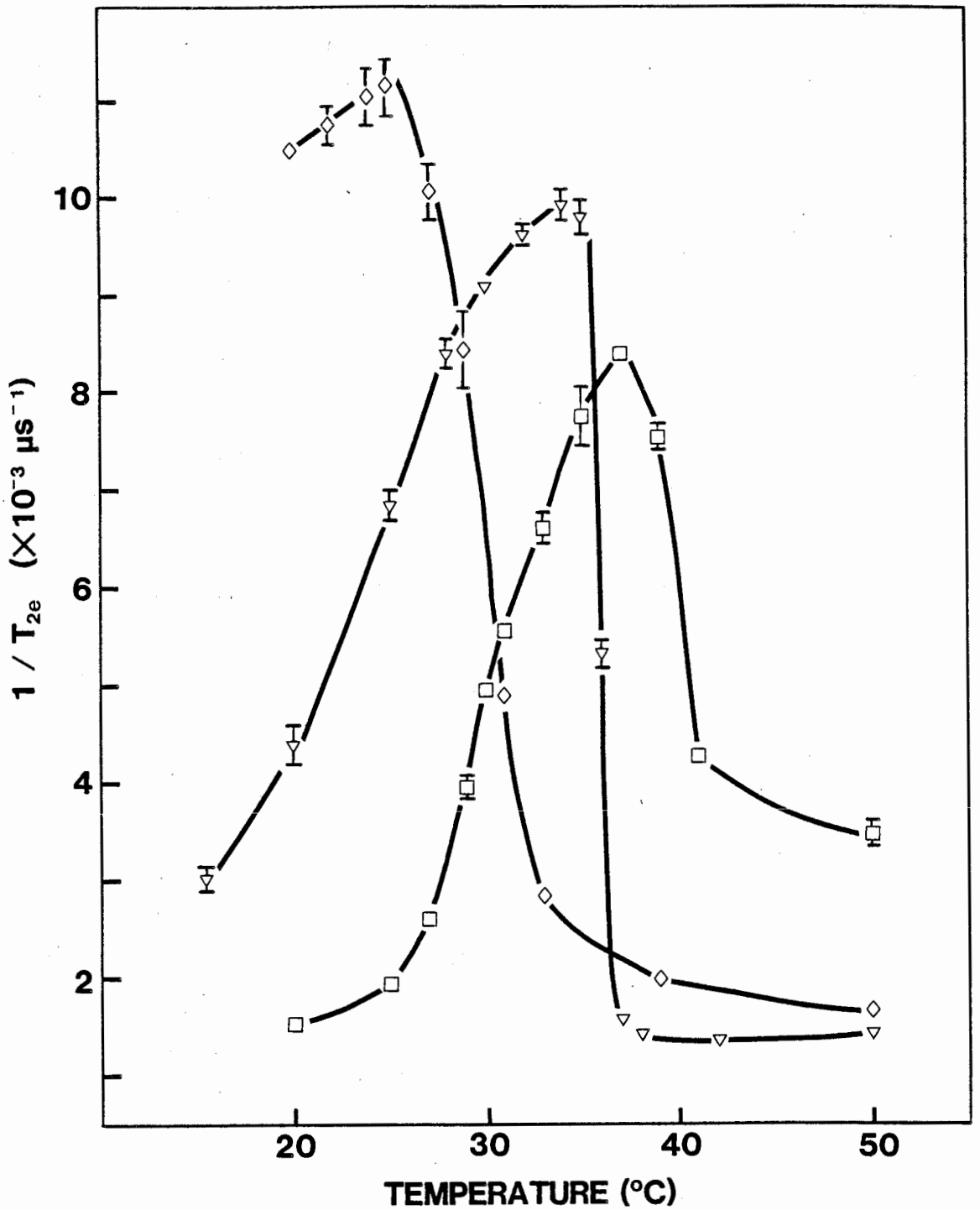
10
8
6
4
2
1 / T2e (X10-3 μs-1)
20
30
40
50
TEMPERATURE (°C)

phospholipid phase transition. Secondly, the maximum $1/T_{2e}$ relaxation rate increases in the order PC-d_{31} < PC-d_{31}/1-decanol < PC-d_{31}/1-octanol. Thirdly, the liquid crystalline $1/T_{2e}$ measured is a factor of two slower in the presence of 25 mol % 1-octanol or 1-decanol. For example, at 50°C, T_{2e} values for PC-d_{31}, PC-d_{31}/25 mol % 1-octanol and PC-d_{31}/25 mol % 1-decanol are 280 μs, 530 μs, and 620 μs, respectively.

The narrowing of the PC-d_{31} spectral lines in Fig. 19b can be attributed to the significantly longer T_{2e}'s of PC-d_{31} in the presence of the anesthetic. The enhanced resolution due to T_{2e} illuminates details of the plateau region in a manner not heretofore obtained in a perdeuterated phospholipid bilayer. As slow motions of the phospholipid acyl chains are usually considered to dominate T_{2e} in the liquid crystalline phase (Davis, 1983), the decreased relaxation rate $1/T_{2e}$ for PC-d_{31} in the presence of 1-alkanols suggests that the 1-alkanols decrease τ_c, the ^2H correlation time for the deuterated phospholipid chains. This agrees with Pauls et al. (1985) who find that, above T_m, $1/T_{2e}$ varies with τ_c. The precise nature of the affected motion is not known. Both chain rotation and director fluctuations are expected to occur at a fast rate ($\geq 10^8$ s^{-1}) in the liquid crystalline phase, with trans-gauche isomerisation being faster still ($\geq 10^9$ s^{-1}) (Meier et al., 1983). Slower ($\approx 10^6$ s^{-1}) motions occurring in lipid bilayers are speculated to include collective director fluctuations such as the twist and splay modes illustrated by Brown et al., 1983. As well, the lamellae may experience periodic, wave-like oscillations. It is

possible that it is the lateral diffusion rate which is affected and that 1-alkanols increase this rate, making $1/T_{2e}$ relaxation less efficient. Lateral diffusion is normally characterized by diffusion coefficients on the order of 10^{-8} cm^2 s^{-1} for bilayers which translates to a time on the order of 10 ms for diffusion through one radian on the surface of a 5 x 10^{-5} cm liposome.

The concentration dependence of the $1/T_{2e}$ vs. temperature plot is shown in Fig. 25. 1-Octanol at 0%, 5% and 25% was incorporated into PC-d_{31} bilayers. The resulting plot is very similar to Fig. 24, indicating that 5 mol % 1-octanol has a similar effect on PC-d_{31} to 25 mol % 1-decanol. The 5 mol % 1-octanol concentration appears to be just as effective as the 25 mol % concentration in slowing the $1/T_{2e}$ rate of PC-d_{31} at 50°C.

These results are viewed as preliminary and further experiments are needed in order to form any firm conclusions concerning the effects of 1-alkanols on the motion of the phosphatidylcholine acyl chains. With regard to the method of measuring $1/T_{2e}$, two points should be made. By measuring the rate of decay of the echo amplitude with increasing pulse spacing all orientations of the molecular and lab axes are combined. We measure the fastest relaxation rate in all cases, and have not attempted to define the orientation-dependence of the relaxation. Also, by using a perdeuterated phosphatidylcholine, we combine the relaxation behaviour for all positions along the acyl chain. Since we measure the initial decay rate, the slower methyl group relaxation is not observed and neither are the different relaxation rates for methylenes near the

Figure 25: The concentration dependence of $1/T_{2e}$ as a function of temperature. Solid line (without symbols): PC-d_{31}; dotted line: PC-d_{31}/25 mol % 1-octanol. (Both are shown in more detail in Fig. 24.) (◇): PC-d_{31}/5 mol % 1-octanol.

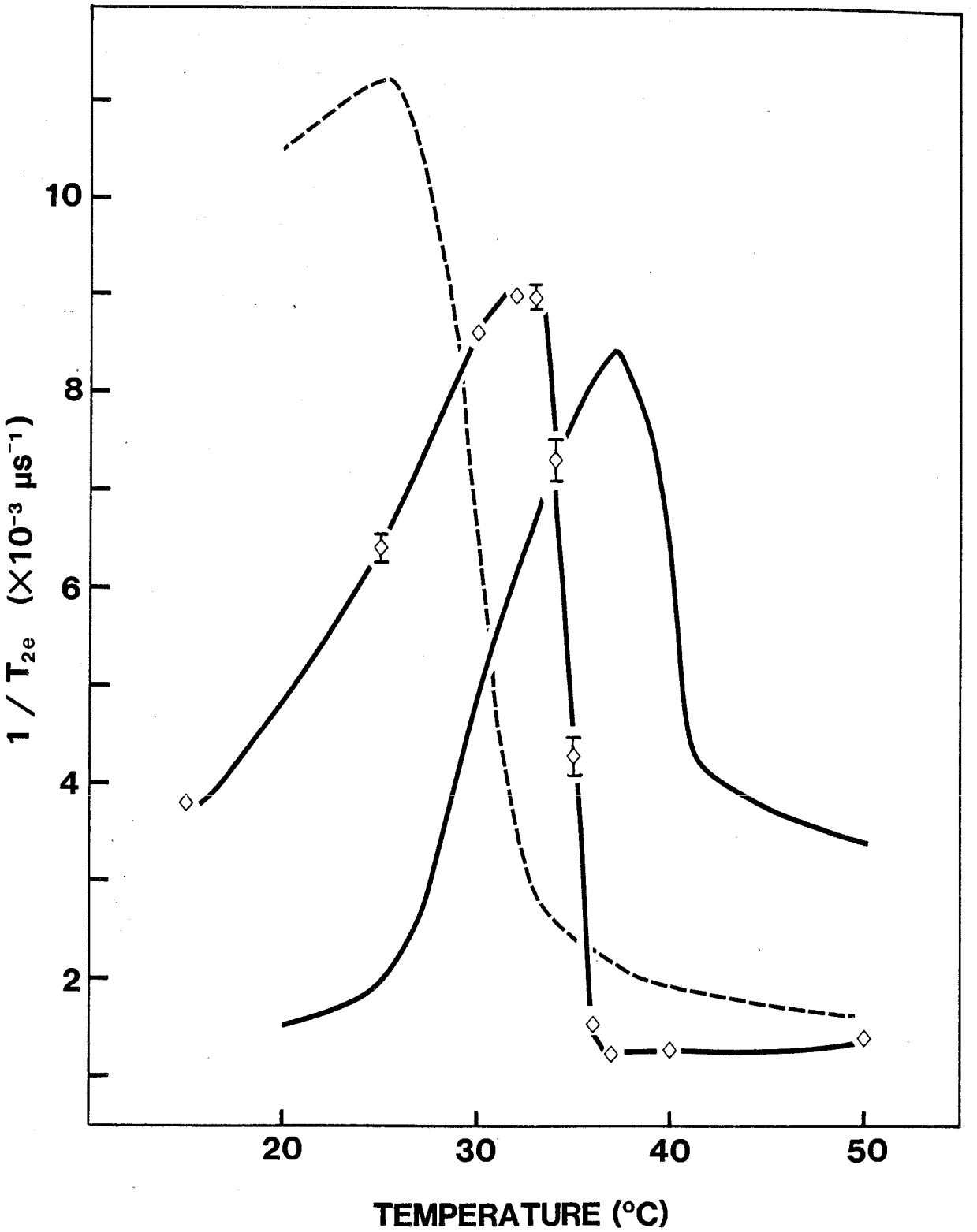
10
8
6
4
2
1 / T2e (×10-3 μs-1)
20
30
40
50
TEMPERATURE (°C)

lipid/water interface compared with those near the center of the bilayer. The use of selectively deuterated phosphatidylcholine and a method of measuring $1/T_{2e}$ from different segments of the Fourier transformed spectrum (angular dependence) could be employed to clarify the motional changes to the phospholipid caused by 1-alkanol anesthetics. An attempt to extract an activation energy from the T_{2e} data presented here via an Arrhenius plot was unsuccessful as the plot was nonlinear.

III. Labelled Anesthetic: 1,2-Dipalmitoyl-*sn*-glycero-3-phosphorylcholine (DPPC)/Deuterated 1-Alkanol

A. DPPC/Selectively Deuterated 1-Decanol

Multilamellar dispersions, 50 wt % in deuterium depleted water, composed of 75 mol % DPPC/25 mol % selectively deuterated 1-decanol have been prepared.

Of the ten carbons in 1-decanol which may be deuterated, eight have been studied. The results are divided into those concerning the temperature dependence of the ^2H NMR spectra of the labelled 1-decanol, and those concerning 1-decanol's order parameter profile in liquid crystalline DPPC.

1. Temperature dependence: DPPC/deuterated 1-decanol

The temperature dependence of the ^2H NMR spectra of DPPC containing 1-decanols deuterated at positions C-2, C-4, C-7, or C-9 has been studied. Fig. 26 shows the ^2H NMR spectrum of DPPC/[4,4-$^2H_2$]-1-decanol dispersions at four different temperatures, illustrating the spectral narrowing that accompanies the lipid gel to liquid crystalline phase transition. At 15°C the DPPC/1-decanol dispersion is in the gel phase and, when the sample is heated to 35°C, only a very gradual sharpening of the vertical edges (≈±30 kHz) takes place. When the temperature is raised further, the central region of the spectrum narrows considerably and the broad shoulders at ±63

Figure 26: The temperature dependence of the ^2H NMR spectrum of 25 mol % [4,4-$^2H_2$]-1-decanol in DPPC multilamellar dispersions. Spectral parameters: 15°C: pulse spacing = 75 μs; pulse length = 8 μs; line broadening = 200 Hz; sweep width = ±250 kHz; number of acquisitions = 16000; 35°C: same as at 15°C except: pulse spacing = 50 μs; line broadening = 300 Hz; 38°C: same as at 15°C except: pulse spacing = 60 μs; line broadening = 300 Hz; number of acquisitions = 32000; 50°C: same as at 15°C except: pulse spacing = 50 μs; line broadening = 100 Hz; sweep width = ±100 kHz; number of acquisitions = 64000.

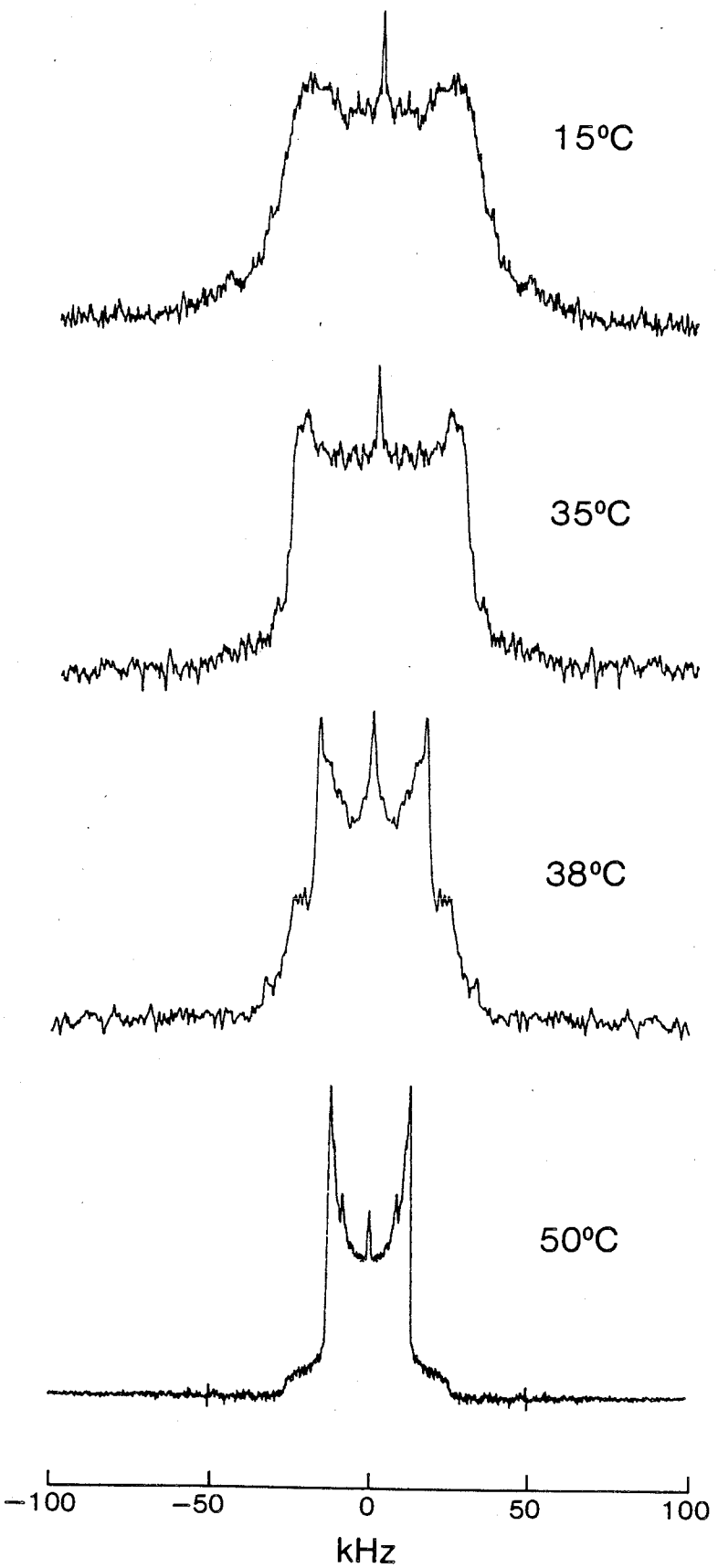
15°C
35°C
38°C
50°C
−100
−50
0
50
100
kHz

kHz are no longer visible. The 38°C spectrum appears to be due to a superposition of the spectra of 1-decanol in two lipid phases: one narrow spectrum, foreshadowing that observed in the liquid crystalline phase with peaks at ±17 kHz, and one broad spectrum with features at ±25 kHz reminiscent of those seen in the gel phase. The 50°C spectrum is a typical powder pattern with narrow resonances arising from 1-decanol intercalated in the liquid crystalline phospholipid phase. (The small peaks at ±9.6 kHz represent ≤ 10% impurity in the [4,4-$^2H_2$]-1-decanol, probably due to contamination with another labelled 1-decanol.) The gel phase spectra of DPPC containing [2,2-$^2H_2$]-, [7,7-$^2H_2$]-, or [9,9-$^2H_2$]-1-decanol are very similar to those shown for [4,4-$^2H_2$]-1-decanol.

At 15°C there is a notable difference between the spectral shapes of deuterated phosphatidylcholine and deuterated alcohol in our phospholipid/1-decanol dispersions. Referring to Fig. 26, the shape of the ^2H NMR spectrum of [4,4-$^2H_2$]-1-decanol in DPPC at 15°C is a broad powder pattern, characteristic of axially symmetric rotation of the 1-decanol about its long axis. Depaking the spectrum results in a broad doublet whose splitting corresponds to $\Delta\nu_Q \approx 56$ kHz. In contrast, the deuterated phosphatidylcholine/1-decanol dispersion has a gel phase spectral shape at 15°C which is also seen in pure lipid lamellar dispersions below T_m. At 38°C, the spectrum of [4,4-$^2H_2$]-1-decanol in DPPC consists of broad and narrow components, presumably due to 1-decanol embedded in gel phase lipid and 1-decanol dissolved in liquid crystalline lipid, respectively.

The 36°C spectrum of PC-d_{31} containing 25 mol % 1-decanol is similarly a superposition of broad and narrow components (Fig. 17). The proportion of 1-decanol in the gel phase lipid at 38°C can be estimated by depaking the spectrum in Fig. 26. As the pulse spacing τ is reduced, however, the broad component in the 38°C spectrum becomes relatively more intense, indicating that T_{2e} is longer for 1-decanol in the liquid crystalline phase than in the gel phase lipid. From a rough extrapolation to zero τ, the proportion of 1-decanol in the gel phase lipid ay 38°C is approximately 60%.

Measurement of the first moment (M_1) (Davis, 1983) of the ^2H NMR spectrum of labelled 1-decanols in DPPC as a function of temperature clarifies the spectral changes illustrated in Fig. 26. Plots of M_1 vs. temperature for 1-decanol deuterated at C-2, C-4, C-7 and C-9 are given in Fig. 27. Below the gel to liquid crystalline phase transition, the M_1 values for all four DPPC/1-decanol dispersions agree closely, with an average value of $1.11 \pm 0.08 \times 10^5$ s^{-1}. Above the phase transition M_1 reflects the quadrupolar splitting of the powder pattern, and hence S_{CD}, so that [4,4-$^2H_2$]-1-decanol has the largest value of M_1, followed by [2,2-$^2H_2$]-1-decanol, [7,7-$^2H_2$]-1-decanol, and [9,9-$^2H_2$]-1-decanol. This agrees with the order parameter profile shown in Fig. 30 (see p. 105).

At the phase transition, M_1 drops suddenly. The increased rate of trans-gauche isomerisation of the phospholipid acyl chains as the sample melts is apparently accompanied by increased trans-gauche isomerisation of the 1-decanol. An

Figure 27: First moment M_1 vs. temperature for four selectively deuterated decanols in multilamellar dispersions of DPPC. (○) [2,2-$^2H_2$]-1-decanol; (▼) [4,4-$^2H_2$]-1-decanol; (●) [7,7-$^2H_2$]-1-decanol; and (△) [9,9-$^2H_2$]-1-decanol. Error bars are given for [2,2-$^2H_2$]-1-decanol indicating a ±0.5°C uncertainty in temperature and an error in the measurement of M_1 which is appreciable only from 30°C to 40°C, where M_1 becomes dependent on the pulse spacing and must be determined by extrapolation.

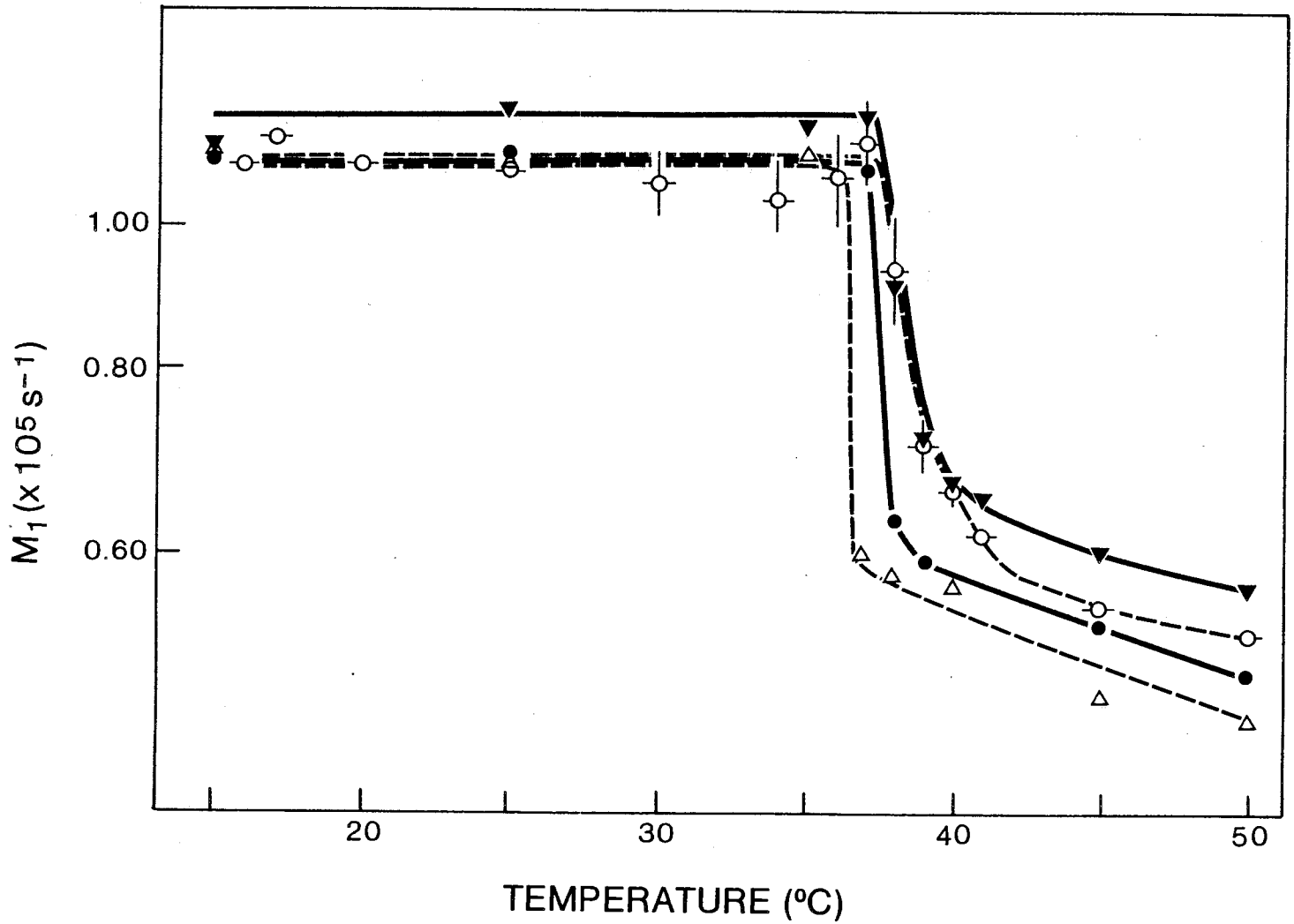
1.00
0.80
0.60
M_1 (x 10^5 s^{-1})
20
30
40
50
TEMPERATURE (°C)

examination of the phase transition region, 36°C to 41°C in Fig. 27, reveals that the labelled carbon positions of 1-decanol monitor the phase change differently depending on their depth in the bilayer. The C-2 label, near the phospholipid/water interface, has a transition from 37°C to 41°C, C-4 has a transition from 37°C to 40°C, C-7 has a slightly sharper transition from 37°C to 39°C, and C-9, toward the middle of the bilayer, has a very short transition region: from 36°C to 37°C. Differential scanning calorimetry on these four DPPC/1-decanol dispersions (Fig. 28) shows a single endothermic phase transition at a temperature of 38.5 ± 0.2°C with a half-height width of 2.9 ± 0.4°C. The observation that the [9,9-$^2H_2$]-1-decanol undergoes a sharp transition at a temperature of 36°C while the other labels have broader transitions beginning at 37°C indicates that the phase change is initiated by increased isomerisation in the middle of the bilayer, while the methylenes near the lipid/water interface remain more restricted.

2. Order parameter: DPPC/selectively deuterated 1-decanol

To determine the order parameter of 1-decanol in liquid crystalline DPPC dispersions the ^2H NMR spectra of 1-decanols labelled at the C-2, C-3, C-4, C-5, C-6, C-7, C-9 and C-10 positions were recorded at 50°C. Representative spectra are shown in Fig. 29. From the splittings $\Delta\nu_Q$ obtained from these powder patterns a detailed order parameter profile (S_{CD} vs. labelled carbon) can be drawn (Fig. 30). This order parameter

Figure 28: DSC traces for selectively deuterated 1-decanols (25 mol %) in DPPC multilamellar dispersions. The position of labelling is indicated beside each trace. Scanning rate: 10°/min. from -30°C to +70°C.

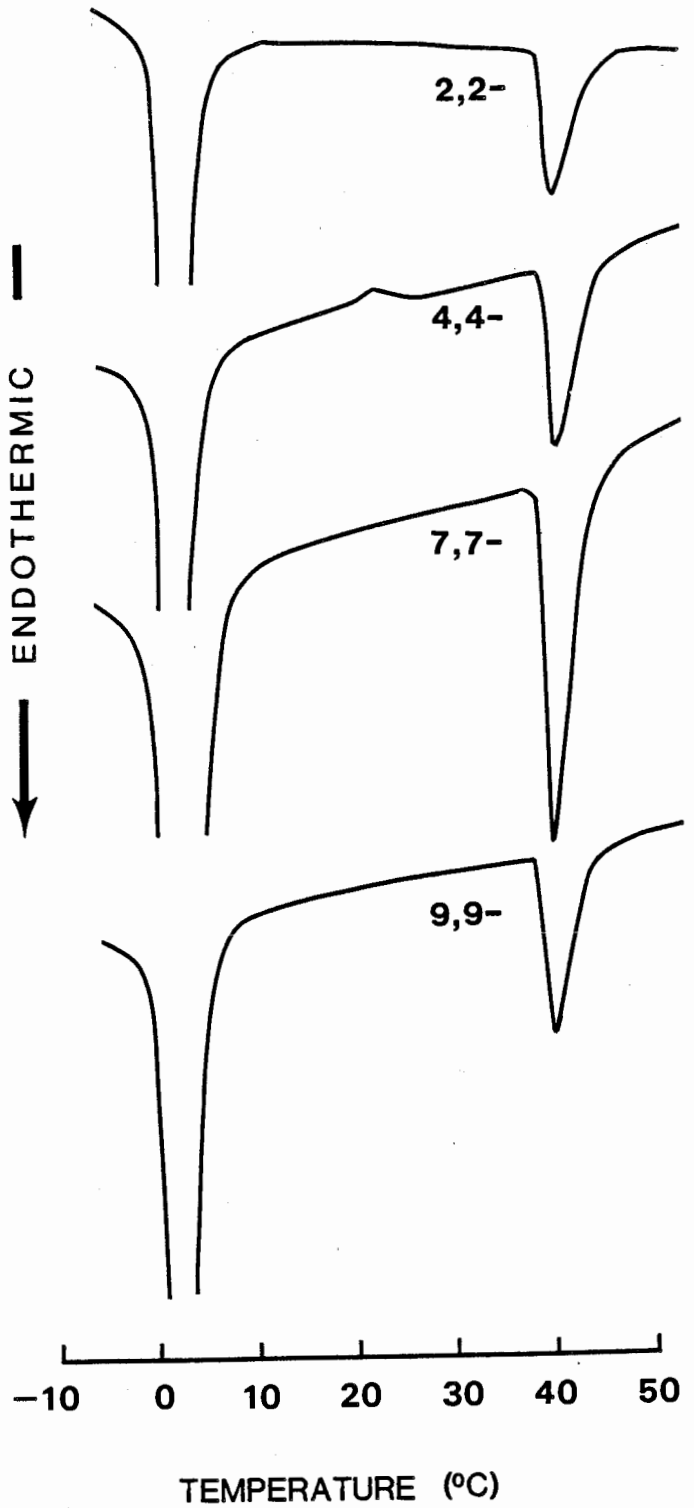
2,2-
4,4-
7,7-
9,9-
ENDOTHERMIC
−10
0
10
20
30
40
50
TEMPERATURE (°C)

Figure 29: Deuterium NMR spectra of 25 mol % selectively deuterated decanols in DPPC multilamellar dispersions at 50°C. The position of deuterium substitution is given to the left of each spectrum. Spectral parameters: 2,2-: pulse spacing = 75 µs; pulse width = 8 µs; line broadening = 100 Hz; sweep width = ±100 kHz; number of acquisitions = 32000; 3,3-: same as for 2,2- except: pulse width = 6.5 µs; line broadening = 50 Hz; number of acquisitions = 48000; 4,4-: same as for 2,2- except: pulse spacing = 50 µs; number of acquisitions = 64000; 7,7- and 9,9-: same as for 2,2-; 10,10,10-: same as for 2,2- except: no line broadening; number of acquisitions = 48000. Peaks marked with a cross are due to small amounts of impurity.

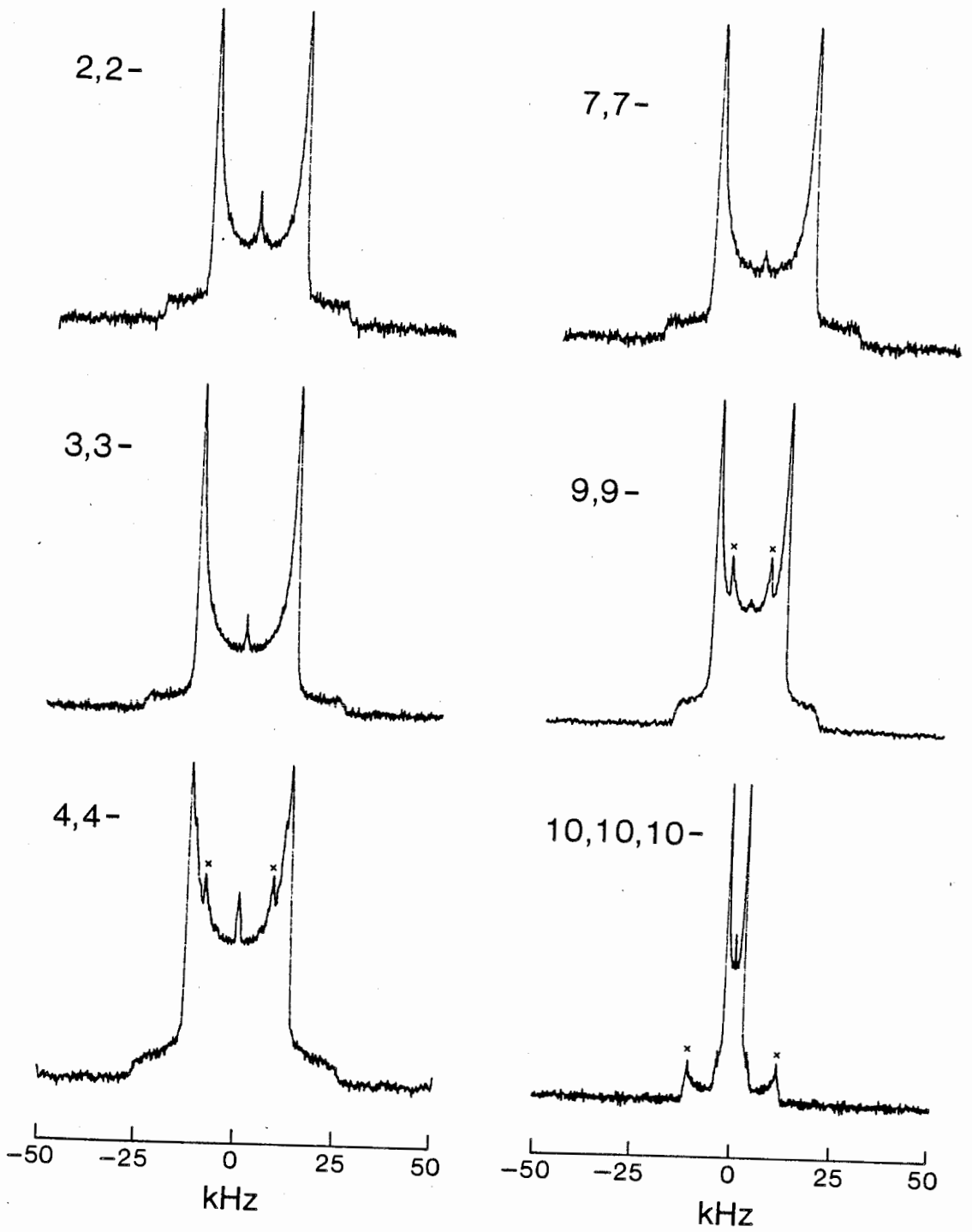
2,2-
7,7-
3,3-
9,9-
4,4-
10,10,10-
-50
-25
0
25
50
kHz
-50
-25
0
25
50
kHz

Figure 30: Order parameter profile $|S_{CD}|$ vs. position of the deuterium label of decanol in DPPC multilamellar dispersions at 50°C. The S_{CD} values at C-2, C-3, C-7, and C-9 are the average of the splittings measured in duplicate samples, with error bars indicating the degree of reproducibility. The largest error bar, at C-7, represents a deviation of ± 4 % from the average value.

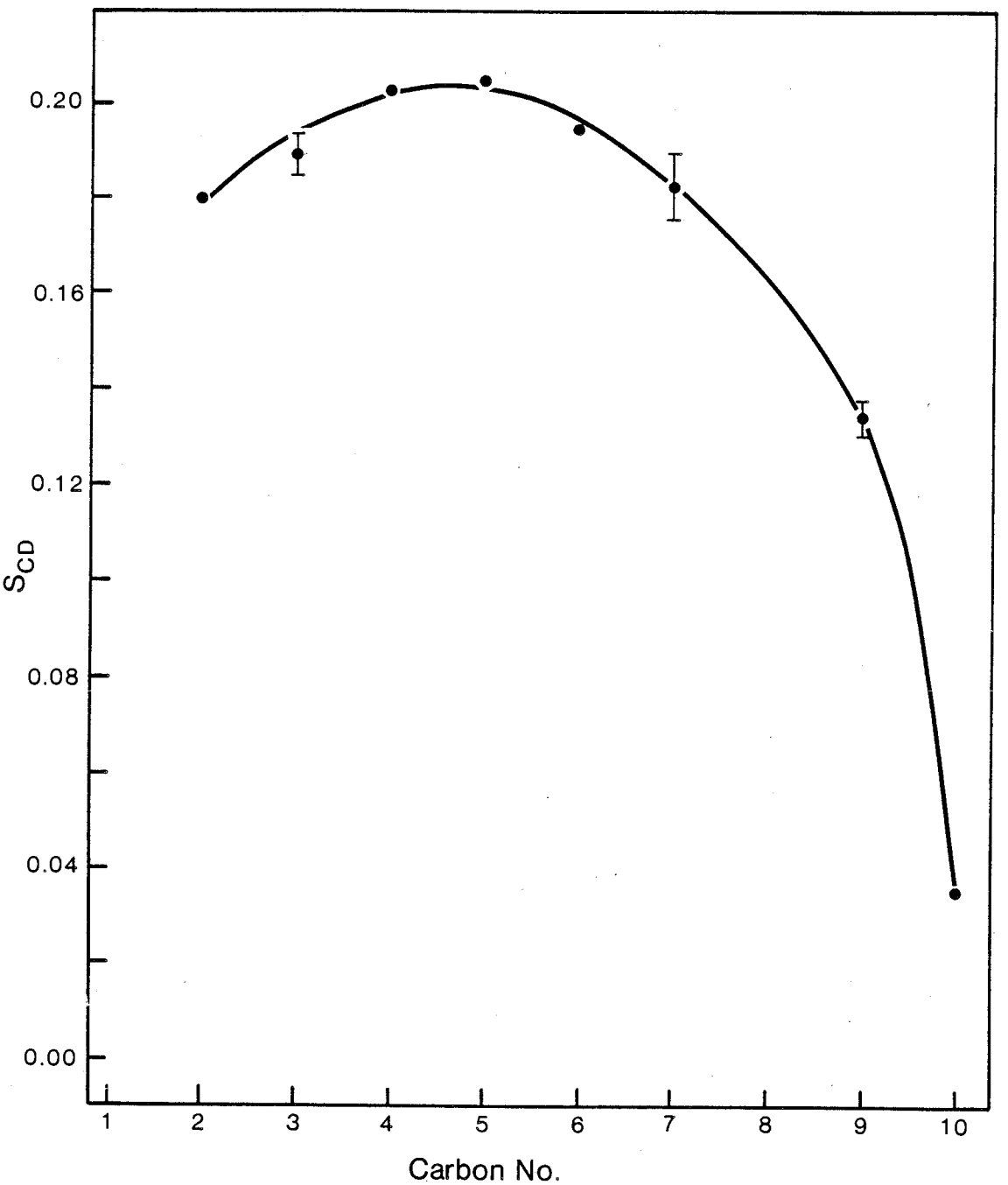
0.20
0.16
0.12
0.08
0.04
0.00
S_{CD}
1
2
3
4
5
6
7
8
9
10
Carbon No.

profile show that 1-decanol in a phospholipid bilayer system has a maximum S_{CD} = 0.20 for C-4 and C-5. Both ends of 1-decanol show reduced splittings with the greatest reduction occurring toward the methyl terminus (C-10).

The shape of the S_{CD} vs. carbon position curve is qualitatively similar to that found for 1-decanol in soap lamellae. Niederberger and Seelig (1974) studied dispersions of sodium decanoate and 1-decanol labelled at the C-1, C-2, C-4, C-7, C-8 and C-10 positions and found that the maximum order parameter S_{CD} = 0.29 occurred at C-4. Klason and Henriksson (1982) studied dispersions of sodium octanoate and 1-decanol selectively labelled at C-1 and C-2 or perdeuterated 1-decanol at 20°C and measured a maximum S_{CD} = 0.28. The order parameter profile of perdeuterated 1-octanol in DMPC at 32°C is also very similar, with a maximum S_{CD} for C-4 and C-5 of 0.27 (Pope et al., 1984). The magnitude of the maximum S_{CD} value of 1-decanol in DPPC multilamellar dispersions found in our study is only about 75% of that found by the previous workers, probably due to the high water content of our system (≈40 H_2O : 1 lipid) compared to the other systems (≈9 H_2O : 1 lipid).

The phenomenon of reduced S_{CD} for carbon positions towards the hydroxyl end of 1-decanol is not peculiar to DPPC. We have found that egg yolk phosphatidylcholine bilayers containing [2,2-$^2H_2$]-1-decanol or [4,4-$^2H_2$]-1-decanol give S_{CD} = 0.18 and 0.21, respectively, at 25°C. This decrease in S_{CD} has also been observed by researchers studying 1-decanol in soap lamellae (Klason and Henriksson, 1982; Niederberger and Seelig, 1974).

Those workers attributed the reduction in S_{CD} to either increased amplitudes of motion of the C-1 to C-3 portion of 1-decanol in comparison with the surrounding lipid, or to the geometric effects of tilting the initial portion of the 1-decanol chain with respect to the bilayer normal in order that hydrogen bonding may occur.

The effect of a tilt would be to reduce S_{CD} but not the C-C segmental order parameter S_{mol} through the relationship $S_{mol} = S_{CD}/S_{geo}$ where $S_{geo} = \langle 3\cos^2\theta' - 1\rangle/2$ and θ' is the angle between the C-^{2}H bond and the molecular long axis (Seelig, 1977; Seelig and Waespe-Sarcevic, 1978). For methylene groups in lipid bilayer acyl chains, θ' is generally taken as 90° (Niederberger and Seelig, 1974). To get an order of magnitude approximation of the degree of tilt that would be necessary to reduce $|S_{CD}|$ to our observed values of 0.18 for C-2 and 0.19 for C-3 we can assume that S_{mol} remains at its plateau level of about 0.41 in this region of the bilayer, as found for phospholipid acyl chains (Thewalt et al., 1985; Paddy et al., 1985). This leads to calculated values of $S_{geo} = -0.44$ for C-2 and $S_{geo} = -0.46$ for C-3, corresponding to a tilt of the decanol backbone away from the bilayer normal of ≈12° at C-2 and ≈9° at C-3. Angles this small would not be expected to significantly disrupt the packing of the lipid acyl chains, but the existence of this type of hydrogen bonding has still to be independently verified. To attempt to clarify this point, ^{13}C NMR spectra of DPPC vesicles with and without 25 mol % 1-decanol were recorded at 52°C. The positions of the lipid acyl chain carbonyl

resonances were unchanged in the presence of 1-decanol, so that ^{13}C NMR gave no evidence of hydrogen bonding. It is possible, however, that the effect of hydrogen bonding on the chemical shifts of the acyl chain carbonyl resonances is too slight to be observed, since DPPC vesicles containing cholesterol, which is known to hydrogen bond, displayed identical carbonyl chemical shifts.

Hydrogen bonding of the carboxyl group of sodium decanoate has been cited as the reason for the larger S_{CD} value displayed by C-2 of the decanoate compared with the C-2 of the 1-decanol in the soap/1-alkanol mixture (Niederberger and Seelig, 1974). The higher hydrophilicity of the carboxyl would restrict the amplitude of the motions of the C-2 position deuterons, thereby increasing S_{CD}. Weaker hydrogen bonding of the decanol's hydroxyl group would not serve to restrict the amplitude of the C-2 deuterons as much, so that S_{CD} is correspondingly reduced. In the case of the phospholipid/1-alkanol dispersions, the lipid acyl chains are covalently bonded to the glycerol backbone, while the 1-decanol, even if some hydrogen bonding were present, would have its hydroxyl end relatively unrestricted, resulting in smaller S_{CD} values for C-1 to C-3.

Table IV compares the splittings obtained from dispersions of PC-d_{31}/1-decanol and DPPC/selectively deuterated 1-decanols. The composition of the dispersions was three moles phospholipid to one mole 1-alkanol in all cases. The phospholipid order parameter is insensitive to variations in the alkanol concentration as shown in Section II of this chapter. As well,

TABLE IV: Comparison of quadrupolar splittings $\Delta\nu_Q$ for 75 mol % phosphatidylcholine/25 mol % 1-decanol, 50 wt % aqueous multilamellar dispersions at 50°C. The splittings arise either from labelled phospholipid *sn*-2 acyl chains or from labelled 1-decanol.

LABELLED PHOSPHATIDYLCHOLINE PC-d_{31}/1-decanol		LABELLED ALCOHOL DPPC/selectively deuterated 1-decanol	
Acyl Chain Position	$\Delta\nu_Q$ (kHz)	Alcohol Chain Position	$\Delta\nu_Q$ (kHz)
C-2	11.4 ± 0.3[a] 17.8 ± 0.4	C-2	22.7 ± 0.0
C-3 to 8	27.4 ± 0.6	C-3	23.9 ± 0.6
C-9	25.6 ± 0.7	C-4	25.6
C-10	23.5 ± 0.6	C-5	25.8
C-11	22.0 ± 0.5	C-6	24.5
C-12	19.9 ± 0.4	C-7	23.0 ± 0.8
C-13	17.8 ± 0.4	C-9	17.0 ± 0.5
C-14	14.7 ± 0.4	C-10	4.4
C-15	11.4 ± 0.3		
C-16	2.66 ± 0.12		

[a] The ± values, where found, are deviations found in duplicate measurements.

comparable order parameters are measured for both selectively deuterated and perdeuterated phospholipid acyl chains (Table II), indicating that mass effects resulting from perdeuteration do not alter the acyl chain order parameters substantially. DSC of the PC-d_{31}/1-decanol and the DPPC/selectively deuterated 1-decanol dispersions used shows that the T_m's differ by less that 2°C (37°C vs. 38.5°C). Thus, 'reduced temperature' effects are negligible. These considerations, together with the comparable chemical structures of the two mixtures, allow the systems to be compared at 50°C. The quadrupolar splittings of the two types of labelled chains in the phosphatidylcholine/1-decanol dispersions are remarkably close. The maximum splitting displayed by the deuterated phospholipid/1-decanol dispersion is 27.4 kHz while that for the DPPC/[5,5-$^2H_2$]-1-decanol dispersion is 25.8 kHz.

To ascertain the depth at which decanol sits in the phospholipid bilayer, it is useful to compare the splittings in the hydrophobic ends of their respective chains. The plateau in the phospholipid acyl chain's quadrepolar splittings extends through C-8, while C-9's splitting is slightly less, and the splittings continue to narrow to the terminal methyl group. For the dispersions containing labelled 1-decanols, C-4 and C-5 display nearly equal splittings, $\Delta\nu_Q$ for C-6 is slightly less, and $\Delta\nu_Q$ for C-7 to C-10 decreases further, monotonically. Thus, it is likely that C-6 of 1-decanol is approximately at the depth of C-9 on the *sn*-2 chain of the phospholipid. This implies that the hydroxyl group of 1-decanol is at the level of C-3 on the

Figure 31: Superimposed order parameter profiles for PC-d_{31}/1-decanol (▲) and DPPC/deuterated 1-decanol (△) at 50°C illustrating the probable location of 1-decanol in the phospholipid bilayer. The thick horizontal bar represents the plateau order parameter, with C-3 to C-8 S_{CD} values falling within range indicated by the error bar.

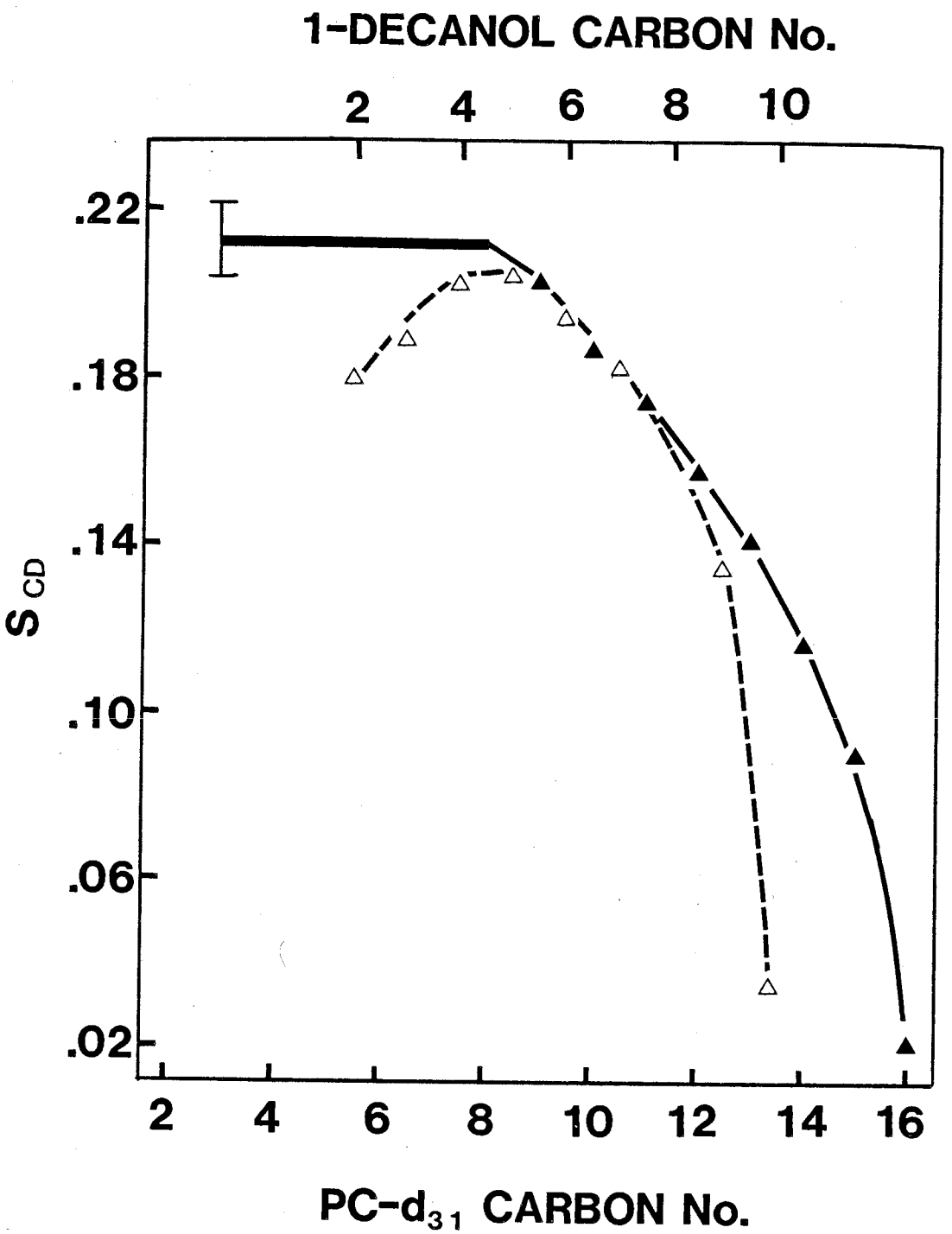
1-DECANOL CARBON No.
2
4
6
8
10
.22
.18
.14
.10
.06
.02
S_{CD}
2
4
6
8
10
12
14
16
PC-d_{31} CARBON No.

sn-2 chain of the phospholipid provided the 1-decanol's long axis is close to being parallel to the bilayer normal. Superimposed order parameter profiles for PC-d_{31}/1-decanol and DPPC/deuterated 1-decanol are shown in Fig. 31, illustrating the corresponding S_{CD}'s described above. By matching the 1-decanol C-5 to C-9 S_{CD} values to the PC-d_{31} profile the alcohol is shown to be situated, on average, with its -OH group between C-3 and C-4 of the phospholipid *sn*-2 chain, and its $-CH_3$ group between C-13 and C-14.

This location of 1-decanol in phospholipid bilayers permits hydrogen bonding, especially with the ester groups of the *sn*-1 chains. The *sn*-2 chain is bent at C-2, so that the *sn*-1 chain C-1 is at about the same depth in the bilayer as the *sn*-2 chain C-3. A recent paper by Brasseur et al. (1985) contains calculations of the depth of a series of *n*-alkanols in DPPC monolayers using a 'semi-empirical conformational analysis'. By calculating the alcohol's minimum energy conformation and the energies of interaction between neighbouring lipids they locate the hydroxyl group of 1-decanol at the level of the ester bond between the phospholipid's glycerol backbone and its polar headgroup, considerably closer to the lipid/water interface than we find. Our method is more direct, however, and the results should consequently be more accurate. As an extension of the results on DPPC/1-decanol it can be predicted that 1-dodecanol would be located slightly deeper in the bilayer, probably approximately parallel to the C-4 to C-16 segments of the *sn*-2 chain. This location would mean that 1-dodecanol's effect on

the DPPC bilayer would be the minimum for the *n*-alkanol series. This is supported by the fact that the temperature of the gel to liquid crystalline phase transition is raised by less than two degrees in the presence of 30 mol % dodecanol (Eliasz et al., 1976). Brasseur et al. (1985) also predict that 1-dodecanol would locate more deeply in the bilayer than 1-decanol.

The question of bilayer solubility of the homologous series of *n*-alkanols is an important one. The anesthetic potency of the alkanols increases with increasing chain length to 1-dodecanol (in tadpoles) while 1-tetradecanol is not anesthetic. This can be explained purely in terms of the limited solubility of 1-tetradecanol in the membrane compared with 1-dodecanol (Pringle et al., 1981). The saturated aqueous concentrations of these alcohols drop with increasing chain length but this is compensated for by increasing membrane/buffer partition coefficients up to 1-dodecanol. 1-Tetradecanol, however, has a membrane/buffer partition coefficient which is smaller than that of 1-dodecanol (Sallee, 1978). This surprising result could be explained if the preferred location of 1-tetradecanol in the bilayer were such that its terminal methyl group extended beyond the terminal methyl groups of the lipid acyl chains. As Sallee's measurements were conducted on intestinal brush border membranes it is not possible to rigorously compare his results with those concerning DPPC. As their chain length is further increased alcohols are known to segregate within the membrane (Grunze et al., 1982). This phase separation implies that alcohol-alcohol interactions are stronger than alcohol-lipid

interactions for these long-chain alkanols.

B. DPPC/1-Octanol

1. Temperature dependence

The temperature dependence of the ^2H NMR spectrum of DPPC dispersions containing 25 mol % [$^2H_{17}$]-1-octanol was investigated and spectra for selected temperatures are presented in Figure 32. The 15°C spectrum in Fig. 32 has a shape generated by superimposed broad and narrow powder patterns. The low, rounded shoulders have a splitting of about 44 kHz, which is comparable to the 48 kHz splitting found for the humps in the spectrum of [4,4-$^2H_2$]-1-decanol in DPPC at 15°C (Fig. 26). In addition, there are sharper structures with smaller splitting (14.4 kHz) which are associated with the -C$^2H_3$ group of the 1-octanol. There is considerable intensity in the center of the 15°C spectrum as well, which, besides the signal from residual ^2HOH, could be due to a small amount of lateral phase separation of the [$^2H_{17}$]-1-octanol, caused by its reduced solubility in gel phase lipid (Jain et al., 1978; Diamond and Katz, 1974). At 28°C the broad component of the spectrum is still present although reduced in intensity because of the fast rate of decay of the quadrupolar echo ($1/T_{2e}$) at this temperature (Thewalt et al., 1985) The peaks due to the methyl group are sharper and closer together, and another pair of peaks, due to the -C$^2H_2$OH group of the 1-octanol, is emerging with $\Delta\nu_Q \approx 23$ kHz. Warming

Figure 32: The temperature dependence of the ^2H NMR spectrum of 25 mol % [$^2H_{17}$]-1-octanol in DPPC multilamellar dispersions. Spectral parameters: 15°C: pulse spacing = 75 μs; pulse length = 8 μs; sweep width = ±250 kHz; line broadening = 50 Hz; number of acquisitions = 2000; 28°C and 33°C: same parameters as at 15°C except: sweep width = ±100 kHz; 50°C: same parameters as at 33°C except: number of acquisitions = 8000.

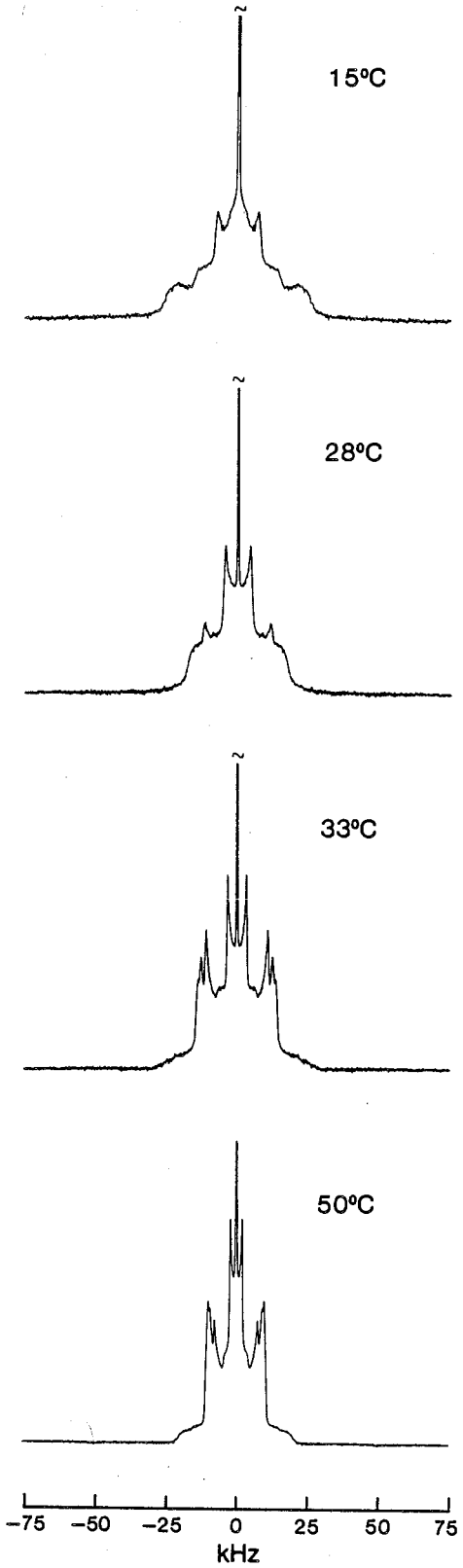
15°C
28°C
33°C
50°C
−75 −50 −25 0 25 50 75
kHz

the DPPC/[$^2H_{17}$]-1-octanol dispersion to 33°C produces a spectrum composed of a superposition of sharper powder patterns arising from the different $-C^2H_2-$ groups and from the $-C^2H_3$ group of the [$^2H_{17}$]-1-octanol. At 50°C, the system is completely in the liquid crystalline phase, and the ^2H quadrupolar splittings of the 1-octanol have narrowed compared with those at 33°C. Due to our method of symmetrizing the solid echo NMR spectra (Experimental Methods, p. 48) the chemical shift between $-C^2H_2OH$ and the remaining $-C^2H_2-$ groups reported by Pope et al. (1984) was not observed.

To improve the resolution of the powder spectra in Fig. 32 they were depaked. The three low temperature spectra from Fig. 32, plus a 25°C spectrum, are shown depaked in Fig. 33. At 15°C this procedure results in three clearly resolved quadrupolar doublets with splittings corresponding to $\Delta\nu_Q$ = 15.0, 28.5 and 50 kHz. These can be matched to the features in the 15°C powder spectrum (Fig. 32) with apparent splitting of 14.4, 28.0, and 44 kHz. The discrepancies in the measured splittings of powder and depaked spectral lines are due to the broadness of the resonance lineshapes at low temperatures.

The 25°C depaked spectrum of [$^2H_{17}$]-1-octanol in DPPC (Fig. 33) shows three resonances, but with narrower splittings of 11.1, 26.0, and 38 kHz. At 28°C three quadrupolar doublets appear at $\Delta\nu_Q$ = 9.04, 24.0, and 34 kHz. When the temperature is raised further the resonances sharpen and more peaks can be resolved, so that at 33°C peaks with $\Delta\nu_Q$ = 6.58, 21.8, 25.4 and 27.8 kHz are found. Based on the temperature dependencies of

Figure 33: The temperature dependence of the depaked ^{2}H NMR spectrum of 25 mol % [$^{2}H_{17}$]-1-octanol in DPPC multilamellar dispersions. Seven iterations were performed for each spectrum shown, with binomial smoothing before plotting.

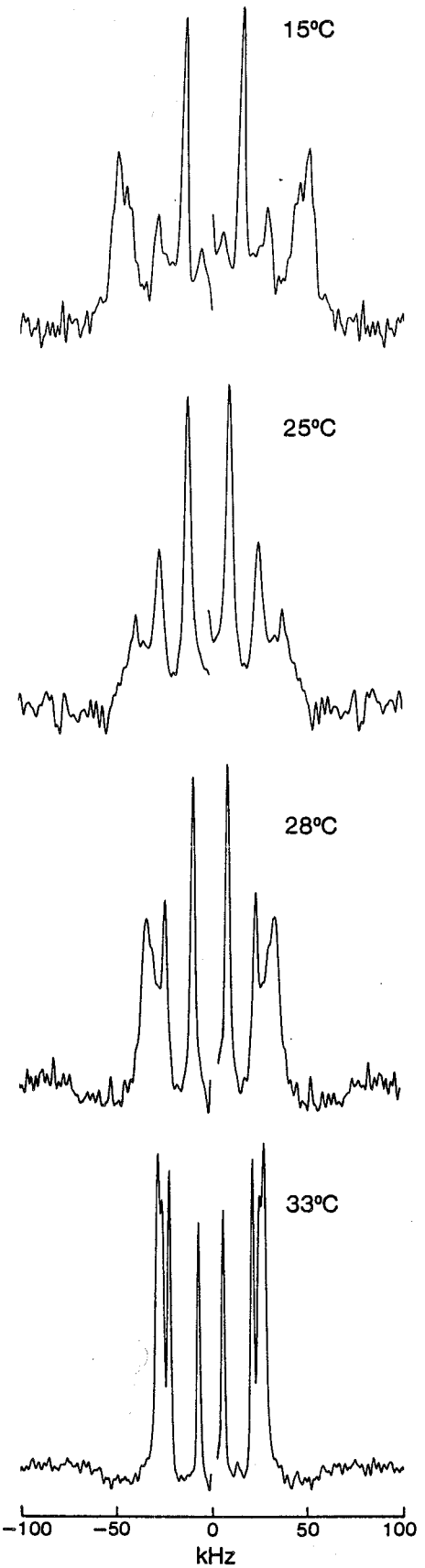
15°C
25°C
28°C
33°C
−100
−50
0
50
100
kHz

the peak positions, some assignments can be made. The inner doublet is due to the $-C^2H_3$ group, while the next narrowest doublet has only a small temperature dependence and is thus assigned to the $-C^2H_2OH$ group (Pope et al., 1984). The intensity of this pair of peaks is increased relative to the other resonances at 25°, 28° and 33°C compared with 15°C (Fig. 33), indicating that, at the higher temperatures, this doublet is the result of a superposition of the signals from the C-1 and, likely, the C-7 deuterons. The remaining $-C^2H_2-$ groups contribute to the broad, unresolved doublet in the 15°, 25° and 28°C spectra. At 33°C, this doublet has split into two, with the inner pair probably due to C-2 and/or C-6, in agreement with Pope et al., (1984).

Fig. 34 plots M_1 vs. temperature for the DPPC/[$^2H_{17}$]-1-octanol system. The discontinuities in the slope of this graph define the phase transition which occurs from ≈25°C to 39°C. All the M_1 values are substantially smaller for [$^2H_{17}$]-1-octanol than for any of the deuterated 1-decanols shown in Fig. 27 at any given temperature. As well, the maximum S_{CD} for [$^2H_{17}$]-1-octanol in DPPC at 50°C is 0.17, compared with S_{CD} = 0.20 for [5,5-$^2H_2$]-1-decanol in DPPC at 50°C. Thus, we conclude that 1-octanol is less ordered than 1-decanol in liquid crystalline DPPC dispersions at any given temperature. However, when the systems are compared at the same reduced temperature (Seelig and Browning, 1978), e.g. T = 37°C for DPPC/1-octanol and T = 50°C for DPPC/1-decanol, the maximum S_{CD} for both [$^2H_{17}$]-1-octanol and for [5,5-$^2H_2$]-1-decanol is 0.20. At 37°C, however, the

Figure 34: Variation of the first moment (M_1) with temperature for the ^2H NMR spectrum of 25 mol % [$^2H_{17}$]-1-octanol in DPPC multilamellar dispersions. Error bars are given for those temperatures where M_1 is a function of pulse spacing and is determined by extrapolation to zero pulse spacing.

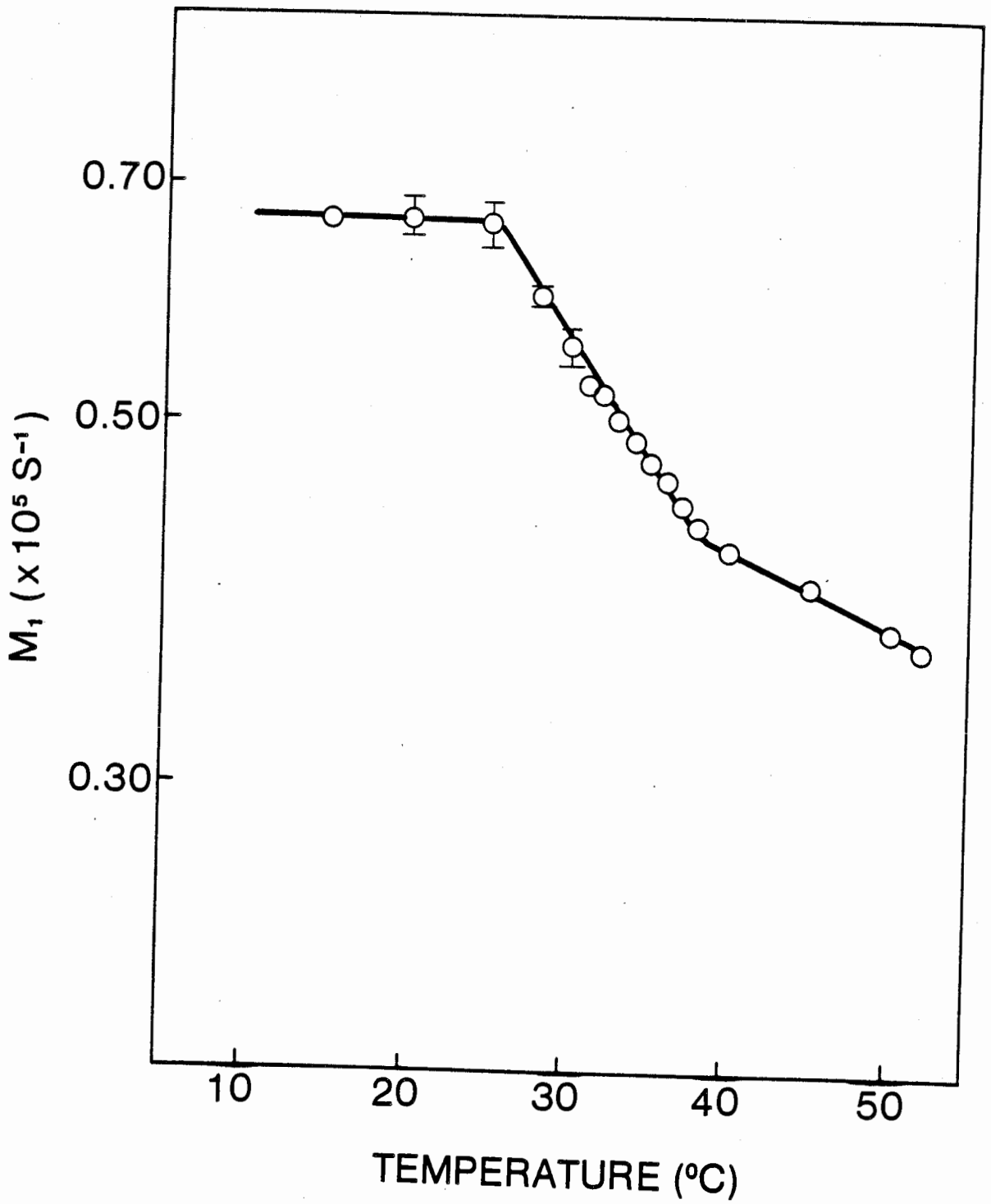
0.70
0.50
0.30
M_1 ($\times 10^5$ S^{-1})
10
20
30
40
50
TEMPERATURE (°C)

DPPC/1-octanol is not completely liquid crystalline so that this comparison may not be entirely valid. (Indeed, recently (Curatolo et al., 1985) the completion temperature of the phase transition instead of its onset temperature has been used to calculate the reduced temperature.) An alternative explanation is that the 1-octanol is too short to have a 'plateau' order parameter as large as that of the lipid acyl chains, and therefore C-4 and C-5 would have lower order due to the effect of increased motion at both ends of 1-octanol. Recently the proposition that 1-alkanols from 1-butanol to 1-octanol will tend to form clusters in DPPC has been made (Brasseur et al., 1985). This could also reduce the order parameter of 1-octanol.

Our work on [$^2H_{17}$]-1-octanol/DPPC multilamellar dispersions complements the recent results of Pope et al. (1984) who studied [$^2H_{17}$]-1-octanol/DMPC dispersions. The high T_m of DPPC (42°C) compared with DMPC (24°C) enabled us to measure the ^2H NMR spectrum of [$^2H_{17}$]-1-octanol in both gel and liquid crystalline phase lipid. At temperatures $\leq$ 25°C the phospholipid/1-octanol dispersion is in the gel phase as shown both by moment analysis (Fig. 34) and DSC (Thewalt et al., 1985). The ^2H NMR spectrum of [$^2H_{17}$]-1-octanol is a superposition of three quite broad powder patterns even at 15°C which means that, like the [4,4-$^2H_2$]-1-decanol already discussed, the 1-octanol is undergoing axially symmetric rotation in the gel phase lipid. The three observed S_{CD} values are: $-C^2H_3$ = 0.12; $-C^2H_2OH$ = 0.23; and $-(C^2H_2)_n-$ $\approx$ 0.4. The intensity in the centre of the 15°C spectrum in Fig. 32 is not consistent with 100 % of the 1-

octanol experiencing axially symmetric rotation, so there could be some proportion (≤15%) of the alcohol which is present in separate pools in the lamellae. No evidence of this second population is observed when the temperature is raised to 28°C.

Plotting $\Delta\nu_Q$ vs. temperature for the various quadrupolar doublets in the depaked spectra of [$^2H_{17}$]-1-octanol in DPPC dispersions yields curves qualitatively similar to those given in Fig. 4 of Pope et al. (1984), although our quadrupolar splittings are consistently smaller at a common reduced temperature, probably due to the much higher water content in our samples. A similar hydration effect has been reported in decanol/octanoate lamellae (Klason and Henrikkson, 1982).

IV. Deuterated Phosphatidylcholine/α-Tocopherol

In order to determine the effect of α-tocopherol on PC-d_{31} aqueous multilamellar dispersions three concentrations of α-tocopherol were employed: 5, 10 and 20 mol %. These dispersions were examined at various temperatures using DSC and ^2H NMR, and order parameter profiles were calculated for the liquid crystalline systems at 50°C.

A. DSC

DSC heating curves for 50 wt % aqueous multilamellar dispersions of PC-d_{31} containing 0, 5, 10 and 20 mol % α-tocopherol are presented in Fig. 35. Fig. 35a, in the absence of α-tocopherol, was discussed in Section I of this chapter. Figs. 35b-d demonstrate that the pretransition is removed, that the onset temperature of the main transition is progressively reduced, and that the main transition broadens as the concentration of α-tocopherol is increased. The temperatures of the main transition in the presence of α-tocopherol are: 5 mol %, 37°C (width at half height = 4°C); 10 mol %, 34°C (width = 5°C); and 20 mol %, 29°C (width = 8°C). These observations are consistent with other DSC studies (Cushley et al., 1979; Pohlmann and Kuiper, 1981; Massey et al., 1982; Lai et al., 1985), as well as with ESR and fluorescence depolarization work using Tempo (2,2,6,6-tetramethylpiperidine-N-oxyl) and DPH (diphenylhexatriene) probes, respectively, to monitor

Figure 35: DSC heating curves for 50 wt % aqueous multilamellar dispersions of: (a) PC-d_{31}; (b) PC-d_{31}/5 mol % α-tocopherol; (c) PC-d_{31}/10 mol % α-tocopherol; and (d) PC-d_{31}/20 mol % α-tocopherol. Scanning rate was 10°C/min over the temperature range -30°C to +70°C.

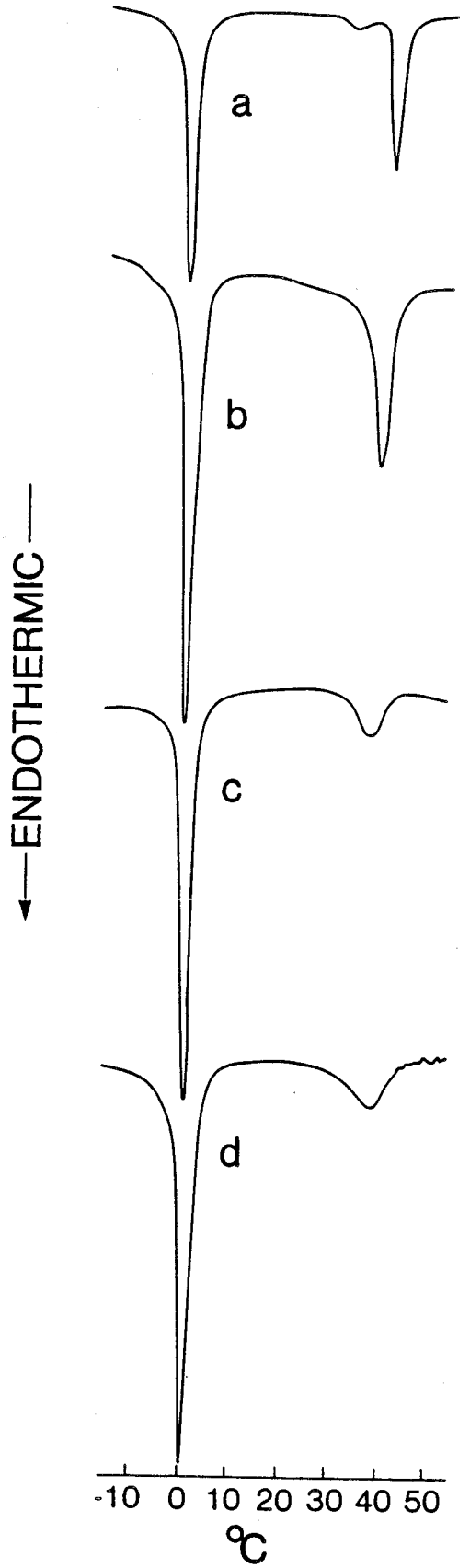
a
b
c
d
ENDOTHERMIC
-10 0 10 20 30 40 50
°C

phospholipid membrane phase (Srivastava et al., 1983; Fukuzawa et al., 1980). Indeed, the agreement with previous DSC data is quantitatively excellent. Pohlmann and Kuiper reported, for instance, that 10 mol % α-tocopherol reduces the onset and peak values for the main transition temperature of DPPC multilayered liposomes by 5°C and 2°C respectively. The corresponding values recorded here for PC-d_{31} are 6°C and 2°C.

B. ^2H NMR

1. Temperature dependence

Deuterium NMR allows the influence of α-tocopherol on aqueous multilamellar dispersions of PC-d_{31} to be examined in much greater detail. Spectra recorded as a function of temperature for 50 wt % aqueous multilamellar dispersions of PC-d_{31}/20 mol % α-tocopherol and PC-d_{31} are compared in Fig. 36. At -15°C, the spectra (Figs. 36a and 36d) are essentially identical for both samples. They have a broad component with edges at ±63 kHz, indicating a substantial proportion of the methylenes are static, and a central component with a pair of peaks split by 17-19 kHz. The large intensity of this central component implies that, in addition to methyls, methylenes contribute and thus are undergoing reorientational motion. Note that the central component has a slightly narrower splitting in the presence of α-tocopherol.

Gel state spectra are obtained at 20°C for the two systems

Figure 36: Temperature dependence of ^2H NMR spectra for 50 wt % aqueous multilamellar dispersions of: (a-c) PC-d_{31}/20 mol % α-tocopherol; and (d-f) PC-d_{31}. Note that (c) and (f) are plotted on an expanded frequency scale. Spectral parameters: pulse spacing = 75μs; pulse length = 6.5 μs; line broadening = 50 Hz; (a), (b), (d) and (e) sweep width = ±250 kHz; number of acquisitions= 1000; (c) and (f) sweep width = ±100 kHz; number of acquisitions = 2000.

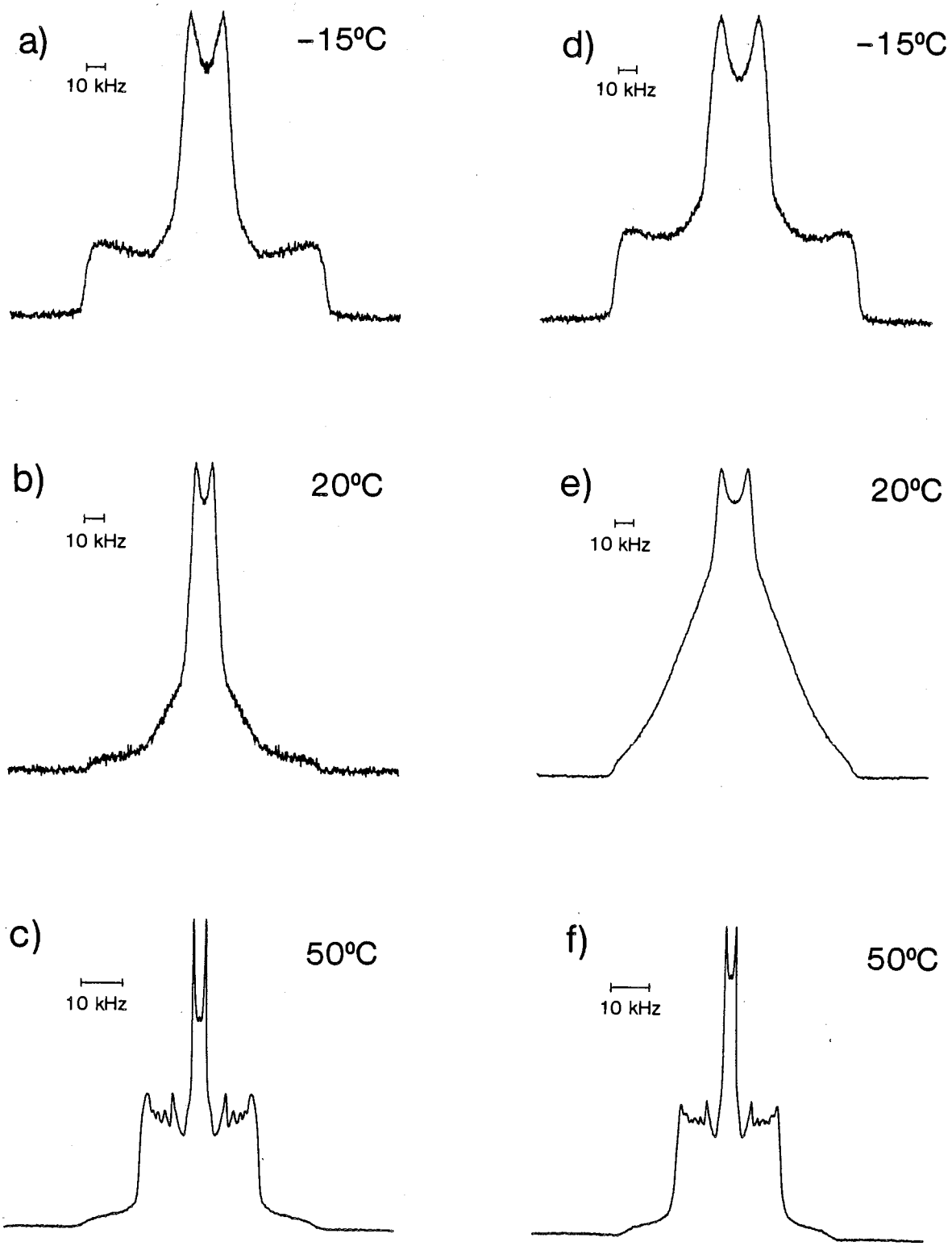
a)
10 kHz
-15°C
d)
10 kHz
-15°C
b)
10 kHz
20°C
e)
10 kHz
20°C
c)
10 kHz
50°C
f)
10 kHz
50°C

(Figs. 36b and 36e). However, quantitatively the shapes of the spectra differ. In the absence of α-tocopherol (Fig. 36e), the shoulders at ±63 kHz have almost disappeared and there has been a broad, featureless increase in intensity towards the center, as discussed in Section I of this chapter. For PC-d_{31}/20 mol % α-tocopherol (Fig. 36b) the spectrum's broad component is reduced in intensity, and the splitting of its narrow component is considerably smaller than the corresponding features in Fig. 36e. At 50°C (Figs. 36c and 36f) both systems are in the liquid crystalline phase, displaying axially symmetric powder patterns possessing well defined, sharp edges (at ±13-14 kHz) associated with a plateau in the variation of the order parameter S_{CD} with position along the phospholipid acyl chain. Upon close examination of these two spectra it is apparent that the PC-d_{31}/20 mol % α-tocopherol spectrum (Fig. 36c) is generally broader than that of pure PC-d_{31}, with larger frequency separations between its components' 90° 'edge' features.

In contrast to the ^2H NMR spectrum of a pure PC-d_{31}/water dispersion, which narrows suddenly at 39-40°C, the spectrum for PC-d_{31}/20 mol % α-tocopherol/water does not undergo an abrupt change from a gel state spectrum of the form observed at 20°C (Fig. 36b) to a spectrum characteristic of the liquid crystalline phase. Instead, a number of gradual temperature dependent changes are exhibited before a liquid crystalline state spectrum of the form depicted in Fig. 36c is attained at temperatures > 38°C.

Fig. 37 elaborates upon the variation with temperature

Figure 37: Examination of changes in ^2H NMR spectra as a function of temperature for aqueous (50 wt % deuterium depleted water) multilamellar dispersions of PC-d_{31}/20 mol % α-tocopherol. Spectral parameters: pulse spacing = 75 μs; pulse length = 6.5 μs; line broadening = 50 Hz; number of acquisitions = 1000; (a)-(e) sweep width = ±250 kHz; (f) sweep width = ±100 kHz.

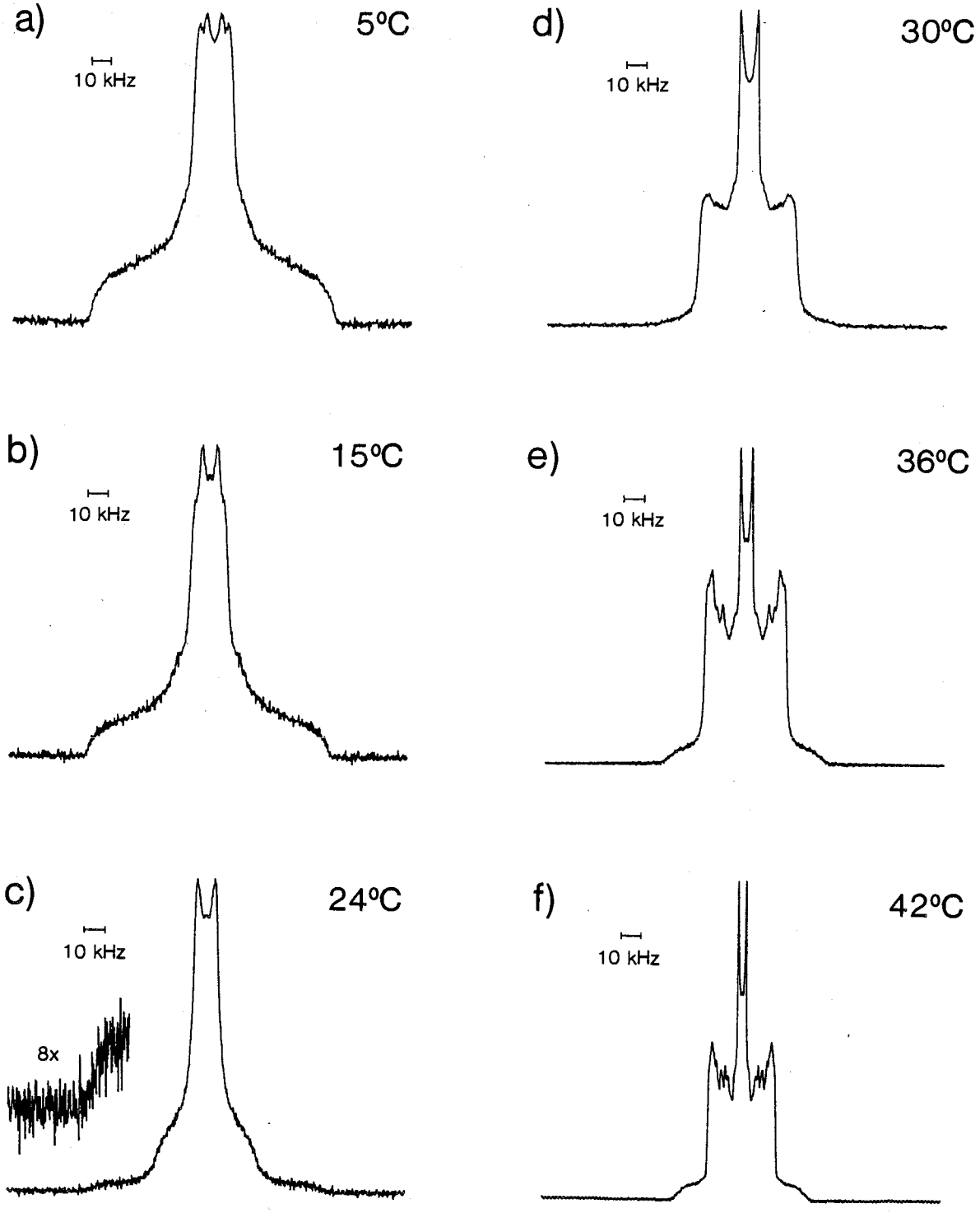
a)
5°C
10 kHz
d)
30°C
10 kHz
b)
15°C
10 kHz
e)
36°C
10 kHz
c)
24°C
10 kHz
8x
f)
42°C
10 kHz

observed for ^2H NMR spectra of PC-d_{31}/20 mol % α-tocopherol aqueous multilamellar dispersions. At 5°C (Fig. 37a), it is apparent that the increase in temperature from -15°C (Fig. 36a) has produced a reduction in intensity in the wings of the spectrum and development of an extra pair of peaks (splitting = 8-10 kHz) in the center. This pair of peaks is presumably due to less ordered methyl groups and, as illustrated by Fig. 37b, increases in intensity with increasing temperature until at 20°C (Fig. 36b) it dominates the central portion of the spectrum. A new component, a rounded "hump" of width ≈ 50 kHz probably representing rapidly reorienting methylenes, is formed at higher temperature (Fig. 37c) and, together with the central methyl component, comprises the entire spectrum at 30°C (Fig. 37d). Figs. 37e and 37f then demonstrate that further increases in temperature lead to resolution of individual peaks within the methylene component. The latter spectrum, at 42°C, essentially corresponds to the characteristic liquid crystalline phase powder pattern obtained at 50°C (Fig. 36c). A possible explanation of this behaviour is in terms of reorientation of the methylene chain as a whole at 30°C, and the increase in rate of trans-gauche isomerization as temperature rises further.

The temperature dependencies of ^2H NMR spectra collected for aqueous multilamellar dispersions of PC-d_{31}/10 mol % α-tocopherol and PC-d_{31}/5 mol % α-tocopherol are qualitatively similar to that seen when 20 mol % α-tocopherol is present. The same spectral changes occur, but over a narrower temperature range. In the presence of 5 mol % α-tocopherol (Fig. 38) a

Figure 38: Temperature dependence of ^2H NMR spectra for 50 wt % aqueous multilamellar dispersions of PC-d_{31}/5 mol % α-tocopherol. Spectral parameters: pulse spacing = 75 μs; pulse length = 6.5 μs; line broadening = 50 Hz; sweep width = ±250 kHz except at 50°C sweep width = ±100 kHz; number of acquisitions = 1000 (15°C, 35°C and 37°C), 2000 (33°C) and 8000 (50°C).

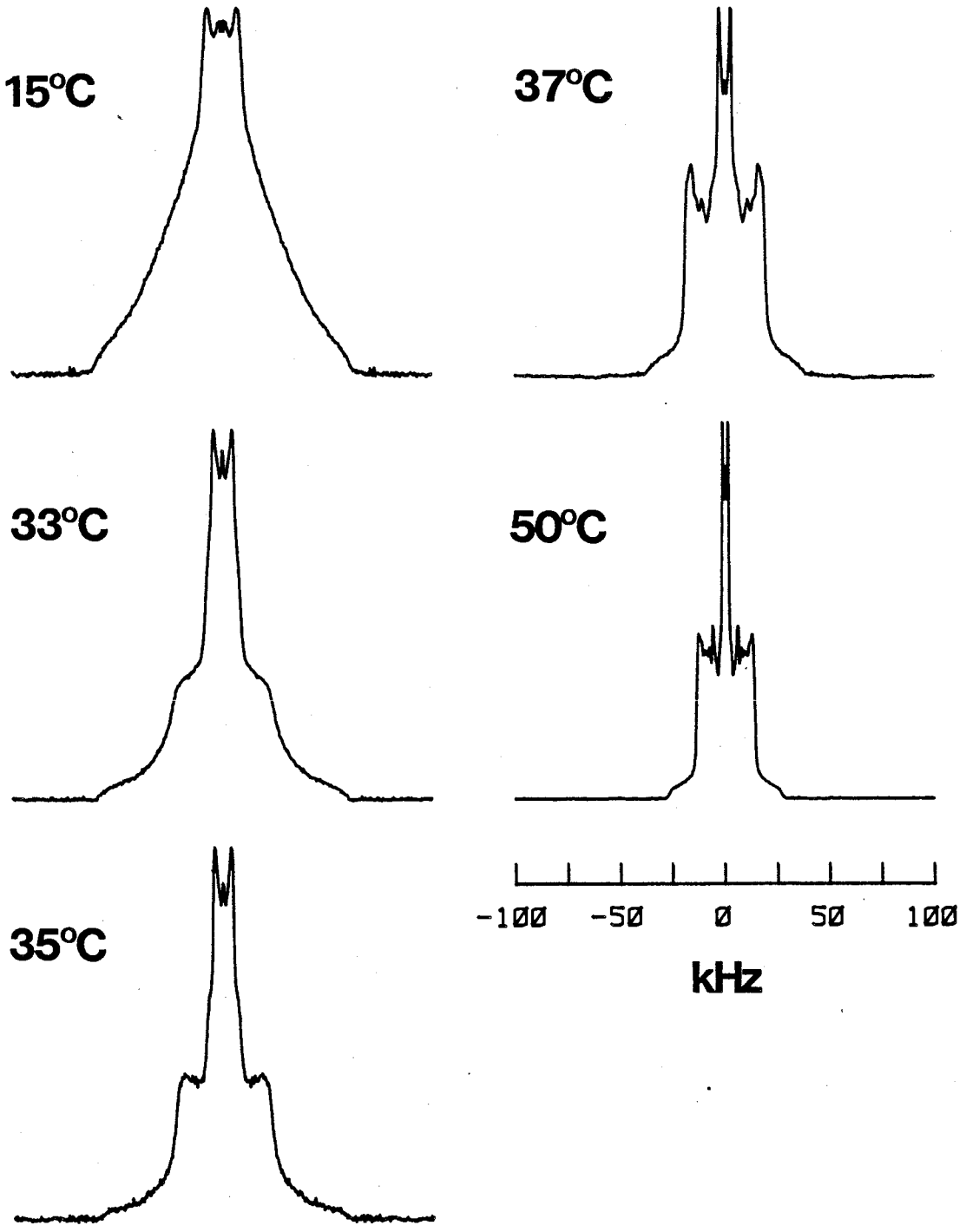
15°C
37°C
33°C
50°C
35°C
-100
-50
0
50
100
kHz

typical gel state spectrum (cf. Fig. 36e) is still recorded at 15°C, while at 35°C the spectrum is qualitatively similar to Fig. 37d (30°C). These spectral changes are illustrated for PC-d_{31}/10 mol % α-tocopherol in Fig. 39, for comparison purposes. For all α-tocopherol concentrations employed, spectra characteristic of liquid crystalline phospholipid are observed at 38-40°C.

Moment analysis facilitates more quantitative interpretation of temperature-dependent spectral changes. First moments M_1 calculated from the ^2H NMR spectra for PC-d_{31}/water, PC-d_{31}/10 mol % α-tocopherol/water and PC-d_{31}/20 mol % α-tocopherol/water samples are plotted vs. temperature in Fig. 40. The uncertainty in the data is $< \pm 1\%$, except in the presence of α-tocopherol when the uncertainty is on the order of ±5% for temperatures approaching the gel to liquid crystalline transition. In this temperature region (15°C to 37°C, depending on α-tocopherol content) the first moment depends markedly on the delay time τ between the two 90° pulses of the solid echo sequence. The values plotted were obtained by extrapolation to zero delay of M_1 measured as a function of τ. Similar behaviour of M_1 vs. τ was discussed in Section II of this chapter. Inspection of Fig. 40 shows that the transition from gel to liquid crystalline state values for the first moment spans a much wider range of temperature when α-tocopherol is present. For PC-d_{31}/20 mol % α-tocopherol/water the onset and completion temperatures of the transition are approximately 28°C and 40°C, respectively. At 10 mol % α-tocopherol incorporation the

Figure 39: Temperature dependence of ^2H NMR spectra for 50 wt % aqueous multilamellar dispersions of PC-d_{31}/10 mol % α-tocopherol. Spectral parameters: pulse spacing = 75 μs; pulse length = 6.5 μs; line broadening = 50 Hz; sweep width = ±250 kHz except at 50°C sweep width = ±100 kHz; number of acquisitions = 1000 (16°C and 28°C), 2000 (32°C), 4000 (35°C) and 8000 (50°C).

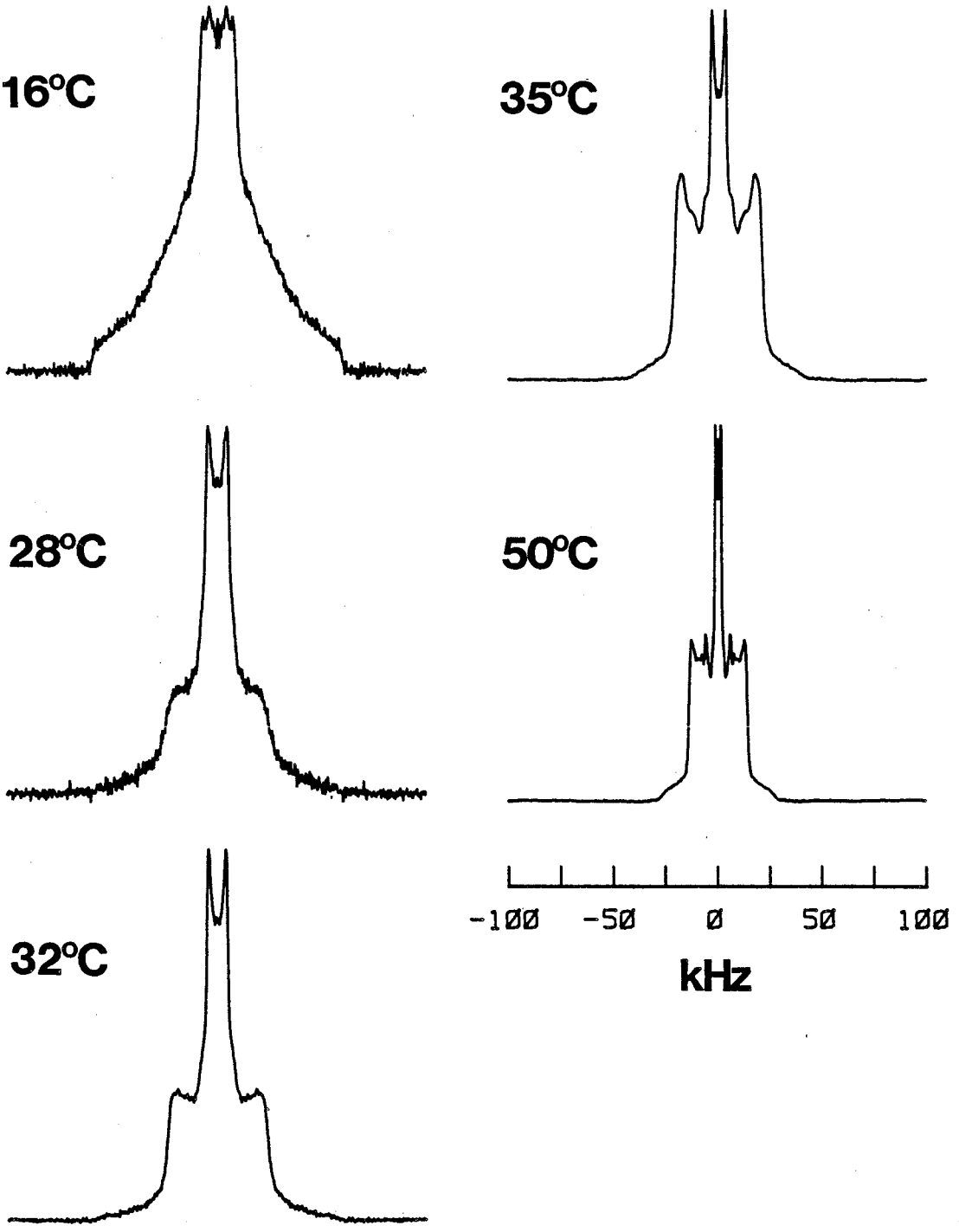
16°C
35°C
28°C
50°C
32°C
-100
-50
0
50
100
kHz

Figure 40: Variation of the first moment M_1 with temperature for 50 wt % aqueous multilamellar dispersions of: (○) PC-d_{31}; (△) PC-d_{31}/10 mol % α-tocopherol; and (□) PC-d_{31}/20 mol % α-tocopherol.

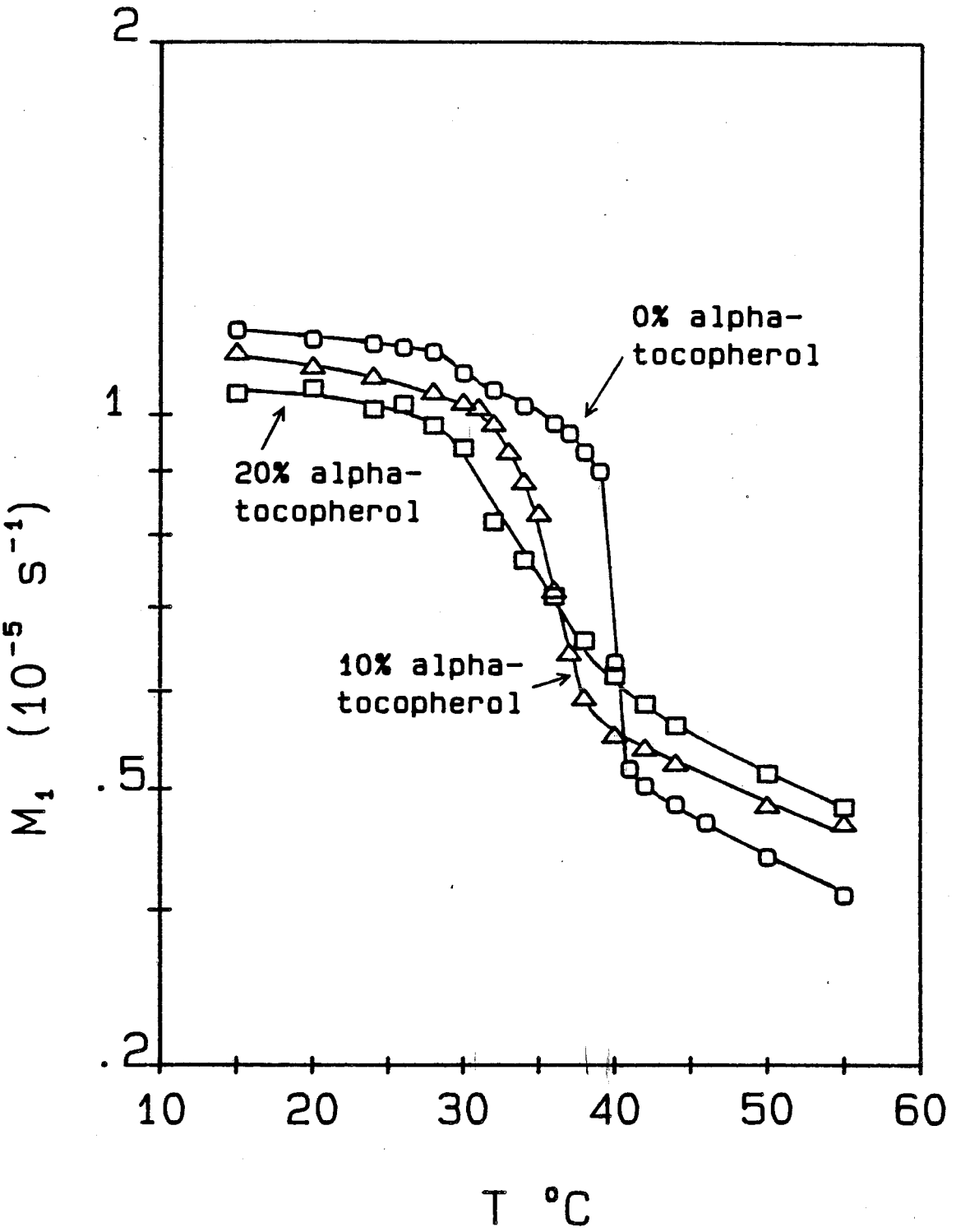
2
1
.5
.2
M_1 (10^{-5} S^{-1})
0% alpha-tocopherol
20% alpha-tocopherol
10% alpha-tocopherol
10
20
30
40
50
60
T °C

transition is broadened to a lesser degree, extending from about 32-40°C. The same trend continues for PC-d_{31}/5 mol % α-tocopherol/water (not included in Fig. 40 for purpose of clarity), with a transition range of 35-40°C. Thus the graphs of first moment M_1 vs. temperature (Fig. 40) display the same trend in phase behaviour as seen by DSC. In the absence of α-tocopherol, the transition from gel to liquid crystalline state values for M_1 is sharp at 39-41°C and is preceded approximately 10°C below by a small discontinuity associated with the pretransition. In the presence of α-tocopherol, no pretransition is discernible and the main transition is increasingly broadened with increasing α-tocopherol concentration. This broadening, also shown by DSC, is a consequence of a depression of the onset temperature for the transition. Little change (< 2°C) occurs in the transition's completion temperature.

Below the main transition temperature, α-tocopherol appears to disrupt the packing of gel-phase phospholipid. This is indicated by the spectral changes which occur upon addition of α-tocopherol to PC-d_{31} as illustrated in Figs. 36-39, and by the reduced values of M_1 at low temperatures in the presence of α-tocopherol shown in Fig. 40. This disruption to the interior of gel state bilayers may be reconciled with permeability measurements on model membrane systems. Specifically, the permeability of DPPC bilayers to water and glucose has been found to be increased below the temperature of the main transition for the unperturbed system when α-tocopherol is

introduced (Fukuzawa et al., 1979; Pohlmann and Kuiper, 1981). Such a response is consistent with increased acyl chain mobility or with the presence of a larger number of packing defects in the gel-phase lipid. The addition of cholesterol is also known to increase permeability below the transition temperature (De Gier et al., 1969) and many of the effects of cholesterol on phospholipid membranes resemble those seen with α-tocopherol. In particular, the gel to liquid crystalline transition is broadened and the onset temperature lowered by cholesterol (McElhaney, 1982). However, the endotherm, as revealed by high sensitivity DSC, is composed of sharp and broad components in the presence of cholesterol whereas, admittedly at lower sensitivity, only a single broad transition is observed with α-tocopherol (Fig. 35). As well, ^2H NMR experiments employing selectively deuterated DMPC indicate that incorporation of cholesterol leads to additional acyl chain motion below the main transition temperature for the pure phospholipid (Haberkorn et al., 1977; Jacobs and Oldfield, 1979; Oldfield et al., 1978).

2. Order parameters

Referring to Fig. 40, at temperatures above the phase transition higher values of first moments demonstrate that introduction of α-tocopherol increases phospholipid acyl chain order within liquid crystalline PC-d_{31} bilayers. More detailed information on the influence of α-tocopherol on acyl chain ordering becomes accessible following depaking (Sternin et al.,

1983) of the ^2H NMR spectra. Depaked ^2H NMR spectra for aqueous multilamellar dispersions of PC-d_{31} in the absence and presence of 20 mol % α-tocopherol at 50°C are compared in Fig. 41. Both spectra contain 5 well resolved doublets, plus a broad, composite pair of outermost peaks possessing a shoulder on its inner side. Similar depaked spectra were obtained at 5 mol % and 10 mol % incorporation of α-tocopherol. The peak labels define assignments to *sn*-2 [$^2H_{31}$]palmitoyl segments.

Profiles of order parameter S_{CD} vs. phospholipid chain position constructed from the depaked spectra in Fig. 41 are plotted in Fig. 42. The shaded areas signify that splittings measured for the outermost pair of peaks do not necessarily correspond to a single mean value but lie within a range determined by the width of the composite signal. The shape of the profile is essentially unaffected by the intercalation of 20 mol % α-tocopherol into the PC-d_{31} bilayer, since in both its absence and presence, the profile consists of a characteristic plateau of almost constant order in the upper portion of the chain and then a gradual decrease in order towards the center of the bilayer. The effect of α-tocopherol appears to be an overall higher degree of ordering along the entire lipid chain. The plateau values of S_{CD} for PC-d_{31}/20 mol % α-tocopherol/water and PC-d_{31}/water are 0.23 and 0.20, respectively. Profiles for PC-d_{31}/5 mol % α-tocopherol/water and PC-d_{31}/10 mol % α-tocopherol/water at 50°C fall between those plotted in Fig. 42, the vertical displacement increasing with α-tocopherol content. For an α-tocopherol content of 5 mol % the plateau value of S_{CD}

Figure 41: Depaked ^2H NMR spectra at 50°C for 50 wt % aqueous multilamellar dispersions of: (a) PC-d_{31}; and (b) PC-d_{31}/20 mol % α-tocopherol. Peak labels specify assignments to *sn*-2 [$^2H_{31}$]palmitoyl segments. Six iterations were performed on the powder pattern data for both (a) and (b).

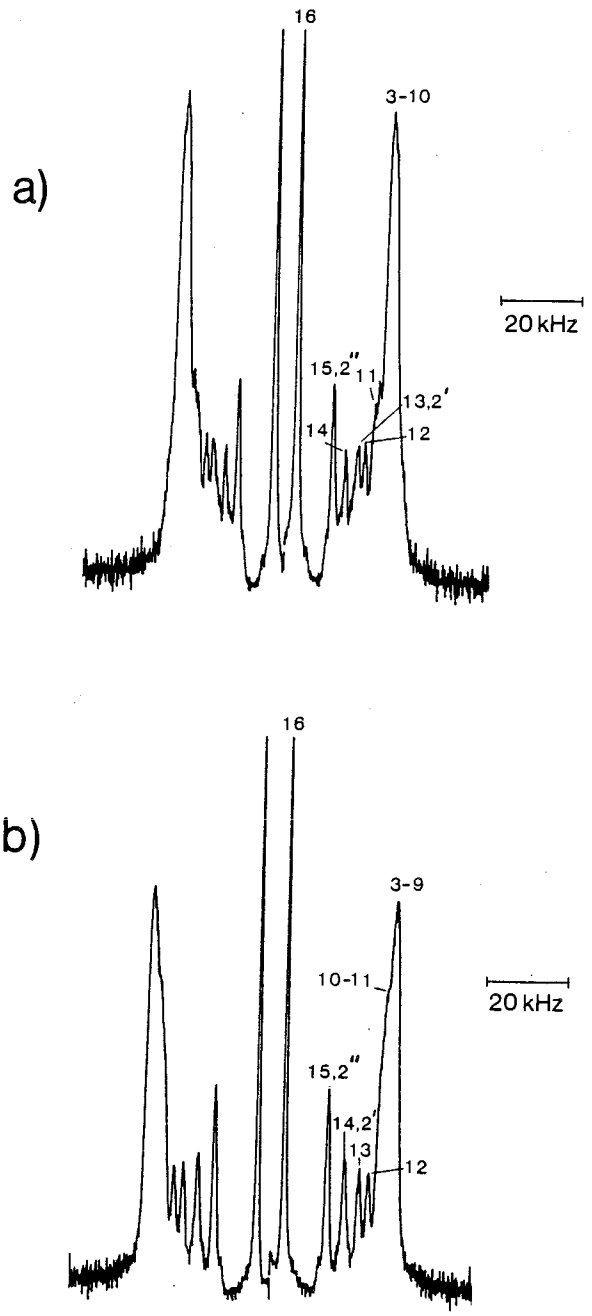
a)
16
3-10
20 kHz
15,2"
11
13,2'
14
12
b)
16
3-9
10-11
20 kHz
15,2"
14,2'
13
12

Figure 42: Order parameter profiles of S_{CD} vs. position along the phospholipid *sn*-2 chain at 50°C for: (○) PC-d_{31}; and (□) PC-d_{31}/20 mol % α-tocopherol. The order parameters for C-3 to C-11 lie within ranges indicated by the shading. The shading represents the S_{CD} values at splittings determined by the width at half-height of the broad composite peaks in Fig. 41.

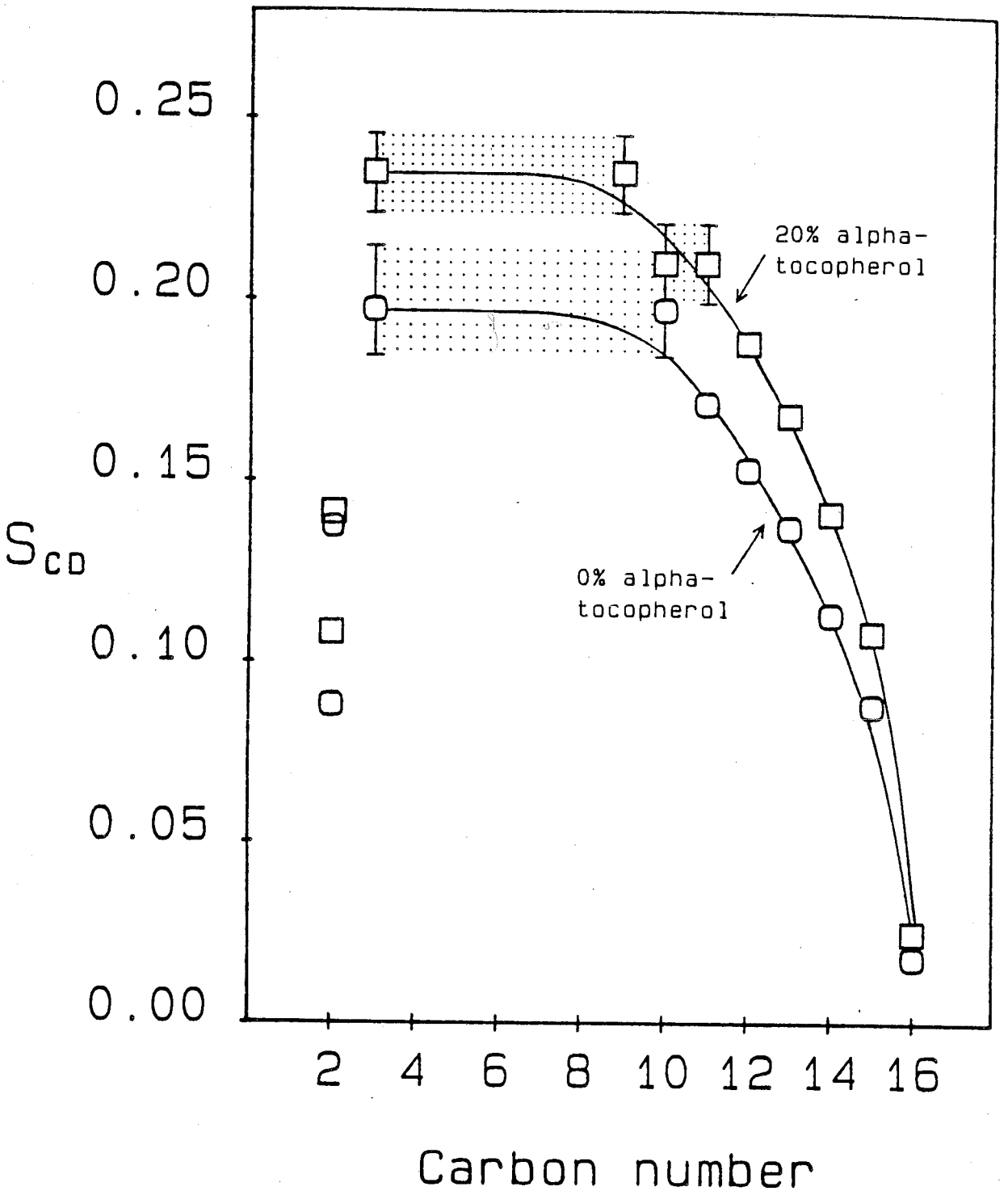
0.25
0.20
0.15
0.10
0.05
0.00
S_{CD}
20% alpha-
tocopherol
0% alpha-
tocopherol
2
4
6
8
10
12
14
16
Carbon number

is 0.21 while for 10 mol % it is 0.22, at 50°C.

In contrast to the gel phase, interpretation of the ^2H NMR spectra recorded for multilamellar dispersions of PC-d_{31}/water and PC-d_{31}/α-tocopherol/water is relatively straightforward above the main transition. Here the spectra with and without α-tocopherol are axially symmetric powder patterns typical of phospholipids in the liquid crystalline state (Figs. 36c and 36f). It may be immediately concluded from the similar overall shape, but increased width, of the spectrum in Fig. 36c compared with Fig. 36f that α-tocopherol orders the membrane interior without appreciably altering the form of the profile of ordering along the PC-d_{31} chain. The average order parameters S_{CD} calculated from the first moments M_1 are increased by α-tocopherol. The extent of this increase is about 17% for 20 mol % incorporation. The profiles of order parameter S_{CD} vs. acyl chain position constructed in Fig. 42 from the depaked spectra (Fig. 41) confirm that the general form of the profile is maintained when α-tocopherol is introduced. The two profiles plotted for PC-d_{31}/water and PC-d_{31}/20 mol % α-tocopherol/water both display the characteristic plateau of almost constant order near the aqueous interface followed by a progressive reduction in order parameter in the lower part of the phospholipid acyl chain. An upward shift of the entire order profile, due to increased ordering throughout the bilayer interior by α-tocopherol, is the only significant difference.

An ESR spin label measurement of order employing 5-doxyl stearic acid in egg yolk phosphatidylcholine (egg PC)

multilayers (Cushley et al., 1979) offers the most direct comparison with the current study. A 20 mol % concentration of α-tocopherol was seen to affect the spin label order parameter S_3 by a negligible amount at 23°C. An explanation for this discrepancy between the ESR and ^2H NMR data is that perturbation problems associated with the bulky nitroxide spin label (especially when it is situated close to the lipid/water interface) are responsible (Taylor and Smith, 1983). The non-perturbing ^2H NMR method more truly reflects the order within the membrane interior. It should be noted that in another ESR investigation using stearic acid spin labels 28 mol % of the closely related compound α-tocopheryl acetate was found to slightly increase order in the inner part of DPPC membranes (Schmidt et al., 1976). This increase in order was only significant at temperatures of 41-55°C, and the differences in order disappeared by 60°C (less than 20° above the phase transition temperature of pure DPPC) for all spin labels. Also, α-tocopheryl acetate is less polar than α-tocopherol and is thus not expected to be located at the same depth in the bilayer.

It is possible to interpret the results of other publications reporting the effects of α-tocopherol on the properties of liquid crystalline model membranes in terms of the possible consequences of an increase in acyl chain order. These include reports of decreased permeability in the presence of α-tocopherol (Diplock et al., 1977; Fukuzawa et al., 1979; Stillwell and Bryant, 1983) and reductions in acyl chain fluidity as indicated by fluorescence polarization experiments

when α-tocopherol is added (Massey et al., 1982) (By "fluidity" it is meant the inverse of the microviscosity of the bilayer interior immediately surrounding the probe. The microviscosity can then be related to the intermolecular free volume (Shinitzky and Yuli, 1982).). Both effects might be expected to accompany increased ordering within the bilayer, although this is not strictly necessary.

The influence of α-tocopherol on liquid crystalline PC-d_{31} resembles that observed with cholesterol in a number of phospholipid bilayer systems. Increased acyl chain order due to cholesterol has been widely described. ^2H NMR studies have shown that while cholesterol leads to higher acyl chain order it does not disturb the overall shape of the ordering profile within the membrane (Oldfield et al., 1978). The extent of the increase is also comparable to that recorded here for α-tocopherol, 17 mol % cholesterol causing approximately 20% higher order in egg PC bilayers as monitored using intercalated [$^2H_{35}$]stearic acid (Stockton and Smith, 1976). The similarity between the effects of α-tocopherol and cholesterol extends even further, since cholesterol is known to decrease rates of permeability to glycerol and erythritol in liquid crystalline membranes such as egg PC (De Gier et al., 1968).

SUMMARY AND CONCLUSIONS

I. Effect of 1-Alkanol Anesthetics on Model Membrane Systems.

A. Phase transition effects

Changes in the thermotropic phase behaviour of aqueous multilamellar dispersions of PC-d_{31} due to incorporation of 1-alkanols can be followed using ^2H NMR or DSC. Pure PC-d_{31}/water dispersions display two phase transitions, a pretransition at 31°C and a main transition at 40°C. These are qualitatively similar to the transitions occurring in aqueous dispersions of DPPC. Phase transition temperatures determined by ^2H NMR are generally 1-3° lower than those obtained by DSC, and correspond more closely with the temperature at which the DSC endotherm first departs from the baseline.

Upon addition of 1-octanol or 1-decanol the PC-d_{31} pretransition disappears. This is likely due to a change in the gel phase packing of the phospholipid. In DPPC dispersions in the gel phase, X-ray diffraction measurements (Tardieu et al., 1973) reveal that the acyl chains are tilted with respect to the bilayer normal. This has been explained as resulting from differences in cross-sectional area between headgroup and acyl chains. The bulky phosphatidylcholine headgroup is larger in cross-section than the two acyl chains, so that if the chains were parallel to the bilayer normal, crowding would occur in the headgroup region. Hence the observation of acyl chain tilt,

which increases the surface area but decreases the thickness of the bilayers. Added 1-alkanols, by acting as molecular 'spacers', would allow the elimination of the acyl chain tilt.

Both 1-octanol and 1-decanol cause the main transition temperature to lower and the width of the main transition to increase. The lowering of T_m means that the alkanols interact preferentially with liquid crystalline phospholipid. They are less soluble in gel phase lipid, acting to disrupt the tight acyl chain packing in this region. 1-Octanol has a larger effect on T_m than 1-decanol as its shorter chain length provides a poorer match with the lipid acyl chains, and hence disrupts the gel phase to a greater extent. The increased width of the phase transition when alcohols are present is ascribed to a reduction in the size of the cooperative unit of the phospholipid. (Cooperativity is a measure of the extent to which phospholipid molecules interact when melting.) Aqueous dispersions of pure DMPC have a cooperative unit which has been measured as being greater than 1700 molecules (Knoll, 1984). Inserting alkanols into the bilayer limits the phospholipid acyl chain interactions and the size of the cooperative unit is correspondingly reduced. The above information is attainable using either DSC or ^2H NMR of PC-d_{31}. DSC allows the pretransition to be defined more easily, but ^2H NMR gives a greater amount of knowledge about the state of the phospholipid dispersions below and above the transition.

When using DPPC containing selectively deuterated 1-decanols ^2H NMR provides a clear picture of the transition in

the local environment of the label. Spectra of DPPC/[9,9-$^2H_2$]1-decanol narrow suddenly from 36°C to 37°C, while those of DPPC/[2,2-$^2H_2$] or [4,4-$^2H_2$]1-decanol narrow more gradually from 37°C to ≈41°C. This indicates that the increased trans-gauche isomerisation rate that accompanies the phase transition occurs first in the centre of the bilayer and then works out to the lipid/water interface.

DPPC/[$^2H_{17}$]1-octanol, being perdeuterated, gives results which are less straightforward to interpret. It is clear, however, that the alcohol's NMR spectra mirror the state of the phospholipid in which it is immersed. Thus the octanol's spectral moment M_1 lessens through the phase transition region, reflecting the greater amount of orientational freedom it has. Similarly, preliminary measurements show that [$^2H_{17}$]1-octanol in egg PC has a narrower spectrum than in egg PC/cholesterol (2:1) at ambient temperature (J. Thewalt, unpublished results), indicating that the alcohol registers the well-known ordering effect of cholesterol in liquid crystalline lamellar systems.

These results confirm what has been found by many other researchers, that octanol and decanol reduce the main phase transition temperature of saturated phosphatidylcholine dispersions. As pointed out in the Introduction, anesthesia mechanisms based on critical regions of lipid poised at their phase transition temperatures are doubtful, largely because of the absence of demonstrable phase changes in mammalian membranes at physiological temperatures. Nevertheless it is important to know the phase transition effects of the membrane perturbant

under study before effects on order parameter can be correctly interpreted. An apparent lowering of the order parameter may in fact be a direct result of a reduction in T_m, rather than an intrinsic disordering capability of the anesthetic. (Since anesthesia is an essentially isothermal process, though, comparative measurements of the state of the lipid at a given temperature are still interesting.)

B. Order parameter effects

The work reported in Sections II and III of the Results and Discussion concerns a binary lipid dispersion whose only components (neglecting water) are phosphatidylcholine and 1-alkanol. This is the simplest type of system possible for such a study and thus represents a logical starting point in the determination of membrane/1-alkanol interactions. The lack of effect of high bilayer concentrations of 1-octanol or 1-decanol on the degree of orientational order at all segments of the phospholipid acyl chains means that in the liquid crystalline phase the alcohol methylene chain is orientationally indistinguishable from neighbouring phospholipid methylene chains, at least on the NMR time scale (microseconds). Thus trans-gauche isomerizations of the phospholipid acyl chains are neither facilitated nor restricted by dissolved 1-octanol or 1-decanol.

The results from the DPPC/deuterated 1-alkanol systems are complementary to those from the more usual deuterated

phospholipid/1-alkanol systems. The major finding is that in the liquid crystalline phase the order parameter profile of 1-decanol is similar to that of the phospholipid acyl chain when the former's shorter chain length and lack of covalent bonding to the glycerol backbone are taken into account. The average depth of 1-decanol in the liquid crystalline DPPC bilayer is from between the *sn*-2 chain's C-3 and C-4 segments to between its C-13 and C-14 segments.

Such a definite statement is not possible with the [$^2H_{17}$]1-octanol results due to the ambiguities associated with the spectra of perdeuterated molecules. The maximum order parameter for an aqueous dispersion of DPPC/[$^2H_{17}$]1-octanol at 50°C is 0.16 (80% of the maximum order parameter of DPPC/selectively deuterated 1-decanol) while the order parameter for the C^2H_3 group of the [$^2H_{17}$]1-octanol is 0.034, nearly as high as [10,10,10-$^2H_3$]1-decanol's S_{CD}=0.035. It is probable that the octanol's chain length is too short for it to have a plateau value of S_{CD} consistent with that of the phospholipid. This seems reasonable given that the "plateau" for 1-decanol in DPPC is only two segments long (C-4 and C-5). As a result the estimation of 1-octanol's depth in the bilayer is not straightforward. The longer 1-alkanols' (eg. 1-dodecanol or 1-tetradecanol) order parameter profiles would presumably give a direct measurement of their depth in DPPC bilayers and would be interesting to study provided that the appropriate deuterium-labelled alcohols were available.

In gel phase DPPC bilayers the selectively deuterated 1-

decanols give very similar spectra whether the label is on C-2, C-4, C-7 or C-9. These spectra appear to be broad powder patterns and are consistent with the alcohol rotating as a whole about its long axis. (There may in addition be some intensity in the centre of the spectrum due to alcohol whose motion is more restricted - this is certainly seen in the low temperature DPPC/[$^2H_{17}$]1-octanol's spectra.) In contrast, chain rotation and other motions in the gel phase phosphatidylcholine are thought to be intermediate or slow on the NMR time scale (Meier et al., 1983), resulting in non-axially symmetric spectral shapes.

Previous workers using ESR spin labelling techniques reported that long chain alcohols disorder multilamellar liposomes (Pringle et al., 1981; Lawrence and Gill, 1975; Lyon et al., 1981). The results in this thesis do not support these findings, since no change in the ^2H NMR order parameter profile was found upon the incorporation of 25 mol % 1-octanol or 1-decanol. This apparent contradiction may be a result of the different membrane systems employed by different researchers. This was noted by Miller and Pang (1976), who surmised that the presence of cholesterol is necessary in order to observe the disordering effect of anesthetics. The reason for this dependence on cholesterol is not known, but any proposed "disordered lipid" hypothesis of anesthesia should be able to explain the absence of disordering of pure phospholipid dispersions by long chain alcohols.

The phase behaviour of phosphatidylcholine/cholesterol

systems is complex (Lentz et al., 1980). Increasing concentrations of cholesterol (up to approximately 50 mol %) cause the main phase transition to broaden and its enthalpy to decrease. Using high-sensitivity DSC the transition in the presence of less than 20 mol % cholesterol is found to consist of a sharp and a broad component attributed to cholesterol-free and cholesterol-rich lipid regions. At higher cholesterol concentrations only the broad component remains.

Addition of 1-alkanols to the phosphatidylcholine/-cholesterol system is not expected to simplify the phase behaviour, but the details of the phase diagram are not known. Previous workers studying model membrane systems (Lawrence and Gill, 1975; Pringle et al., 1981) employed at least a 33 mol % concentration of cholesterol in egg yolk phosphatidylcholine. They found that added 1-alkanols reduced membrane order as determined by ESR. However the temperature was not varied and so the question of the degree to which the alkanols modify the egg PC/cholesterol phase behaviour remains to be answered.

A logical extension of the work reported in this thesis would be to include cholesterol in the PC-d_{31} or PC-d_{31}/1-alkanol dispersions. Preliminary results (J. Thewalt and R.J. Cushley, unpublished) show that at 50°C an aqueous dispersion of PC-d_{31}/cholesterol/1-octanol (mol ratio 2:1:1) has a significantly narrower ^2H NMR spectrum than PC-d_{31}/cholesterol (2:1). The former has an M_1 value of 0.69×10^5 s^{-1} while the latter's is 0.85×10^5 s^{-1}, 23 percent larger. Varying the temperature reveals increases in slope of the M_1 vs. temperature plots at

between 15 and 20°C for PC-d_{31}/cholesterol/1-octanol and at about 35°C for the PC-d_{31}/cholesterol. (The high-temperature levelling off of these plots, if existent, is indistinct but is certainly greater than 50°C for both samples. The width of the "transition" is thus not determined.) Further work pursuing this topic would employ a 3:1 phospholipid to cholesterol ratio which should give a shorter, more easily-defined transition.

C. Relaxation

An unexpected finding of the PC-d_{31}/1-alkanol studies is that the spin-spin relaxation behaviour of the phospholipid is markedly affected by dissolved 1-octanol or 1-decanol. Relaxation as reflected by the rate of decay of the quadrupolar echo is slowed in liquid crystalline PC-d_{31}/1-alkanol dispersions, resulting in sharper lines in their ^2H NMR spectra. This is apparent even when the concentration of 1-octanol is low (5 mol %). The relaxation rate in the absence of alcohol is approximately twice the rate in the presence of alcohol, at 50°C.

The decay of the quadrupolar echo height is thought to be related to the slow motions of the lipid acyl chains (Davis, 1979). In the liquid crystalline phase most motions such as trans-gauche isomerisations and chain rotations are rapid (with characteristic times of $\leq 10^{-8}$ s). The nature of the motion(s) causing the T_{2e} relaxation is unspecified. One can speculate that the motion(s) must be cooperative, involving a population

of phospholipids, which would account for the effectiveness of 5 mol % 1-octanol in disrupting the relaxation mechanism. ("Disrupting" includes two opposite meanings: the alcohol might either disable the motion(s) responsible for relaxation or speed the motion(s) up, making relaxation less effective.)

There is ample room to extend these results. Selectively deuterated phospholipids could be used to determine the orientation dependence of the T_{2e} relaxation, and other deuterium relaxation times could be measured. It is difficult to see how the T_{2e} results could have direct bearing on the mechanism by which 1-alkanols induce anesthesia, however, since the heterogeneity of natural membranes would presumably preclude cooperative modes of relaxation.

II. Effect of Alpha-Tocopherol on Model Membrane Systems

A. Phase transition effects

In agreement with previous studies (Cushley et al., 1979; Pohlmann and Kuiper, 1981; Massey et al., 1982; Lai et al., 1985; Srivastava et al., 1983; Fukuzawa et al., 1980) the ^2H NMR and DSC results presented in Section IV of the Results and Discussion clearly demonstrate that PC-d_{31} multilamellar dispersions containing α-tocopherol have altered phase behaviour in comparison with the pure phospholipid. With increasing concentrations of α-tocopherol the gel to liquid crystalline transition becomes progressively broader and its onset temperature decreases. This type of transition effect implies that α-tocopherol is more soluble in liquid crystalline than in gel phase phospholipid, a conclusion which is further supported by the lack of change observed in the completion temperature of the transition.

It is interesting to compare the phase behaviour of phosphatidylcholine/α-tocopherol dispersions and phosphatidylcholine/cholesterol dispersions. Both α-tocopherol and cholesterol (at concentrations > 20 mol %) reduce the enthalpy of the transition and broaden it. The major difference seems to be that while both additives lower the phase transition onset temperature, cholesterol also has the effect of increasing the completion temperature of the transition (Mabrey et al., 1978). It is likely that cholesterol/phosphatidylcholine interactions

are such that a regular network of the two components can form which resists complete conversion to the random liquid crystalline phase. The phase diagram of α-tocopherol/phosphatidylcholine is apparently simpler, although high sensitivity DSC would be required to verify that the transition is a single broad peak.

B. Order parameter effects

Below the gel to liquid crystalline transition for PC-d_{31}/-water, the ^2H NMR spectra of α-tocopherol-containing PC-d_{31} dispersions establish that α-tocopherol significantly perturbs the interior of the gel state membrane. The spectra obtained for aqueous multilamellar dispersions of PC-d_{31} are essentially independent of temperature in the range 5-30°C, consisting of a broad and rather featureless pattern. In contrast, the ^2H NMR spectra obtained for aqueous multilamellar dispersions of PC-d_{31} in the presence of α-tocopherol exhibit a series of spectral changes over the same temperature range. The most notable changes are the growth of a narrow component (between approximately -5°C to 20°C for 20 mol % α-tocopherol), followed by the appearance of a broader intermediate component (between approximately 20°C to 30°C for 20 mol % α-tocopherol). Attributing the central and intermediate components to rapidly rotating methyls and methylenes, respectively, it is proposed that α-tocopherol disrupts packing within the gel state bilayer to enable free rotation of the phospholipid chains about their

long axes. Indeed, the 38°C spectrum of PC-d_{31}/water is qualitatively the same shape as the 15°C spectrum in the presence of α-tocopherol. As chain rotation is thought to occur in intermediate-phase phosphatidylcholine dispersions (Meier et al., 1983) this observation of similar spectral shapes supports the above proposal. The increase in rate of trans-gauche isomerisation during the main gel to liquid crystalline transition accounts for the accompanying resolution of individual peaks in the intermediate component (between approximately 30°C to 40°C with 20 mol % α-tocopherol).

These results on gel phase phospholipid/α-tocopherol interactions indicating disruption of the gel by α-tocopherol addition are supported by permeability studies by Pohlmann and Kuiper (1981) and Fukuzawa et al. (1979). They found that α-tocopherol enhanced water and glucose permeability, respectively, in gel phase phosphatidylcholine. Thus there is a link between increased permeability and looser or more imperfect acyl chain packing in the gel phase. The biphasic variation of glucose permeability with increasing concentrations of α-tocopherol in DPPC at 37°C observed by Fukuzawa et al. (1979) is explained by a progressive reduction in phase transition onset temperature of DPPC as α-tocopherol is added. These workers found that α-tocopherol concentrations below 5 mol % resulted in enhanced permeability and at this level of α-tocopherol the data presented in Section IV of the Results and Discussion indicates that the dispersions would be in the gel phase at 37°C. At higher α-tocopherol concentrations they would

be primarily liquid crystalline and the reduced permeability observed is then consistent with more organized acyl chains, as summarized next.

In the liquid crystalline phase ^2H NMR clearly demonstrates that increased phosphatidylcholine acyl chain ordering results upon α-tocopherol incorporation, and that the degree of ordering varies directly with α-tocopherol concentration (at least up to a 4:1 phospholipid:α-tocopherol ratio). Published observations of reduced permeability and mobility in liquid crystalline phospholipid dispersions containing α-tocopherol (Diplock et al., 1977; Stillwell and Bryant, 1983; Srivastava et al., 1983; Fukuzawa et al., 1980; Massey et al.,1982) are consistent with the observed increase in order. Reports of increased permeability of egg PC vesicles to Pr^{3+} (Cushley and Forrest, 1977; Cushley et al., 1979) and of DPPC vesicles to sodium ascorbate (Srivastava et al., 1983) are, on the surface, in disagreement. Vesicles and multilamellar dispersions are different systems, however, and have been reported to display differences in acyl chain ordering (Parmar et al., 1984). Thus their response to α-tocopherol incorporation may be different including their change in permeability.

Further work to determine the structural effects of α-tocopherol on phosphatidylcholine multilamellar dispersions would incorporate unsaturated fatty acids or phospholipids into the system, to test the hypothesis that interactions between α-tocopherol and unsaturated fatty acyl chains stabilize the membrane (Diplock and Lucy, 1973; Maggio et al., 1977). The

relevance of such an investigation is confirmed by a recent report that α-tocopherol and fatty acids form complexes and that the equilibrium constants characterizing the complex formation are substantially higher for unsaturated fatty acids (Erin et al., 1984).

REFERENCES

Bloom, M., Davis, J.H., and MacKay, A.L. (1981) Chem. Phys. Lett. 80, 198-202.

Bloom, M., Davis, J.H. and Valic, M.I. (1980) Can. J. Phys. 58, 1510-1517.

Bloom, M. and Smith, I.C.P. (1985) in Progress in Protein-Lipid Interactions (J.J.H.H.M. du Pont and A. Watts, eds.) Vol. 1, pp. 61-88.

Boigegrain, R.A., Fernandez, Y., Massol, M. and Mitjavila, S. (1984) Chem. Phys. Lipids 35, 321-330.

Boroske, E. and Trahms, L. (1983) Biophys. J. 42, 275-283.

Boss, W.F., Kelley, C.J. and Landsberger, F.R. (1975) Anal. Biochem. 64, 289-292.

Brasseur, R., Chatelain, P., Goormaghtigh, E. and Russchaert, J.-M. (1985) Biochim. Biophys. Acta 814, 227-236.

Brown, M.A. (1983) Radiat. Res. 95, 303-316.

Brown, M.F., Ribeiro, A.A. and Williams, G.D. (1983) Proc. Natl. Acad. Sci. USA 80, 4325-4329.

Burnett, L.J. and Muller, B.H. (1971) J. Chem. Phys., 55, 5829-5831.

Chen, S.C. and Sturtevant, J.M. (1981) Biochemistry 20, 713-718.

Chen, S.C., Sturtevant, J.M. and Gaffney, B.J. (1980) Proc. Natl. Acad. Sci. USA 77, 5060-5063.

Cohen, M.H. and Reif, F. (1957) Solid State Phys. 5, 321-438.

Colley, C.M. and Metcalfe, J.C. (1972) FEBS Lett. 24, 241-246.

Curatolo, W., Jungalwala, F.B., Sears, B., Tuck, L. and Neuringer, L.J. (1985) Biochemistry 24, 4360-4364.

Curatolo, W., Sears, B. and Neuringer, L.J. (1985) Biochim. Biophys. Acta 817, 261-270.

Cushley, R.J. and Forrest, B.J. (1977) Can. J. Chem. 55, 220-226.

Cushley, R.J., Forrest, B.J., Gillis, A., and Tribe, J. (1979) Can. J. Chem. 57, 458-465.

Davis, J.H. (1979) Biophys. J. 27, 339-358.

Davis, J.H. (1983) Biochim. Biophys. Acta 737, 117-171.

Davis, J.H., Jeffrey, K.R., Bloom, M., Valic, M.J. and Higgs, T.P. (1976) Chem. Phys. Lett. 42, 390-394.

De Gier, J., Mandersloot, J.G., and Van Deenen, L.L.M. (1968) Biochim. Biophys. Acta 150, 666-675.

De Gier, J., Mandersloot, J.G., and Van Deenen, L.L.M. (1969) Biochim. Biophys. Acta 173, 143-145.

Diamond, J.M. and Katz, Y. (1974) J. Membrane Biol. 17, 121-154.

Diplock, A.T., and Lucy, J.A. (1973) FEBS Lett. 29, 205-210.

Diplock, A.T., Lucy, J.A., Verrinder, M., and Zieleniewski, A. (1977) FEBS Lett. 82, 341-344.

Dluzewski, A.R., Halsey, M.J. and Simmonds, A.C. (1983) Molec. Aspects Med. 6, 459-573.

Eliasz, A.W., Chapman, D. and Ewing, D.F. (1976) Biochim. Biophys. Acta 448, 220-230.

Erin, A.N., Spirin, M.M., Tabidze, L.V. and Kagan, V.E. (1984) Biochim. Biophys. Acta 774, 96-102.

Fesik, S.W. and Makriyannis, A. (1985) Mol. Pharmacol. 27, 624-629.

Fukuzawa, K., Chida, H. and Suzuki, A. (1980) J. Nutr. Sci. Vitaminol. 26, 427-434.

Fukuzawa, K., Ikeno, H., Tokumura, A. and Tsukatani, H. (1979) Chem. Phys. Lipids 23, 13-22.

Grover, A.K. and Cushley, R.J. (1979) J. Label. Comp. Radiopharm. 16, 307-313.

Grunze, M., Haest, C.W.M. and Deuticke, B. (1982) Biochim. Biophys. Acta 693, 237-245.

Haberkorn, R.A., Griffin, R.J., Meadows, M.D. and Oldfield, E. (1977) J. Amer. Chem. Soc. 99, 7353-7355.

Harris, R.K. (1983) Nuclear Magnetic Resonance Spectroscopy, Pitman Books Ltd., London.

Heyn, M.P. (1979) FEBS Lett. 108, 359-364.

Hill, M.W. (1974) Biochim. Biophys. Acta 356, 117-124.

Hsiao, C.Y.Y., Ottaway, C.A. and Wetlaufer, D.B. (1974) Lipids 9, 913-915.

Ingram, L.O., Carey, V.C. and Dombek, K.M. (1982) Subst. Alc. Actions/Misuse 2, 213-224.

Jacobs, R., and Oldfield, E. (1979) Biochemistry 18, 3280-3285.

Jacobs, R.E. and White, S.H. (1984) J. Am. Chem. Soc. 106, 915-920.

Jahnig, F. (1979) Proc. Natl. Acad. Sci. USA 76, 6361-6365.

Jain, M.K., Gleeson, J., Upreti, A. and Upreti, G.C. (1978) Biochim. Biophys. Acta 509, 1-8.

Jain, M.K., Wu, N.M. (1977) J. Membrane Biol. 34, 157-201.

Jain, M.K., Wu, N.M., and Wray, L.V. (1975) Nature 255, 494-496.

Janoff, A.S. and Miller, K.W. (1982) in Biological Membranes (D. Chapman, ed.) Vol. 4, pp. 417-476.

Jeffrey, K.R. (1981) Bull. Magn. Reson., 3, 69-82.

Klason, T. and Henriksson, U. (1982) in: Solution Behaviour of Surfactants, Vol.1, (Mittal, K.L. and Fondler, E.I., eds.), Plenum Press, New York pp.417-429.

Knoll, W. (1984) Thermochim. Acta 77, 35-47.

Lai, M., Duzgunes, N. and Szoka, F.C. (1985) Biochemistry 24, 1646-1653.

Lawrence, D.K. and Gill, E.W. (1975) Mol. Pharmacol. 11, 595-602.

Lee, A.G. (1976a) Biochemistry 15, 2448-2454.

Lee, A.G. (1976b) Nature 262, 545-548.

Lentz, B.R., Barrow, D.A. and Hoechli, M. (1980) Biochemistry 17, 1943-1954.

Lucy, J.A. and Dingle, J.T. (1964) Nature 204, 156-160.

Lyon, R.C., McComb, J.A., Schreurs, J. and Goldstein, D.B. (1981) J. Pharm. Exp. Ther. 218, 669-675.

Mabrey, S., Mateo, P.L. and Sturtevant, J.M. (1978) Biochemistry 17, 2464-2468.

MacDonald, A.G. (1978) Biochim. Biophys. Acta 507, 26-37.

Machlin, L.J. (ed.) (1980) Vitamin E: A Comprehensive Treatise, Marcel Dekker, Inc., New York.

Maggio, B., Diplock, A.T. and Lucy, J.A. (1977) Biochem. J. 161, 111-121.

Mansfield, P. (1965) Phys. Rev. 137, A961-974.

Marder, M., Frisch, H.L., Langer, J.S. and McConnell, H.M. (1984) Proc. Natl. Acad. Sci. USA 81, 6559-6561.

Massey, J.B., Hoyan, S.S. and Pownall, H.J. (1982) Biochem. Biophys. Res. Commun. 106, 842-847.

McElhaney, R.N. (1982) Chem. Phys. Lipids 30, 229-259.

Meier, P., Ohmes, E., Kothe, G., Blume, A., Weldner, J. and Elbl, H.-J. (1983) J. Phys. Chem. 87, 4904-4912.

Miller, K.W. and Pang, K.-Y.Y. (1976) Nature 263, 253-255.

Niederberger, W. and Seelig, J. (1974) Ber. Bunsenges. Physik. Chem. 78, 947-949.

Oldfield, E., Chapman, D. and Derbyshire, W. (1971) FEBS Lett. 16, 102-104.

Oldfield, E., Meadows, M., Rice, D., and Jacobs, R. (1978) Biochemistry 17, 2727-2740.

Paddy, M.R. Dahlquist, F.W., Dratz, E.A. and Deese, A.J. (1985) Biochemistry 24, 5988-5995.

Parmar, Y.I. (1985) NMR Studies of Human Plasma High Density Lipoproteins, Ph.D. Thesis, Simon Fraser University, Burnaby, B.C.

Parmar, Y.I., Wassall, S.R. and Cushley, R.J. (1984) J. Amer. Chem. Soc. 106, 2434-2435.

Paterson, S.J., Butler, K.W., Huang, P., Labelle, J., Smith, I.C.P. and Schneider, H. (1972) Biochim. Biophys. Acta 266, 597-602.

Pauls, K.P., MacKay, A.L. and Bloom, M. (1983) Biochemistry 22, 6101-6109.

Pauls, K.P., MacKay, A.L., Soderman, O., Bloom, M., Tanjea, A.K. and Hodges, R.S. (1985) Eur. Biophys. J. 12, 1-11.

Perly, B., Smith, I.C.P., Hughes, L., Burton, G.W. and Ingold,

K.U. (1985a) Biochim. Biophys. Acta 819, 131-135.

Perly, B., Smith, I.C.P. and Jarrell, H.C. (1985b) Biochemistry 24, 4659-4665.

Pohlmann, F.W. and Kuiper, P.J.C. (1981) Phytochemistry 20, 1525-1528.

Pringle, M.J., Brown, K.B. and Miller, K.W. (1981) Mol. Pharmacol. 19, 49-55.

Pope, J.M., Walker, L.W. and Dubro, D. (1984) Chem. Phys. Lipids 35, 259-273.

Rance, M.A. (1981) Deuterium Nuclear Magnetic Resonance Studies of Unsaturated Lipids in the Membranes of Acholeplasma Laidlawii, Ph.D. Thesis, University of Guelph, Guelph, Ontario.

Richards, C.D., Keightley, C.A., Hesketh, T.R. and Metcalfe, J.C. (1980) in Progress in Anesthesiology (R.A. Fink, ed.) Vol. 2, pp. 337-351.

Ruocco, M.J. and Shipley, G.G. (1982a) Biochim. Biophys. Acta 684, 59-66.

Ruocco, M.J. and Shipley, G.G. (1982b) Biochim. Biophys. Acta 691, 309-320.

Sallee, V.L. (1978), J. Membrane Biol. 43, 187-201.

Schmidt, D., Steffen, H., and Von Planta, C. (1976) Biochim. Biophys. Acta 443, 1-9.

Seelig, A. and Seelig, J. (1974) Biochemistry 13, 4839-4845.

Seelig, J. (1977) Q. Rev. Biophys. 10, 353-418.

Seelig, J. and Browning, M.L. (1978) FEBS Lett. 92, 41-44.

Seelig, J. and Waespe-Sarcevic, N. (1978) Biochemistry 17, 3310-3315.

Slichter, C.P. (1978) Principles of Magnetic Resonance, Harper & Row, New York.

Smith, I.C.P. and Butler, K.W. (1985) in Effects of Anesthesia (Proceedings, American Physiological Society) pp. 1-11.

Solomon, I. (1958) Phys. Rev. 110, 61-65.

Spiess, H.W. and Sillescu, H. (1980) J. Magn. Res. 42, 381-389.

Srivastava, S., Phadke, R.S., Govil, G. and Rao, C.N.R. (1983) Biochim. Biophys. Acta 734, 353-362.

Stanley, H.E. (1971) Phase Transitions and Critical Phenomena, Clarendon Press, Oxford, London.

Sternin, E. (1982) Depakeing of NMR Spectra, M.Sc. Thesis, The University of British Columbia, Vancouver, B.C.

Sternin, E., Bloom, M. and MacKay, A.L. (1983) J. Magn. Res. 55, 274-282.

Stillwell, W., and Bryant, L. (1983) Biochim. Biophys. Acta 731, 483-486.

Stockton, G.W., and Smith, I.C.P. (1976) Chem. Phys. Lipids 17, 251-263.

Tardieu, A., Luzzati, V. and Reman, F.C. (1973) J. Mol. Biol. 75, 711-733.

Taylor, M.G. and Smith, I.C.P. (1983) Biochim. Biophys. Acta 733, 256-263.

Thewalt, J.L., Wassall, S.R., Gorrissen, H. and Cushley, R.J. (1985) Biochim. Biophys. Acta 817, 355-365.

Trudell, J.R. (1977) Anesthesiology 46, 5-10.

Tulloch, A.P. (1985a) Chem. Phys. Lipids 37, 197-213.

Tulloch, A.P. (1985b) Lipids 20, 404-411.

Turner, G.L. and Oldfield, E. (1979) Nature 277, 669-670.

Wassall, S.R., Thewalt, J.L., Wong, L., Gorrissen, H. and Cushley, R.J. (1986) Biochemistry (in press).

Zavoico, G.B., Chandler, L. and Kutchai, H. (1985) Biochim. Biophys. Acta 812, 299-312.

Zavoico, G.B. and Kutchai, H. (1980) Biochim. Biophys. Acta 600, 263-269.